

5-2010

## Osteopontin and cadherin 11 are novel mediators and drug targets for chronic lung diseases

Daniel J. Schneider

Follow this and additional works at: [https://digitalcommons.library.tmc.edu/utgsbs\\_dissertations](https://digitalcommons.library.tmc.edu/utgsbs_dissertations)



Part of the [Circulatory and Respiratory Physiology Commons](#), [Pathology Commons](#), and the [Respiratory Tract Diseases Commons](#)

---

### Recommended Citation

Schneider, Daniel J., "Osteopontin and cadherin 11 are novel mediators and drug targets for chronic lung diseases" (2010). *The University of Texas MD Anderson Cancer Center UTHealth Graduate School of Biomedical Sciences Dissertations and Theses (Open Access)*. 47.  
[https://digitalcommons.library.tmc.edu/utgsbs\\_dissertations/47](https://digitalcommons.library.tmc.edu/utgsbs_dissertations/47)

This Dissertation (PhD) is brought to you for free and open access by the The University of Texas MD Anderson Cancer Center UTHealth Graduate School of Biomedical Sciences at DigitalCommons@TMC. It has been accepted for inclusion in The University of Texas MD Anderson Cancer Center UTHealth Graduate School of Biomedical Sciences Dissertations and Theses (Open Access) by an authorized administrator of DigitalCommons@TMC. For more information, please contact [digitalcommons@library.tmc.edu](mailto:digitalcommons@library.tmc.edu).

# **Osteopontin and cadherin 11 are novel mediators and drug targets for chronic lung diseases**

By

Daniel J. Schneider, B.S.

APPROVED:

---

Michael R. Blackburn, Ph.D.

Supervisory Chair

---

Sandeep K. Agarwal, M.D., Ph.D.

---

Russel Broddus, MD, Ph.D.

---

Rodney E. Kellems, Ph.D.

---

Renhao Li, Ph.D.

---

APPROVED:

---

George Stancel, Ph.D.  
Dean, The University of Texas  
Health Science Center at Houston  
Graduate School of Biomedical Sciences

# **Osteopontin and cadherin 11 are novel mediators and drug targets for chronic lung diseases**

A

## **DISSERTATION**

Presented to the Faculty of

The University of Texas

Health Science Center at Houston

and

The University of Texas

M.D. Anderson Cancer Center

Graduate School of Biomedical Sciences

in Partial Fulfillment

of the Requirements

for the Degree of

## **Doctor of Philosophy**

by

Daniel Schneider, B.A

Houston, TX

May, 2010



# Acknowledgements

I wish to acknowledge my first two mentors, Dr. Shawn Newlands at UTMB in Galveston and Dr. Ruth Anne Eatock formerly at Baylor College of Medicine. My work in their labs represented my first research experiences. Had those experiences been less than favorable, I would likely never have realized my passion for research and surely would not have matriculated into the MD PhD program here at UT Houston. With Dr. Eatock's encouragement, I applied to transfer into the program after two years of medical school. On that note, I want to thank the MD PhD program directors and committee members, especially Dr. Dianna Milewicz and Dr. Russel Broadus, for their mentorship and for my unconventional admission into the program.

I'd like to thank all my committee members including Dr. Rodney Kellems and Dr. Renhao Li for the work they put in and all their help and support. I'd like to specifically thank Dr. Sandeep Agarwal for the opportunity to work on the cadherin 11 project and for his mentorship for me as an MD PhD in training. I certainly would like to thank my thesis advisor Dr. Michael Blackburn for all his help with everything. To be concise, I am very grateful for all his time, his insights, and the intangible skills I have adopted as a result of my time with him over the last three years. It is unsettling to contemplate what my graduate training and its result may have been had I not chosen him as the principle investigator for whom I wished to study under.

I'd like to thank current and past members in Dr. Blackburn's and collaborator's labs. Jose Molina in Dr. Blackburn's lab and Minghua Wu in Dr. Agarwal's Lab for their help with the mice. Special thanks go to Eva Morschl, Yang Zhou, and Amir Mohsenin for helping me get started in the lab and for helping me understand many of the techniques I utilized to answer the questions proposed in this dissertation. I would also like to acknowledge Dr. Joseph Alcorn and Dr. Seo-Hee Cho in the Department of Pediatrics for their help with various imaging techniques. I would like to thank Dr. Gregory Shipley for his time and help with the high-throughput RT-PCR reactions and our attempts at multiplex protein analysis. I'd also like to thank all the students in the MD PhD and biochemistry programs. It's been a great social and intellectual environment to be around.

Finally, I would like to give my thanks and appreciation to members of my family: my wife Allison, my son Aspen, my mother Dr. Cynthia Schneider, my father Dr. David Schneider, my sister Gina Schneider and other members of my immediate and extended family. It is a constant battle to split time between work and family. Their love and support make balancing those areas of my life manageable and certainly contributed to my success in the lab. Though, I have a long way to go in terms of my training as a physician scientist, I would like to dedicate this dissertation to all that have played a role in facilitating my accomplishments as a graduate student. My sincere thanks go to everyone mentioned. I hope to have made you all proud.

Chronic lung diseases (CLDs) are a considerable source of morbidity and mortality and are thought to arise from dysregulation of normal wound healing processes. An aggressive feature of many CLDs is pulmonary fibrosis (PF) and is characterized by excess deposition of extracellular matrix (ECM) proteins from myofibroblasts in airways. However, factors regulating myofibroblast biology are incompletely understood. Proteins in the cadherin family contribute epithelial to mesenchymal transition (EMT), a suggested source of myofibroblasts. Cadherin 11 (CDH11) contributes to developmental and pathologic processes that parallel those seen in PF and EMT. Utilizing *Cdh11* knockout (*Cdh11*<sup>-/-</sup>) mice, the goal of this study was to characterize the contribution of CDH11 in the bleomycin model of PF and assess the feasibility of treating established PF. We demonstrate CDH11 in macrophages and airway epithelial cells undergoing EMT in lungs of mice given bleomycin and patients with PF. Endpoints consistent with PF including ECM production and myofibroblast formation are reduced in CDH11-targeted mice given bleomycin. Findings suggesting mechanisms of CDH11-dependent fibrosis include the regulation of the profibrotic mediator TGF- $\beta$  in alveolar macrophages and CDH11-mediated EMT. The results of this study propose CDH11 as a novel drug target for PF. In addition, another CLD, chronic obstructive pulmonary disease (COPD), is characterized by airway inflammation and destruction. Adenosine, a nucleoside signaling molecule generated in response to cell stress is upregulated in patients with COPD and is suggested to contribute to its pathogenesis. An established model of adenosine-mediated lung injury exhibiting features of COPD is the *Ada*<sup>-/-</sup> mouse. Previous studies in our lab suggest features of the *Ada*<sup>-/-</sup> phenotype may be secondary to adenosine-dependent expression of osteopontin (OPN). OPN is a protein implicated in a variety of human pathology, but its role in COPD has not been examined. To address this, *Ada/Opn*<sup>-/-</sup> mice were generated and endpoints consistent with COPD were examined in parallel with *Ada*<sup>-/-</sup> mice. Results demonstrate OPN-mediated pulmonary neutrophilia and airway destruction in *Ada*<sup>-/-</sup> mice. Furthermore, patients with COPD exhibit increased OPN in airways which correlate with clinical airway obstruction. These results suggest OPN represents a novel biomarker or therapeutic target for the management of patients with COPD. The importance of findings in this thesis is highlighted by the fact that no pharmacologic interventions have been shown to interfere with disease progression or improve survival rates in patients with COPD or PF.

# Table of contents

<b>List of illustrations</b>	ix
------------------------------	----

<b>List of abbreviations</b>	xi
------------------------------	----

## Chapter 1

### Introduction

Chronic lung disease	2
COPD	3
Pulmonary Fibrosis	3
Dissertation Overview	4

## Chapter 2

### Experimental Procedures

<i>Ada</i> <sup>-/-</sup> mice	7
<i>Opn</i> <sup>-/-</sup> mice	7
CD44 neutralization	7
Bleomycin installation	7
CDH11 neutralization	7

Mice	7
BAL, airway inflammatory cells, and differentials	9
Histology, air-space size and fibrosis assessment	9
Immunostaining	9
Immunofluorescence	10
Western blot for CDH11	10
Analysis of whole lung mRNA	11
Analysis of A549 cells	11
<i>In vivo</i> neutrophil migration	12
Human lung samples	12
Whole mount immunohistochemistry for CD31 on tracheas	12
Mucus quantitation	13
Peripheral blood differentials	13
Statistics	13

## Chapter 3

### Osteopontin and adenosine contribute to COPD

#### Introduction

COPD	15
Adenosine	15
<i>Ada</i> <sup>-/-</sup> mice	18
Adenosine receptor signaling in the <i>Ada</i> <sup>-/-</sup> model	19

<i>Ada</i> <sup>-/-</sup> mice, the A <sub>2B</sub> receptor, and OPN	20
Osteopontin	23
Osteopontin in cancer	23
Osteopontin as a modulator of immunity in human disease	25
OPN in lung disease	25

## Results

Histopathology in <i>Ada/Opn</i> <sup>-/-</sup> mice	27
Quantification of pulmonary inflammation in <i>Ada/Opn</i> <sup>-/-</sup> mice	27
OPN contributes to air-space enlargement in <i>Ada</i> <sup>-/-</sup> mice	27
OPN increases mediators of air-space enlargement	31
OPN-dependent <i>in vivo</i> neutrophil recruitment	31
CD44 expression, localization, and neutralization in <i>Ada</i> <sup>-/-</sup> mice	35
OPN and the regulation of proinflammatory cytokines	38
OPN and peripheral blood neutrophilia	38
OPN and alveolarization	38
OPN-mediated angiogenesis in <i>Ada</i> <sup>-/-</sup> mice	42
Mucus metaplasia in <i>Ada/Opn</i> <sup>-/-</sup> mice	42
OPN-dependent airway remodeling and fibrosis	42
OPN expression, localization, and association with severity of COPD in humans	46

Discussion	52
------------	----

## Chapter 4 - Cadherin 11 and pulmonary fibrosis

## Introduction

Pulmonary fibrosis	59
TGF- $\beta$ in pulmonary fibrosis	60
Epithelial to mesenchymal transition (EMT)	60
Cadherins and EMT	61
Cadherin 11 (CDH11)	62

## Results

Expression and localization of CDH11 in patients with ILD	63
Expression and localization of CDH11 in bleomycin model of pulmonary fibrosis	63
Immunofluorescence detection of CDH11 on alveolar macrophages	63
Contribution of CDH11 to features of pulmonary fibrosis	67
CDH11 blocking Ab improves established pulmonary fibrosis	67
CDH11 contributes to EMT in airway epithelial cells	71
Role of CDH11 in pulmonary inflammation	71
CDH11-dependent regulation of TGF- $\beta$	78

Discussion	80
------------	----

## Chapter 5 - Future Directions

Characterize the contribution of $\alpha_v\beta_3$ integrin to the <i>Ada</i> <sup>-/-</sup> pulmonary phenotype	88
OPN-dependent regulation of adhesion molecules	88
Role of OPN in alternative models of emphysema/COPD	89

Localization of $\beta$ catenin	89
CDH11-dependent expression of TGF- $\beta$ in alveolar macrophages	91
CDH11-dependent clearance of 'debris' by alveolar macrophages	91
Further characterization of pulmonary endpoints in the bleomycin and <i>Ada</i> <sup>-/-</sup> model	93
Overlap between CDH11 and OPN?	93
<b>References</b>	95
<b>Vita</b>	113

## List of illustrations

Figure 2.1	Bleomycin model and CDH11 treatment strategy	8
Figure 3.1	Generation of extracellular adenosine	16
Figure 3.2	Adenosine receptor activities in the lungs of <i>Ada</i> <sup>-/-</sup> mice	21
Figure 3.3	A <sub>2B</sub> R-dependent OPN expression in macrophages of <i>Ada</i> <sup>-/-</sup> mice	22
Figure 3.4	Primary sequence and post-translational modification sites of OPN	24
Figure 3.5	Histopathology associated with genetic removal of <i>Opn</i> in <i>Ada</i> <sup>-/-</sup> mice	28
Figure 3.6	Airway inflammatory cells in <i>Ada</i> <sup>-/-</sup> and <i>Ada/Opn</i> <sup>-/-</sup> mice	29
Figure 3.7	Alveolar air-space size in <i>Ada</i> <sup>-/-</sup> and <i>Ada/Opn</i> <sup>-/-</sup> mice	30
Figure 3.8	OPN-dependent regulation of air-space enlargement mediators	32
Figure 3.9	Lung neutrophilia and MMP-9 immunolocalization	33
Figure 3.10	OPN-mediated neutrophil recruitment in an in vivo model	34
Figure 3.11	CD44 expression in <i>Ada</i> <sup>-/-</sup> mice	36



Figure 3.12	CD44 neutralization in <i>Ada</i> <sup>-/-</sup> mice	37
Figure 3.13	OPN-dependent regulation of proinflammatory cytokines	39
Figure 3.14	Quantification of blood leukocytes in <i>Opn</i> <sup>-/-</sup> mice	40
Figure 3.15	OPN and alveolarization	41
Figure 3.16	Angiogenesis and OPN in the <i>Ada</i> <sup>-/-</sup> model	43
Figure 3.17	Role of OPN in mucus production in the <i>Ada</i> <sup>-/-</sup> model	44
Figure 3.18	Myofibroblasts and collagen	45
Figure 3.19	Profibrotic mediators	47
Figure 3.20	Fibronectin	48
Figure 3.21	OPN expression in patients with COPD	49
Figure 3.22	OPN expression associates with clinical indicators of COPD	51
Figure 3.23	Schematic representation of OPN-mediated air-spaces	53
Figure 4.1	Cadherin 11 expression and immunolocalization in human IPF patients	64
Figure 4.2	Cadherin 11 expression and localization in bleomycin-induced fibrosis	65
Figure 4.3	CDH11 immunolocalization on alveolar macrophages	66
Figure 4.4	Cadherin 11-dependent histopathology	68
Figure 4.5	Histologic evidence of CDH11-dependent myofibroblast formation and collagen deposition	69
Figure 4.6	Quantifiable fibrotic endpoints <i>Cdh11</i> <sup>-/-</sup> mice given bleomycin	70
Figure 4.7	CDH11 blocking antibody improves established pulmonary fibrosis	72
Figure 4.8	CDH11 blocking antibody reduces lung myofibroblasts and collagen	73
Figure 4.9	TGF- $\beta$ -induced EMT and <i>Cdh11</i> expression in A549 lung epithelial cells	74

Figure 4.10	<i>Cdh11</i> knockdown prevents TGF- $\beta$ -induced EMT of lung epithelial cells	75
Figure 4.11	<i>Cdh11</i> knockdown prevents TGF- $\beta$ -induced transition to mesenchymal morphology in lung epithelial cells	76
Figure 4.12	Contribution of CDH11 to pulmonary inflammation	77
Figure 4.13	CDH11-dependent regulation of TGF- $\beta$	79
Figure 4.14	Working model of cadherin 11-dependent pulmonary fibrosis	81
Figure 5.1	Dual CDH11 $\beta$ -catenin immunofluorescence on ILD macrophages	90
Figure 5.2	'Inclusion' cells in <i>Cdh11</i> <sup>-/-</sup> alveolar macrophages	92

# List of abbreviations

Ab	antibody
ADA	adenosine deaminase
ADP	adenosine diphosphate
AEC	airway epithelial cell
AMP	adenosine monophosphate
ARDS	acute respiratory distress syndrome
ATP	adenosine triphosphate
BAL	bronchoalveolar lavage
BSA	bovine serum albumin
CDH11	cadherin 11
COPD	chronic obstructive pulmonary disease
CCL	C-C motif ligand
CD	cluster of differentiation
CSE	cigarette smoke extract
CXCL	C-X-C motif ligand
DMEM	Dulbecco's Modified Eagle's Medium
DPLD	diffuse proliferative lung disease
ECL	enhanced chemiluminescence
ECM	extracellular matrix
ELISA	enzyme-linked immunosorbent assay

EMT	epithelial to mesenchymal transition
FBS	fetal bovine serum
FEV1	forced expiratory volume in 1 second
FVC	forced vital capacity
HRP	horseradish peroxidase
IL	interleukin
ILD	interstitial lung disease
IP	intraperitoneal
IPF	idiopathic pulmonary fibrosis
LPS	lipopolysaccharide
MAP	mitogen activated protein
MMP	matrixmetalloprotease
NECA	N-ethylcarboxamide adenosine
OPN	osteopontin
PAI	plasminogen activator inhibitor
PAS	Periodic Acid Schiff
PBS	phosphate-buffered saline
PDGF	platelet-derived growth factor
PEFR	peak expiratory flow rate
PEG	polyethylene glycol
PF	pulmonary fibrosis
PFT	pulmonary function test

PPIA	peptidylprolyl isomerase A (Cyclophilin A)
PVDF	polyvinylidene fluoride
RT-PCR	reverse transcriptase polymerase chain reaction
SEM	standard error of the mean
SMA	smooth muscle actin
TBS/T	tris buffered saline + tween
TGF	transforming growth factor
TIMP	tissue inhibitor of matrixmetalloprotease
uPA	urokinase plasminogen activator

# **Chapter 1**

## **Introduction**

## **Chapter 1 - Introduction**

### **Chronic lung disease**

Acute lung injuries arise from many well-recognized etiologies. Examples include environmental insults, particularly cigarette smoke, infections, and allergens. These injuries lead to disrupted endothelial and epithelial cell integrity and pulmonary edema. Under normal conditions, there are established response mechanisms for lung tissue repair. These include inflammation, ECM production, deposition, and angiogenesis all encompassing the process of normal wound healing. In the scenario of acute lung injury, tissue undergoes normal healing until repair is complete and there is full recovery of function with no long term sequelae.

For reasons poorly understood, pathways involved in normal wound healing become dysregulated or excessive in the context of chronic lung disease. Hence, these diagnoses, in contrast to acute lung injuries, comprise a group of conditions where sustained insults lead to permanent changes in lung architecture and its ability to exchange gases. This leads to progressive dyspnea, chronic cough, shortness of breath, and fatigue. In addition, patients are highly sensitive to infections that can lead to acute exacerbations of these symptoms. Furthermore, substantial complications occur outside the lung as a consequence of destroyed lung parenchyma and disrupted gas exchange. These include anorexia, cardiac arrhythmias, muscle wasting, and pulmonary hypertension, all of which contribute significantly to the overall morbidity and mortality of these conditions.

Examples of chronic lung diseases include asthma, chronic obstructive pulmonary disease (COPD), and interstitial lung disease (ILD). Asthma is characterized by chronic inflammation and remodeling of the airways. Most recognizable features of asthma, however, are acute episodes of airway edema, constriction and collapse leading to sudden onset of dyspnea. In addition, asthma may present in a patient at any age. These features are in contrast to COPD and ILD which commonly present in the fourth to sixth decades of life with a progressive, insidious onset of dyspnea.

Although many triggers associated with development of disease are established, the details regarding specific factors that drive the chronic nature of these processes remain unknown. Hence, these conditions are irreversible and effective treatments are lacking. This

thesis will focus on novel signaling pathways involved in promoting the chronic features of COPD and ILD contributing to the fund of knowledge that will ultimately lead to the development of disease-modifying treatments for these devastating conditions.

### **Chronic obstructive pulmonary disease (COPD)**

Patients with COPD comprise the majority of conditions termed “chronic diseases of the lower respiratory tract” which include chronic bronchitis, emphysema, and asthma. COPD affects six percent of the American population, contributes to seven percent of all hospitalizations and harbors direct and indirect costs on the order of tens of billions in US dollars annually (1). These conditions are the leading cause of death in America after cardiovascular diseases and cancer (2) and the incidence of COPD is projected to increase in the next 30 years (3).

Emphysema, a well-recognized feature of COPD and is most common in people aged 50 to 65 years who have a history of smoking (4). However, other less common etiologies of emphysema exist including HIV,  $\alpha_1$  antitrypsin deficiency, and hypersensitivity pneumonitis. Emphysema is defined as destructive, permanent alveolar airspace enlargement in the adult lung in contrast to enlarged distal airways secondary to abnormal alveolar development in the neonatal lung. These destructive changes result in progressive loss of patency and elasticity of medium and small airways leading to airway obstruction and collapse.

Most notable histopathologic features of emphysema are the loss of alveolar sacs and enlargement of distal air-spaces. This is accompanied by an inflammatory cell infiltrate (5) consisting of neutrophils, CD8+ T-lymphocytes, and macrophages throughout the airways and lung parenchyma. Gene expression and proteomic profiling of samples obtained from patients and animal models of emphysema yield select cytokines, growth factors and proteases upregulated during this disease. The roles of these proteins in the contribution to inflammation and tissue damage in the acute setting are well-documented. Despite this knowledge, there is a complete lack of therapies that alter disease progression or improve survival rates for patients with COPD/emphysema (6). Signaling pathways involved in the maintenance of the chronic inflammation and tissue destruction seen in COPD remain poorly defined. Understanding these processes will aid the development of novel treatment strategies and yield adequate prognostic biomarkers for better disease management and optimization of treatment



options. Aspects of this thesis will address these gaps in our knowledge with the goal of identifying novel pathways that can be targeted for the treatment of COPD.

## **Pulmonary fibrosis**

The term fibrosis refers to excessive and dysregulated deposition of extracellular matrix in an organ. In many cases, this can be linked to exposure to environmental or iatrogenic irritants such as allergens, toxic chemicals, particulate matter, radiation, or chemotherapy. In other cases, particularly in the lung, it may be secondary to systemic inflammatory disorders and connective tissue diseases such as sarcoidosis and scleroderma (7-9). Fibrosis is the cardinal feature of a group of chronic lung diseases termed diffuse proliferative lung diseases (DPLD) or interstitial lung diseases (ILD). A particularly deadly form of unknown etiology is idiopathic pulmonary fibrosis (IPF). Less than ten percent of patients show a response to available treatments (10) and the condition carries a mean survival time of two to three years at time of diagnosis. Unfortunately, this is attributable to the total absence of disease-modifying therapies (11) and a deficiency in understanding the fundamental pathogenic mechanisms of the disease. In addition, many recent studies have impressed that pulmonary fibrosis is a compounding pathologic feature in chronic stages of asthma and COPD (12-14). Hence, while sources report pulmonary fibrosis affects roughly 200,000 Americans (15, 16), estimates of prevalence and incidence are often understated given its exhibition in this vast array of clinical conditions.

Established histopathologic features of pulmonary fibrosis include variable inflammation and the appearance of myofibroblasts in fibrotic foci of the distal airways. Myofibroblasts exhibit contractile properties and a propensity for the synthesis and deposition of extracellular matrix proteins (17). Through these functions, they play a physiologic role in the maintenance of structure of the large airways and vessels under normal conditions. At sites of injury in any organ, the appearance of myofibroblasts is a necessary process of normal wound healing (18). Naturally, a critical step in repair at sites of injury is the disappearance of myofibroblasts once wound healing is complete. Thus, over-activity and enhanced survival of myofibroblasts is a defining feature of pathologic fibrosis. However, molecular mechanisms promoting the formation and survival of myofibroblasts in pathologic situations are not well-understood. Detailed investigation into the origin of myofibroblasts and their corresponding processes will

be critical in developing therapeutic measures for pulmonary fibrosis. These concepts and their individual contribution to pulmonary fibrosis are explored in this thesis.

## **Dissertation overview**

The importance of studying the pathogenesis of COPD and ILD is highlighted by the fact that no current pharmacologic treatment has been shown to prolong the life of patients with these diseases. In this dissertation, I will introduce adenosine signaling and its role in chronic lung disease. In an effort to understand some of the direct consequences of adenosine signaling, I will examine the contribution of osteopontin (OPN) to adenosine dependent lung disease. Results of this investigation displayed that adenosine-dependent upregulations in OPN promote recruitment of neutrophils leading to pathologic destruction of alveolar airways. This work also demonstrates OPN expression in patients with COPD in association with clinical endpoints of disease severity. These findings highlight OPN and adenosine signaling in the continuing pursuit of novel drug targets for the treatment of COPD. In the second half of this dissertation I examined another molecule, cadherin 11 (CDH11), and its specific influence on lung myofibroblasts and pulmonary fibrosis. Findings include CDH11 expression on alveolar macrophages and hyperplastic airway epithelial cells playing a role in CDH11-dependent expression of the profibrotic mediator TGF- $\beta$  and epithelial to mesenchymal transition (EMT). We also demonstrate improved fibrotic endpoints in mice treated with CDH11-blocking antibodies. These results reveal CDH11 as a novel player in regulating macrophage, airway epithelial cell, and myofibroblast biology in the context of pulmonary fibrosis. Further, we introduce CDH11 as a promising drug target for the treatment of pulmonary fibrosis.

# **Chapter 2**

## **Experimental Procedures**

## **Chapter 2 - Experimental procedures**

*Ada*<sup>-/-</sup> mice. *Ada*<sup>-/-</sup> mice were genotyped and generated as previously described (19, 20). Mice homozygous for the *Ada* null allele were designated *Ada*<sup>-/-</sup>, while control mice, designated *ADA*<sup>+</sup>, were heterozygous for the *Ada* null allele. *Ada*<sup>-/-</sup> mice were congenic on a C57BLk/6J background. All comparisons were made amongst *Ada*<sup>+</sup> littermates.

*Opn* knockout (*Opn*<sup>-/-</sup>) mice (21) were acquired from Jackson labs where mice were previously backcrossed fully onto a C57Bl/6 background. *Ada/Opn* double knockout mice (*Ada/Opn*<sup>-/-</sup>) were generated by breeding *Ada*<sup>-/-</sup> mice with *Opn*<sup>-/-</sup> mice. *Ada*<sup>-/-</sup> mice were identified at birth by screening for ADA enzymatic activity in the blood as described previously (22). For alveolarization experiments, endpoints were collected on postnatal day 10. For all other *Ada/Opn*<sup>-/-</sup> studies, *Ada*<sup>-/-</sup> mice were maintained on ADA enzyme therapy from postnatal day 2 until postnatal day 21 (22). Endpoints were collected on postnatal day 37.

*CD44 neutralization experiments.* *Ada*<sup>-/-</sup> mice were on a 129/Sv C57BL/6 mixed background. These mice were maintained on ADA enzyme therapy from postnatal 2 until postnatal 25. Beginning at postnatal day 33, mice were given intraperitoneal (IP) injections of CD44 blocking antibody (Ab) (100 µg in 100 µl, Rat monoclonal KM114, BD Biosciences) or the manufacturer's isotype control Ab every other day until postnatal day 40. Endpoints were collected on postnatal day 41.

*Bleomycin installation.* Eight to twelve week old mice were anesthetized with 250 mg/kg IP avertin and received 50 µl intratracheal sterile saline or bleomycin (Blenoxane, Teva Pharmaceuticals) at 3.5U/kg diluted in sterile saline. All endpoints were examined at day 21 after exposure.

*CDH11 neutralization experiments.* Delivery schedule for CDH11-blocking Abs was based on a previous report of systemic CDH11 neutralization experiments (23). For our purposes, mice were given IT bleomycin as above and treated with a loading dose of 500 µg Ab (clone 23C6, clone 13C2, or isotype control Ab (mouse monoclonal, MOPC 31C clone, Sigma)) resuspended in 100 µL sterile, endotoxin-free PBS at 10 days after bleomycin exposure. Mice were subsequently administered 100 µg Ab in 100 µL PBS every other day until day 20. All endpoints were collected on day 21 (Figure 2.1).

*Mice.* Eight to twelve week old C57BLk/6J female mice used for peritoneal lavage and CDH11 neutralization experiments were purchased from Harlan. Cadherin 11-null (*Cdh11*<sup>-/-</sup>)

mice on the C129 background were previously backcrossed onto the C57/B6 background (23, 24). These studies were reviewed and approved by the University of Texas Health Science

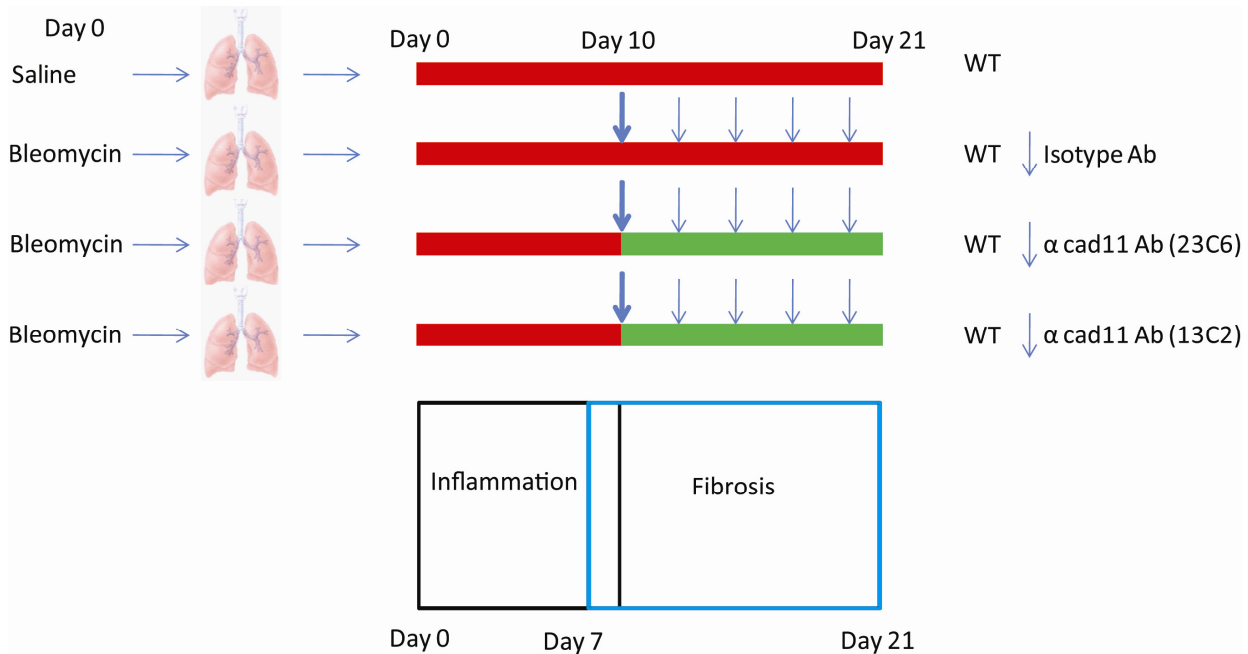


**Figure 2.1 - Bleomycin model and CDH11 treatment strategy**

The intratracheal bleomycin model of pulmonary fibrosis can be divided into two stages: “Inflammation” and “Fibrosis”. The upregulation of profibrotic mediators and appearance of ECM and myofibroblasts begins at day 7 after bleomycin exposure. The CDH11 treatment was designed such that mice would receive CDH11 antibody (blue arrows) after the onset of fibrosis.

Center at the Houston Animal Welfare Committee in Houston, Texas, USA. All mice were housed in ventilated cages equipped with microisolator lids and maintained under strict containment protocols. No evidence of bacterial, parasitic, or fungal infection was found, and serologies on cage littermates were negative for 12 of the most common murine viruses.

*Bronchoalveolar lavage (BAL), airway inflammatory cell counts, and differentials.* Mice were anesthetized with avertin, lungs were lavaged 4 times with 0.3 to 0.4 mL PBS and 1.0 mL of pooled lavage fluid was recovered. Total BAL inflammatory cells were counted with a hemocytometer. BAL samples were spun at 4 °C and cell pellets were spun on microscope slides and stained with Diff-Quick (Dade Behring) for cellular differential determination. BAL cell pellets and supernatants were aliquoted and saved for protein quantification (Sircol collagen assay, Biocolor Assays) (Mouse TGF- $\beta$ , CXCL-1, TIMP-1 Quantikine ELISAs, R&D systems) performed according to manufacturer's instructions.

*Histology, air-space size, and fibrosis assessment.* Mouse lungs were inflated at 25 cm H<sub>2</sub>O pressure and fixed with 10% phosphate buffered formalin. Fixed lungs were dehydrated through ethanol gradient, embedded in paraffin, and 5  $\mu$ m sections were cut. Lung sections were rehydrated through graded ethanol to water and stained with H&E (Thermo Electron Corp) or Masson's trichrome (EM Science) according to manufacturer's instructions. Eight unique, representative digital images were taken from each H&E stained mouse lung section at 20X magnification and alveolar airway size was assessed by mean chord length measurement. A line grid spaced at 10.5  $\mu$ m intervals was overlaid on each image using image analysis software (Image Pro Plus 4.0, Media Cybernetics). The resultant lines were measured and averaged to give mean chord length of the alveolar airways. Fibrosis was quantified using the Ashcroft scoring method (25) on 20 images per H&E-stained mouse lung. Analyses were performed blinded with regard to animal genotype and/or treatment.

*Immunostaining.* Sections were rehydrated, endogenous peroxidases were quenched with 1% hydrogen peroxide, antigen retrieval was performed (Dako), and endogenous avidin and biotin was blocked with the Biotin-Blocking System (Dako). Slides were incubated with primary Abs for  $\alpha$  SMA (1:500 dilution, 4<sup>o</sup> overnight, mouse monoclonal, Sigma-Aldrich), MMP-9 (1:50 dilution, 1 hr room temperature, goat monoclonal, R&D Systems), neutrophil marker (1:200 dilution, overnight 4<sup>o</sup>C, rat anti-mouse allotypic neutrophil marker, AbD Serotec), CD44

(1 µg/ml, 1 hr room temperature, rabbit polyclonal, Abcam), CDH11 (10 µg/ml, overnight 4 °C, mouse monoclonal, invitrogen) human OPN (1:250 dilution, 1 hr room temperature, rabbit polyclonal, Calbiochem). For  $\alpha$  SMA staining, sections were processed with the Mouse on Mouse kit (VectorLabs). All sections were incubated with ABC Elite Streptavidin reagents and appropriate secondary Abs, developed with 3,3'-diaminobenzidine (Sigma-Aldrich) and counterstained with methyl green. Quantification of distal airway neutrophils and MMP-9 positive cells was performed on 20 fields per mouse lung section at 20X magnification. Positive staining cells were identified and counted using software analysis (Image Pro Plus 4.0, Media Cybernetics).

*Immunofluorescence.* Sections were rehydrated and fixed with acetone and methanol. Endogenous fluorescence was quenched with NaBH<sub>4</sub>. Slides were incubated with primary Ab to fibronectin (1:400 dilution, 1 hr room temperature, rabbit polyclonal, Sigma-Aldrich) followed by secondary Ab (1:1000 dilution, 1 hr room temperature, donkey anti-rabbit IgG Alexa fluor 555-red, Invitrogen). Sections were covered with Vectashield anti-fade medium with DAPI (VectorLabs). BAL cell pellets were cytopspun onto microscope slides, allowed to air-dry, and fixed in acetone and methanol. Slides were incubated with primary Abs for mouse CDH11 (5 µg/ml, 1 hr room temperature, clone 23C6 mouse monoclonal), mouse CDH11 (1:100 dilution, 1 hr room temperature, Invitrogen, mouse monoclonal), N cadherin (1:100 dilution, 1 hr room temperature, Invitrogen, mouse monoclonal), and human  $\beta$  catenin (1:100 dilution, 1 hr room temperature, Invitrogen, rabbit polyclonal) followed by secondary Abs (1:1000 dilution, 1 hr room temperature, donkey anti-mouse IgG Cy3, Jackson ImmunoResearch Laboratories) (1:1000, 1 hr room temperature, goat anti-rabbit Alexa flour 488, Invitrogen), and covered with Prolong Gold anti-fade medium with DAPI (Invitrogen). Confocal images on BAL cytopspins were obtained using a TCS SP5 confocal laser microscope (Leica).

*Western blot detection of CDH11.* Protein lysates were prepared from homogenization of frozen tissue in cold lysis buffer (150 mM NaCl, 50 mM Tris, pH 7.4, 1% Triton X-100) containing protease inhibitor cocktail (Roche) in a Polytron homogenizer. Protein concentrations from BAL cell pellets, mouse and human lungs were determined by Bradford assay (Bio-Rad). Equal protein quantities were diluted 1:1 by volume with Laemmli sample buffer (BioRad) and incubated at 95 °C for 5 minutes. Samples were then added to 10% Tris-HCl SDS Ready-Gels (Bio-Rad), separated by electrophoresis, and transferred onto PVDF membranes (Millipore). Membranes were blocked with 5% dehydrated milk and 0.02% sodium azide in TBS/T (1 hour, room temperature), incubated with primary Ab (CDH11, mouse

monoclonal, 1:500, Invitrogen), ( $\alpha$ -tubulin, mouse monoclonal, 1:5000, Sigma-Aldrich) diluted in 0.5% BSA and 0.02% sodium azide in TBS/T at 4 °C overnight, incubated with secondary Abs conjugated to HRP (1:5000, eBiosciences), and detected with ECL reagents (Amersham).

*Analysis of whole lung mRNA.* Mice were anesthetized with avertin and lungs were quickly removed and frozen in liquid nitrogen. RNA was isolated from frozen lung tissue using TRIzol reagent (Invitrogen) according to the manufacturer's instructions. RNA was then DNase (Invitrogen) treated and used for quantitative real time RT-PCR analysis. Primer sequences for uPA: forward 5' CCTACAATGCCACAGACCT 3' and reverse 5' GCTGCTCCACCTCAAACCTTC 3'. For CD44: forward 5' AGAGATCGAGACTCATCCAA 3' and reverse 5' CCCAATCTTCATGTCCACAC 3'. Other primers, probes, and procedures for real time RT-PCR were as described previously (19, 26). Sample reactions were performed on a SmartCycler System (Cepheid). Specific transcript levels for mouse OPN were determined through comparison to a standard curve generated from the PCR amplification of template dilutions or measured in parallel with  $\beta$ -actin and presented as mean %  $\beta$ -actin. Transcripts for human OPN, CXCL1, CCL7, and  $\alpha_1$  procollagen were measured in parallel with 18S rRNA and values are presented as mean %18S rRNA. Transcripts for mouse and human CDH11 obtained with corresponding Taqman probes (Applied Biosystems) and measured in parallel with PPIA and values are presented as mean normalized transcript levels using the comparative Ct method ( $2^{\Delta\Delta C_t}$ ) (27). Remaining transcript levels were calculated using SYBR Green method in SmartCycler Software (version 4.0, Cepheid) and normalized to transcript levels of 18S rRNA in the corresponding sample and are presented as mean normalized transcript levels using the comparative Ct method ( $2^{\Delta\Delta C_t}$ ).

*Analysis of A549 cells.* A549 cells (ATCC) were seeded in 96 well plates and grown overnight in DMEM containing 10% FBS and 1% antibiotics. For siRNA knockdown of *Cdh11*, cells were washed with antibiotic free media and subsequently incubated with Optimem (Invitrogen) with Lipofectamine RNAiMax (Invitrogen) and either non-targeting siRNA or human *Cdh11* siRNA (antisense sequence: 5'-UUUGAAUGGAGUCAUAAGGUU) (Dharmacon RNAi technologies, Thermo) for 48 hours. Cells were then trypsinized and reseeded in antibiotic free medium. Six hours later, cells were serum-starved overnight in DMEM containing 0.1% BSA. Cells were then stimulated with or without TGF- $\beta$  at 10 ng/ml in DMEM + 0.1% BSA for 24 hours. RNA was isolated using Cell to Ct reagents (Ambion) according to manufacturer's instructions. Transcripts for CDH11, COL1A1, N cadherin (*Cdh2*), and E cadherin (*Cdh1*) were obtained with corresponding Taqman probes (Applied Biosystems) and presented as mean fold



change versus control. Imaging of A549 cells was performed with a BX60 inverted phase contrast microscope (Olympus) for determination of cellular morphology.

*In vivo neutrophil migration.* Wild type C57/B6 female mice were anesthetized with isofluorane and pretreated with intraperitoneal (IP) injection of 300  $\mu$ L isotype control Ab,  $\beta_3$  integrin neutralizing Ab (Biolegend), or CD44 neutralizing Ab (BD Pharmingen). After 15 minutes, neutrophil recruitment *in vivo* was assessed with 100  $\mu$ L intraperitoneal (IP) administration of PBS alone or containing BSA, CXCL-1 (R&D Systems), OPN (R&D Systems), or BAL fluid isolated from one of four mouse genotypes at postnatal day 37 as described above. After 3.5-4.5 hours, mice were killed and 2 mL of PBS was used to lavage the peritoneal cavity to recover peritoneal inflammatory cells. Cellular differentials were determined on cell suspensions cytopspun on microscope slides and stained with Diff-Quick (Dade-Behring).

*Human lung samples.* Deidentified human lung tissue samples were obtained from the Lung Tissue Research Consortium (Bethesda, MD, USA). Patients were classified as at risk COPD (Gold Stage 0), severe COPD (Gold Stage 4), Mild IPF, and severe IPF according to spirometry, pathological specimen and high resolution CT scan. Mild/at risk COPD/IPF patients were used as controls in comparison to corresponding severe COPD/IPF patients. Quantification of OPN positive staining cells in each group was performed on 12 images of the alveolar airways per human lung section at 10X magnification. Positive staining cells were identified and counted using software analysis (Image Pro Plus 4.0, Media Cybernetics).

*Whole mount immunohistochemistry for CD31 on tracheas.* Methods for tracheal whole mount immunohistochemistry were as previously described (28). Briefly, mice were anesthetized, tracheas were excised, surrounding soft tissue was removed, and tracheas were pinned flat onto silicone polymer. Tracheas were subsequently fixed with zync fixative (BD Pharmingen) for 72 hours at 4  $^{\circ}$ C. Following fixation, tracheas were washed, permeabilized with 1% Triton X-100, and endogenous peroxidases were quenched with 0.06% hydrogen peroxide. Immunohistochemistry for CD31 (1:250 dilution, room temperature overnight, rat anti-mouse, BD Pharmingen) was performed according to the manufacturer's guidelines with anti-rat Ig horseradish peroxidase detection kit (BD Pharmingen). Tracheas were dehydrated and mounted onto microscope slides with Permount (Fisher Scientific). Number of CD31 positive vessels traversing tracheal cartilage rings was determined to estimate angiogenesis present in the lung (29). This value was determined with placement of a line of known length

parallel to the long axis of a cartilage ring and counting the number of vessels intersecting the line.

*Mucus quantitation.* Mouse lung sections collected and prepared as above were stained with Periodic Acid-Schiff and counterstained with Alcian Blue. Quantification of mucus production was obtained by mucus index scoring (Image Pro Plus 4.0, Media Cybernetics) (30) determined by dividing ((area of PAS staining) x (mean PAS intensity)) by the total airway epithelium area.

*Peripheral blood differentials.* Mice were anesthetized with avertin and peripheral blood was collected into tubes containing 0.5M EDTA from subaxillary arteries, bilaterally. Red blood cells were removed through dextran sedimentation and hypotonic lysis (dH<sub>2</sub>O followed by 0.6 M KCl). Absolute leukocyte count (per mL) was determined by hemocytometer. Isolated leukocytes were cytopun onto microscope slides, stained with Diff-Quick, and differentials were determined by light microscopy.

*Statistics.* Values are expressed as mean  $\pm$  SEM. As appropriate, groups were compared by analysis of variance (ANOVA) and follow-up comparisons between groups were conducted using 2-tailed Student's t test. The correlation of OPN immunostaining and clinical endpoints was determined by Pearson correlation. The P value of  $\leq 0.05$  was considered to be significant.

# **Chapter 3**

**Osteopontin and adenosine  
contribute to features COPD**

## **Chapter 3 - Introduction**

### **COPD**

COPD is a chronic condition affecting the lung characterized by progressive dyspnea secondary to collapse, obstruction, and loss of elastic recoil of large airways, and destruction of smaller alveolar air-spaces (4). Many inciting factors have been associated with the development of COPD including cigarette smoke, infections, and environmental agents/allergens. These various insults converge on the induction of cell stress and injury. Adenosine is a nucleoside signaling molecule generated in excess at these sites of tissue damage. Not surprisingly, adenosine levels are elevated in bronchoalveolar lavage (BAL) fluid from patients with COPD (31). Furthermore, bronchoconstriction, a pathologic feature of COPD, is elicited by exogenous adenosine administration in patients with obstructive airway disease, but not in normal patients (32). This suggests altered adenosine signaling exists in patients with COPD. Additionally, adenosine signaling has been shown to influence the processes of inflammation, angiogenesis, and fibrosis (33-35). These are primary histopathologic features of COPD; thus adenosine signaling represents an important area of study for the pathogenesis of this disease.

### **Adenosine**

Adenosine is a nucleoside signaling molecule produced at sites of tissue stress or injury (Figure 3.1). Under normal conditions, circulating concentrations of adenosine vary from 40-600 nM (36). In these scenarios, the majority of adenosine is generated as a result of increased intracellular generation from ATP leading to passive transfer through equilibrative transporter proteins (37). In contrast, in the setting of acute cellular stress, the predominant origin of adenosine arises from the dephosphorylation of released adenine nucleotides (38, 39). ATP and ADP can escape cells through transporters present on the plasma membrane (40-45), via fusion of vesicles, or from degranulating inflammatory cells. These nucleotides are dephosphorylated to AMP by the ectonucleoside triphosphate diphosphohydrolase CD39 (46). AMP is subsequently dephosphorylated to adenosine by the ecto-5'-nucleotidase CD73 (47). These enzymes are upregulated following injury leading to enhanced adenosine generation (38, 39).

Adenosine signaling has diverse effects on human physiology and pathophysiology and is centered on a wide tissue distribution of adenosine receptors and the variety of signaling pathways to which they are coupled. Four unique, seven membrane spanning, G protein-

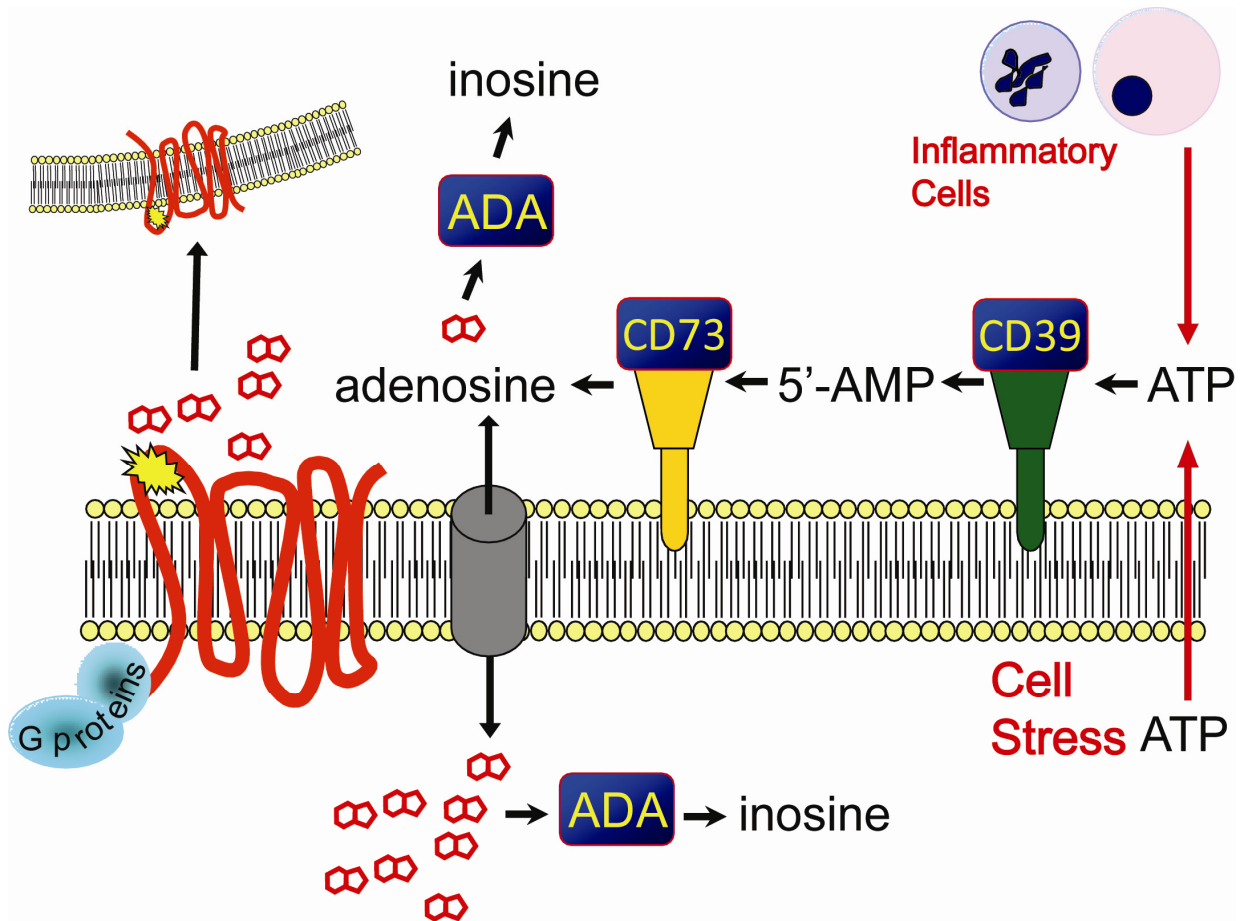


**Figure 3.1 - Generation of extracellular adenosine**

Cellular stress and inflammatory cell infiltration yield the liberation of ATP into the extracellular space. Adenosine is generated via the actions of two extracellular enzymes, CD39 and CD73, present on the cell surface. Adenosine is free to interact with one of four cell surface receptors resulting in changes in many intracellular signaling pathways.

coupled adenosine receptors have been described (48): A<sub>1</sub> receptor (A<sub>1</sub>R), A<sub>2A</sub>R, A<sub>2B</sub>R, and A<sub>3</sub>R. Classically, A<sub>1</sub> and A<sub>3</sub> are coupled to G<sub>ai</sub>-proteins leading to the decreased production of the second messenger cyclic AMP through the inhibition of adenylate cyclase (49, 50). Conversely, A<sub>2A</sub> and A<sub>2B</sub> are frequently coupled to G<sub>os</sub>-proteins resulting in increased cyclic AMP levels via stimulation of adenylate cyclase (49, 50). Additionally, other intracellular pathways involved include G<sub>q</sub> protein-mediated stimulation of phospholipase C and various kinase pathways including MAP kinase, protein kinase C, and phosphoinositide 3 kinase.

Under physiologic conditions, the engagement of adenosine receptors promotes the regulation of a variety of homeostatic functions including heart rate (51, 52) and body temperature (53). Additionally, adenosine signaling mediates a variety of adaptive functions. These include response to pain (54), adaptation to hypoxia (55), and the regulation of blood flow through vasoconstriction (56), vasodilation (57), and platelet aggregation (54).

In addition to homeostatic functions, adenosine has multiple effects on the regulation of immune responses in the setting of pathology. Acute tissue injury such as sepsis or ischemia yields adenosine concentrations reaching 10  $\mu$ M (58). Increased adenosine concentrations in the setting of acute pathology generally access tissue protective and anti-inflammatory pathways through the high affinity A<sub>1</sub> and A<sub>2A</sub> receptors. For example, activation of the A<sub>1</sub> and A<sub>2A</sub> receptors attenuates inflammation in models of ischemia-reperfusion and LPS-induced injury in multiple organs (59-65).

Furthermore, concentrations in excess of 100  $\mu$ M are reported in chronic conditions such as rheumatoid arthritis (66), asthma and COPD (31). Hence, chronic adenosine elevations in persistent inflammatory conditions, particularly chronic lung diseases, have proinflammatory and tissue destructive consequences through engagement of the low affinity A<sub>2B</sub> and A<sub>3</sub> receptors. For example, features of asthma, such as mast cell degranulation (67-69) and eosinophil trafficking (22), are promoted through engagement of the A<sub>3</sub> receptor. Suggested mediators of chronic lung disease are elicited from bronchial smooth muscle cells (22), fibroblasts, and macrophages (70, 71) through engagement of the A<sub>2B</sub> receptor. Furthermore, activation of the A<sub>2B</sub> receptor on fibroblasts induces differentiation into myofibroblasts (72) suggesting a mechanism of adenosine-dependent airway remodeling and fibrosis. Despite these findings, the detailed molecular mechanisms of adenosine-dependent lung injury remain unknown. To address this, *in vivo* studies conducted in a mouse model are a necessary step toward a full understanding of the role of adenosine in lung disease.

### ***Ada*<sup>-/-</sup> mice**

The *Ada*<sup>-/-</sup> mouse is a well-established model designed to investigate the sequelae of increased concentrations of adenosine *in vivo*. Degradation of extracellular adenosine and deoxyadenosine is accomplished through the activity of the enzyme ADA (Figure 3.1). Thus, genetic ablation of *Ada* results in considerable systemic elevations of these substrates which directly promote multi-organ pathology (30). For example, deoxyadenosine accumulation in the spleen and thymus leads to a severe combined immunodeficiency displayed in this model. Most notably, adenosine concentrations in the lungs of *Ada*<sup>-/-</sup> mice correlate with measured levels in lungs of patients with asthma and COPD (31). In parallel with adenosine accumulations, *Ada*<sup>-/-</sup> mice exhibit pulmonary inflammation and histopathologic changes in lung architecture that resemble findings in human lung disease (30). Namely, features consistent with asthma include eosinophilia, mucus metaplasia, and mast cell degranulation. Neutrophilia, activation of alveolar macrophages, and distal air-space enlargement are features consistent with COPD.

*Ada*<sup>-/-</sup> mouse lungs display upregulations of cytokines and mediators commonly elevated in association with asthma and COPD. For example, serum IgE and TH<sub>2</sub> cytokines are increased in *Ada*<sup>-/-</sup> mice (30) and patients with asthma. Similarly, *Ada*<sup>-/-</sup> mice and humans with COPD display increases in chemokines and cytokines that recruit macrophages and neutrophils to the lungs (71, 73). In addition, both exhibit upregulations in mediators of air-space enlargement such as MMPs and cathepsins (71, 73). Grossly, these mice will display labored breathing and dehydration. Thus, findings that adenosine concentrations exceeding the normal physiologic range are associated with pathology suggest that adenosine directly promotes these disease processes.

ADA enzyme replacement therapy utilized to reduce systemic adenosine levels support the suggestion that features of the lung phenotype are a direct consequence of adenosine signaling. Administration of ADA covalently linked to polyethylene glycol (PEG-ADA) to *Ada*<sup>-/-</sup> mice prevents and reverses every aspect of the pulmonary phenotype and maintains the health of the animal indefinitely (30). Other mouse models of lung injury, including transgenic IL-4 and IL-13 mice exhibit elevated adenosine levels concurrent with active lung disease consistent with emphysema and fibrosis. Furthermore, these features were also abolished by lowering adenosine levels with PEG-ADA in these models. These findings reveal an obvious

correlation between adenosine concentrations, lung pathology, and its contribution to overall morbidity.

Additionally, the use of PEG-ADA permits the study of pulmonary fibrosis in *Ada*<sup>-/-</sup> mice (26). Without PEG-ADA these animals die at three weeks of age from presumed respiratory complications before the onset of fibrosis. By administering a tapered regiment of PEG-ADA, adenosine levels will elevate slowly, life spans of mice are prolonged, and pulmonary fibrosis will develop. Lung sections from *Ada*<sup>-/-</sup> mice in this scenario exhibit increased alveolar and peribronchial staining for collagen and myofibroblasts. In parallel, measurable elevations in soluble collagen are present in BAL samples. Finally, *Ada*<sup>-/-</sup> mouse lungs also have upregulations in established profibrotic mediators. These include TGF- $\beta$ , IL-1 $\beta$ , IL-13, MMP-2, osteopontin (OPN), and PAI-1. Concurrent with histological findings, these results display that adenosine signaling accesses profibrotic pathways contributing to the overall chronic pulmonary disease phenotype these mice display.

As with features in this model consistent with COPD and asthma, fibrotic endpoints can be prevented and reversed by maintaining low adenosine concentrations with PEG-ADA (26). Additionally, elevated adenosine levels are present in the standard model of bleomycin-induced fibrosis and all features of this model are prevented and reversed by diminishing adenosine levels with PEG-ADA. Overall, adenosine concentrations are clearly associated with many features of chronic lung disease and these findings underscore the necessity of understanding the role of adenosine in promoting the chronic nature of these pathologic processes.

### **Adenosine receptor signaling in the *Ada*<sup>-/-</sup> model**

Genetic and pharmacologic targeting of adenosine receptors in the *Ada*<sup>-/-</sup> model suggest that adenosine signaling may directly influence changes that lead to the development of chronic lung disease features. Increased expression of the A<sub>3</sub>R is localized to key effector cells mediating features of asthma including eosinophils, mast cells, and bronchial epithelial cells (22, 69). Genetic and pharmacologic targeting of the A<sub>3</sub>R in *Ada*<sup>-/-</sup> mice displayed diminished mast cell degranulation, eosinophil trafficking, and mucus production. Additionally, levels of TH<sub>2</sub> cytokines commonly elevated in allergic airway disease were reduced in these studies. These findings highlight the pathologic role of A<sub>3</sub>R signaling.

Similar to roles in acute tissue injury in other models, other work in the *Ada*<sup>-/-</sup> model shows a protective role of adenosine signaling through the A<sub>1</sub> and A<sub>2A</sub> receptors. Specifically,



genetic knockout of these receptors results in enhanced pulmonary inflammation, mucus production, and pathologic air-space enlargement in association with increases in proinflammatory cytokines and mediators of air-space enlargement (19, 28). In contrast, similar to the pathologic role of the A<sub>3</sub>R, most recent work in the *Ada*<sup>-/-</sup> model demonstrates that these features are promoted by A<sub>2B</sub>R signaling. Selective antagonism of the A<sub>2B</sub>R in *Ada*<sup>-/-</sup> mice prevented features of emphysema including influx and activation of macrophages and neutrophils, air-space enlargement, and upregulations in proinflammatory cytokines and mediators of air-space enlargement. Additionally, features of pulmonary fibrosis are also regulated by A<sub>2B</sub>R signaling. Namely, treatment with the selective A<sub>2B</sub>R antagonist yields a reduction in distal airway collagen and  $\alpha$  SMA in addition to a reduction in the profibrotic mediators TGF- $\beta$ , PAI-1, and OPN (71).

In summary, these results suggest that the A<sub>2A</sub>R and A<sub>1</sub>R promote tissue protection and the A<sub>2B</sub>R and A<sub>3</sub>R are playing a pathologic role (Figure 3.2). These results displayed in *Ada*<sup>-/-</sup> mice support the suggested benefit of selective adenosine receptor agonists and antagonists in the treatment of chronic lung diseases. This highlights the importance of understanding the consequences of adenosine receptor signaling in humans and other animal models of lung disease.

### ***Ada*<sup>-/-</sup> mice, the A<sub>2B</sub> receptor, and OPN**

Despite the clear association of adenosine levels and lung pathology, the mechanisms of adenosine-dependent lung injury are incompletely defined. To identify pivotal mediators in the *Ada*<sup>-/-</sup> model, gene array profiling was performed in comparison to *Ada*-competent (*Ada*<sup>+</sup>) littermates (73). Results of this study demonstrated that OPN was the most highly upregulated gene and that its expression was lowered to baseline by administration of PEG-ADA. Subsequent studies in *Ada*<sup>-/-</sup> mice display adenosine-dependent OPN expression in alveolar macrophages during active disease (71). In this study, systemic pharmacologic neutralization of the A<sub>2B</sub>R prevented all aspects of the pulmonary phenotype in *Ada*<sup>-/-</sup> mice and concurrently reduced expression of OPN in alveolar macrophages. Follow-up studies confirmed increased expression of OPN in lungs of *Ada*<sup>-/-</sup> mice (Figure 3.3A, B), displayed elevated levels of OPN in BAL fluid (Figure 3.3C), and confirmed A<sub>2B</sub>R-dependent expression of OPN in alveolar macrophages (Figure 3.3D, E). These findings suggest that adenosine signaling through the A<sub>2B</sub>R regulates the expression of OPN on alveolar macrophages. As discussed in detail later in this chapter, many recent studies in mouse models and humans have showcased OPN as a

major mediator of lung injury. Therefore, many of the pathologic features of A<sub>2B</sub>R signaling displayed in the *Ada*<sup>-/-</sup> model may be a consequence of A<sub>2B</sub>R-dependent upregulations in OPN.

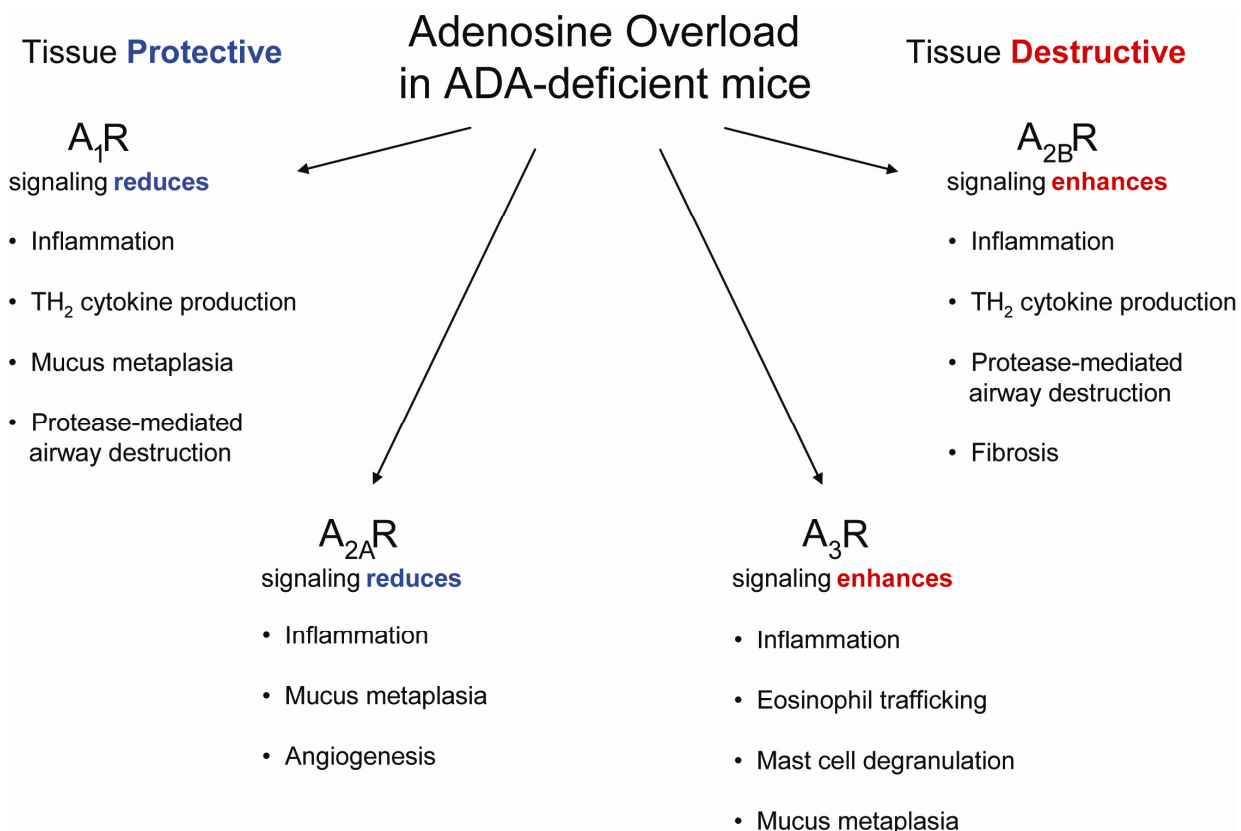


**Figure 3.2 - Adenosine receptor activities in the lungs of *Ada*<sup>-/-</sup> mice**

Genetic and pharmacologic studies in the *Ada*<sup>-/-</sup> model suggest that adenosine receptor signaling influences both tissue-protective and tissue-destructive pathways in the lungs.

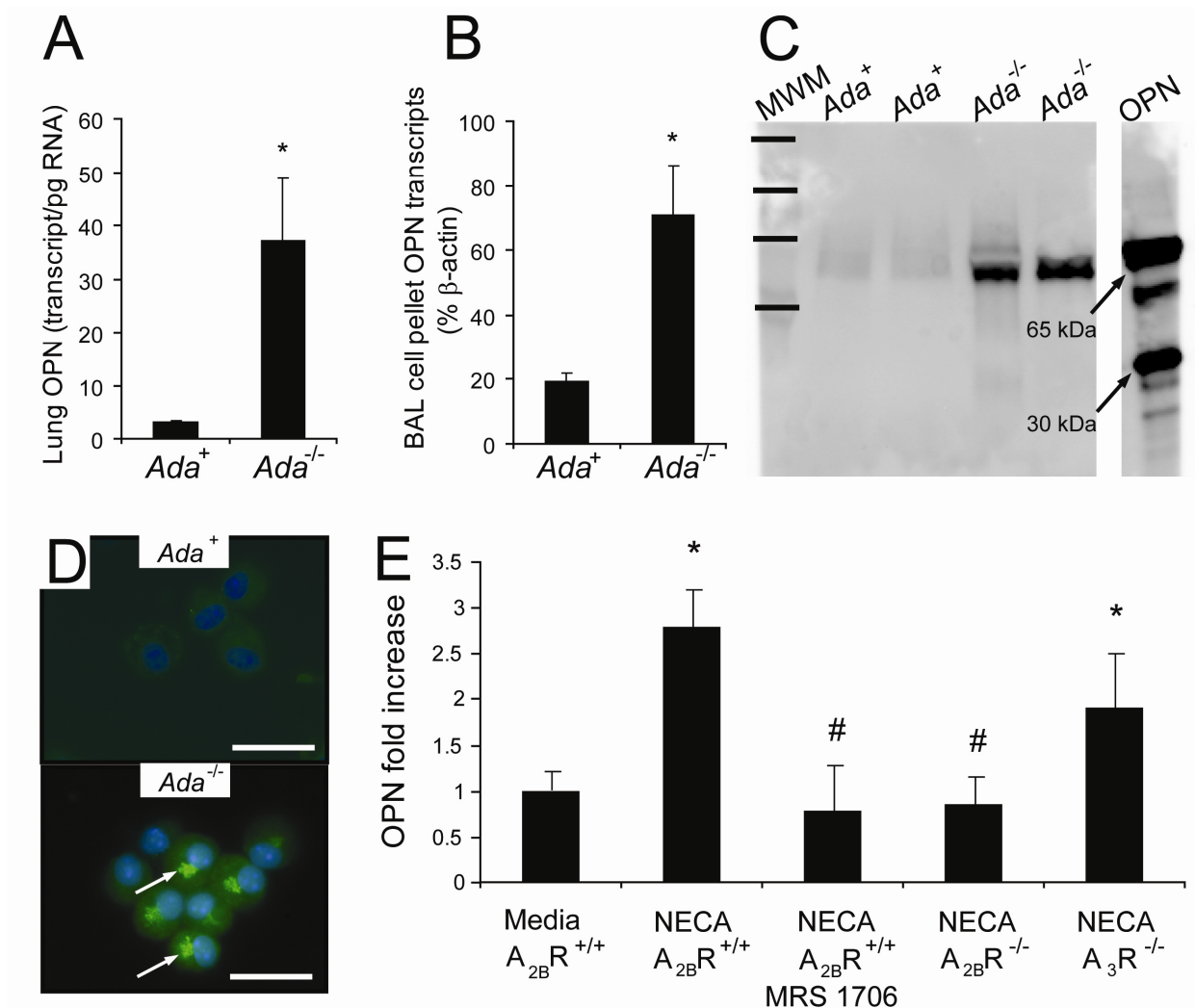


**Figure 3.3 - *A*<sub>2B</sub>*R*-dependent OPN expression in alveolar macrophages of *Ada*<sup>-/-</sup> mice**

Quantitative RT-PCR measuring OPN transcripts in RNA extracts from (A) whole lung and (B) BAL cell pellets. For (A), data are presented as mean transcripts per picogram RNA  $\pm$  SEM.  $n = 4$  mice. For (B), data are presented as mean transcripts as a percent of  $\beta$ -actin  $\pm$  SEM.  $n = 5$  mice. \* $P \leq 0.05$  versus *Ada*<sup>+</sup> mice. (C) Western blot of secreted OPN in BAL fluid. (Left) MWM, (Right) recombinant OPN showing full length (65 kDa) and cleaved (30 kDa) protein. (D) Immunofluorescence detection of OPN (green) in primary alveolar macrophages isolated from BAL fluid of *Ada*<sup>+</sup> and *Ada*<sup>-/-</sup> mice. Compartmentalized localization of OPN (arrow). Scale bars: 50  $\mu$ m. (E) Primary alveolar macrophages isolated from *Ada*<sup>+</sup> or *A*<sub>2B</sub>*R*<sup>-/-</sup> mouse lungs incubated with the non-specific adenosine receptor agonist, NECA and/or the selective *A*<sub>2B</sub>*R* antagonist, MRS 1706. Data are presented as normalized mean fold change  $\pm$  SEM. \* $P \leq 0.05$  versus media *A*<sub>2B</sub>*R*<sup>+/+</sup> macrophages; #  $P \leq 0.05$  versus NECA *A*<sub>2B</sub>*R*<sup>+/+</sup> macrophages.

Experiments performed by Janci C. Lindsay.

## **Osteopontin**

The manner in which OPN entered the scientific literature conveys its diverse, widely-expressed, multifunctional nature. Its primary structure was originally discovered in the late 1970s as a protein secreted from malignant tumors, but was twice independently discovered as a protein isolated from bone extracellular matrix (74) and activated T cells (75). OPN functions in a variety of physiologic and pathologic processes including bone remodeling, cancer, immunity and inflammation. These processes can be influenced through changes in gene expression, alternate splicing, and post-translational modifications (Figure 3.4) such as glycosylation, phosphorylation, and proteolytic cleavage by thrombin and MMPs (76, 77).

OPN is a mediator of cell adhesion and migration through its interactions with various integrin receptors. The primary protein sequence of OPN (Figure 3.4) includes an Arg-Gly-Asp (RGD) domain common to many ECM proteins which mediates adhesion to various integrin receptors. Adjacent to the RGD domain is a separate SVVYGLR sequence (Figure 3.4) that mediates cellular adhesion via many integrins including  $\alpha_9\beta_1$  and  $\alpha_4\beta_1$  (78, 79). Of these OPN-integrin interactions, binding with integrin  $\alpha_v\beta_3$  has been shown to promote cellular migration. OPN- $\alpha_v\beta_3$ -dependent cellular migration has been described in smooth muscle cells (80), endothelial cells (81), alveolar epithelial cells (82), tumor cells (83), and macrophages (84). Additionally, OPN, through non-RGD and SVVYGLR-containing domains, interacts with variants of the hyaluronic acid receptor CD44. These interactions promote cell migration in various cell types including tumor cells (83, 85), lymphocytes, fibroblasts (75, 82, 86) and macrophages (87). Thus,  $\alpha_v\beta_3$  integrin and CD44 are considered the putative OPN receptors.

## **Osteopontin in cancer**

In addition to promoting cellular migration of tumor cells through interactions with CD44 and  $\alpha_v\beta_3$ , OPN interactions with these receptors have been shown to promote malignancy and metastasis. Several studies in multiple forms of cancer cite OPN- $\alpha_v\beta_3$ -dependent angiogenesis as a factor in tumor growth and metastatic potential (76, 81). Furthermore, the presence and activation of matrix degrading proteases facilitates the migration and metastasis of tumor cells. Studies in prostate cancer and melanoma have demonstrated OPN promotes regulation and activation of multiple proteases through interactions with CD44 and  $\alpha_v\beta_3$  (88-90). Thus, OPN directly influences three independent mechanisms facilitating malignancy and metastasis.

Importantly, dysregulation of these three processes, cell migration, extracellular matrix turnover, and angiogenesis, are major mechanisms in the pathogenesis of chronic lung

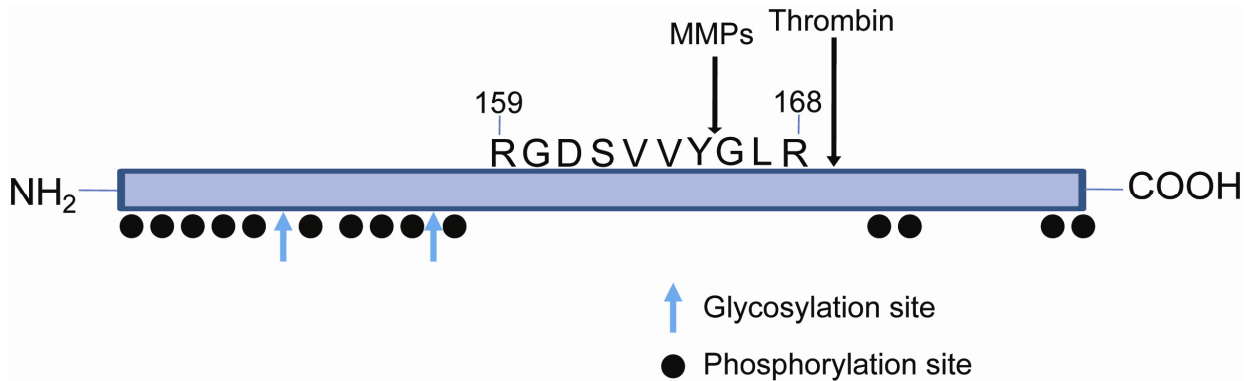


**Figure 3.4 - Primary sequence and post-translational modification sites of osteopontin**

Schematic representation of the protein sequence of human OPN depicting RGD, SVVYGLR functional domains, and post-translational modification sites (proteolytic cleavage, glycosylation and phosphorylation).

disease. Through these studies in cancer, it follows that OPN has the potential to be an important mediator of chronic lung diseases.

### **OPN as a modulator of immunity in human disease**

OPN interactions with the two putative OPN receptors modify immune responses that are pivotal in the pathogenesis of human disease outside the cancer field. Classically, OPN is a known regulator of TH1 cytokine profiles. Specifically, OPN binding  $\alpha_v\beta_3$  yields IL-12 expression from macrophages and, through interaction with CD44 inhibits the production of IL-10 (84). OPN- $\alpha_v\beta_3$  interaction also upregulates IFN- $\gamma$  expression in natural killer T-Cells (91). These features are central in the role of OPN in granulomatous lung diseases including tuberculosis, silicosis, and sarcoidosis (92-94). In addition, OPN-dependent TH1 linked responses are demonstrated in a variety of *in vivo* models. Namely, *Opn*<sup>-/-</sup> mice display diminished immunity to viruses (84) and are protected from experimental autoimmune encephalomyelitis (95) and keratitis (84). In contrast, it was recently reported that OPN also influences TH2 cytokine response patterns (96). This study demonstrated that OPN, through regulation of TH2 cytokine expression from dendritic cells, has an important role in allergic airway disease. These results demonstrate the wide capacity of OPN to affect conditions to promote human disease, including lung disease.

### **OPN in lung disease**

The aforementioned studies facilitated the investigation of OPN in chronic forms of lung pathology. Microarray studies in patients with IPF show upregulation of OPN when compared to normal patients (82). Furthermore, OPN<sup>-/-</sup> mice are protected from pulmonary fibrosis in the standard model of intratracheal bleomycin installation (97, 98). Despite the fact that OPN has been extensively associated with the development of pulmonary fibrosis in patients and animal models, the mechanisms of OPN-driven fibrosis have not been elucidated.

The role of OPN in lung pathology has expanded recently to include other diseases such as acute respiratory distress syndrome (99) and bronchiolitis obliterans (100). These conditions display inflammation and protease dependent destruction and remodeling of the alveolar air-spaces. These pathologic features exist in a more chronic form known as emphysema and the role of OPN in emphysema has received limited attention. However, one study demonstrated elevated OPN expression in alveolar macrophages of smokers and



correlated OPN expression levels with the degree of airway obstruction in these patients (101). Other studies in patients and animal models of emphysema (102-105), including the *Ada*<sup>-/-</sup> model (71), link the activity of certain MMPs with the development of air-space destruction. As mentioned previously, *in vitro* studies of tumor cells demonstrate OPN-dependent activation and expression of MMPs (88, 89), which suggest a potential mechanism of OPN-mediated air-space enlargement.

Associations of OPN and these chronic lung diseases are consistent with studies in cancer showing OPN can influence cell migration, angiogenesis, and matrix degrading proteases. Furthermore, these studies are supported by findings in the *Ada*<sup>-/-</sup> model that display upregulations in OPN during active pulmonary disease consisting of inflammation, air-space enlargement, and fibrosis. Taken together, these studies led to the development of the **hypothesis that OPN contributes to pulmonary phenotypic features in *Ada*<sup>-/-</sup> mice.**

To investigate this, *Ada/Opn*<sup>-/-</sup> mice were generated and their pulmonary phenotype was assessed in parallel with *Ada*<sup>-/-</sup> mice. Results indicate that the genetic removal of *Opn* in *Ada*<sup>-/-</sup> mice leads to reduced histopathologic and biochemical features of pulmonary inflammation and emphysema. In addition, results demonstrate novel OPN interactions on neutrophils offering a mechanism for increased protease concentrations within alveolar air-spaces. Furthermore, these studies demonstrate that OPN is not required for the development of pulmonary fibrosis in this model but influences select mediators and features of the phenotype. Finally, OPN expression is increased in distal air-spaces of lung samples obtained from patients with COPD. Thus, OPN may represent a novel drug target and/or clinical indicator of COPD.

## **Chapter 3 - Results**

### **Histopathology in *Ada/Opn*<sup>-/-</sup> mice**

OPN is suggested to contribute to pathology in animal models (97, 98, 106) and humans (82) with chronic lung disease. To determine the contribution of OPN to the *Ada*<sup>-/-</sup> pulmonary phenotype, *Ada/Opn*<sup>-/-</sup> mice were generated and compared in parallel with *Ada*<sup>-/-</sup> mice. *Ada*<sup>-/-</sup> mice were treated with PEG-ADA from birth until postnatal day 21 to prevent defects in lung development. All pulmonary endpoints were assessed 16 days after cessation of PEG-ADA treatment at postnatal day 37, a stage when adenosine levels are elevated in association with severe pulmonary inflammation and damage (71). Examination of H&E stained lung sections demonstrated no discernable difference in pulmonary histology between *Ada*<sup>+</sup> and *Opn*<sup>-/-</sup> mice (Figure 3.5). *Ada*<sup>-/-</sup> mice exhibited characteristic increases in pulmonary inflammation and destruction of the alveolar air-spaces. In contrast, *Ada/Opn*<sup>-/-</sup> mice showed reduced pulmonary inflammation and distal air-space destruction. Overall, these findings suggest that OPN contributes to histopathologic features of *Ada*<sup>-/-</sup> mice.

### **Quantification of pulmonary inflammation in *Ada/Opn*<sup>-/-</sup> mice**

The characteristic inflammatory cell infiltrate in lungs of *Ada*<sup>-/-</sup> mice includes macrophages, neutrophils and lymphocytes (30, 71). To confirm histologic findings of reduced pulmonary inflammation in *Ada/Opn*<sup>-/-</sup> mice, inflammatory cells were quantified by counting total cells recovered in BAL fluid with a hemocytometer. Results showed characteristic increases in total inflammatory cells in *Ada*<sup>-/-</sup> versus *Ada*<sup>+</sup> mice, and a significant reduction between *Ada/Opn*<sup>-/-</sup> and *Ada*<sup>-/-</sup> mice (Figure 3.6A). Analysis of BAL cellular differentials displayed significant reductions in neutrophils and lymphocytes (Figure 3.6C, D). These results suggest that OPN contributes to pulmonary inflammation in *Ada*<sup>-/-</sup> mice.

### **OPN contributes to alveolar air-space enlargement in *Ada*<sup>-/-</sup> mice**

*Ada*<sup>-/-</sup> mice exhibit histopathologic features resembling COPD in parallel with upregulations in OPN (71) in alveolar macrophages. In addition, alveolar macrophages isolated from smokers display upregulations in OPN (101). To investigate OPN-dependent emphysematous changes, alveolar air-space size was quantified in H&E stained lung sections from *Ada*<sup>-/-</sup> and *Ada/Opn*<sup>-/-</sup> mice utilizing mean chord length calculations. Results of this

analysis (Figure 3.7) showed typical increases in average distal air-space size of *Ada*<sup>-/-</sup> versus *Ada*<sup>+</sup> mice. Furthermore, *Ada*<sup>-/-</sup> mice without *Opn* had dramatically reduced average size of

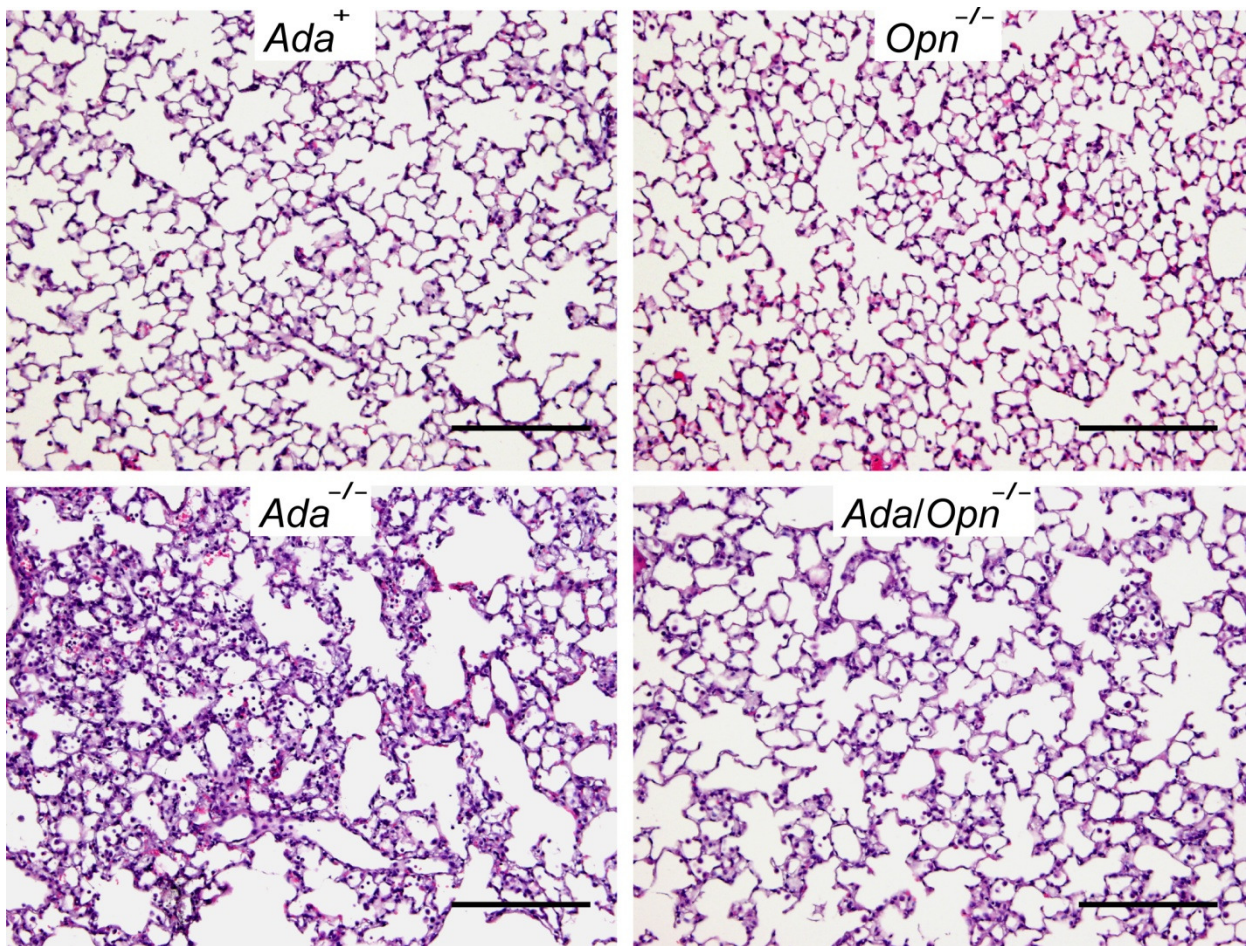


**Figure 3.5 - Histopathology associated with genetic removal of *Opn* in *Ada*<sup>-/-</sup> mice**

Lungs isolated from *Ada*<sup>+</sup>, *Opn*<sup>-/-</sup>, *Ada*<sup>-/-</sup>, and *Ada/Opn*<sup>-/-</sup> mice at postnatal day 37 were processed for sectioning and H&E staining. Displayed sections are representative of 9-12 mice from each genotype. Scale bars: 200 μm.

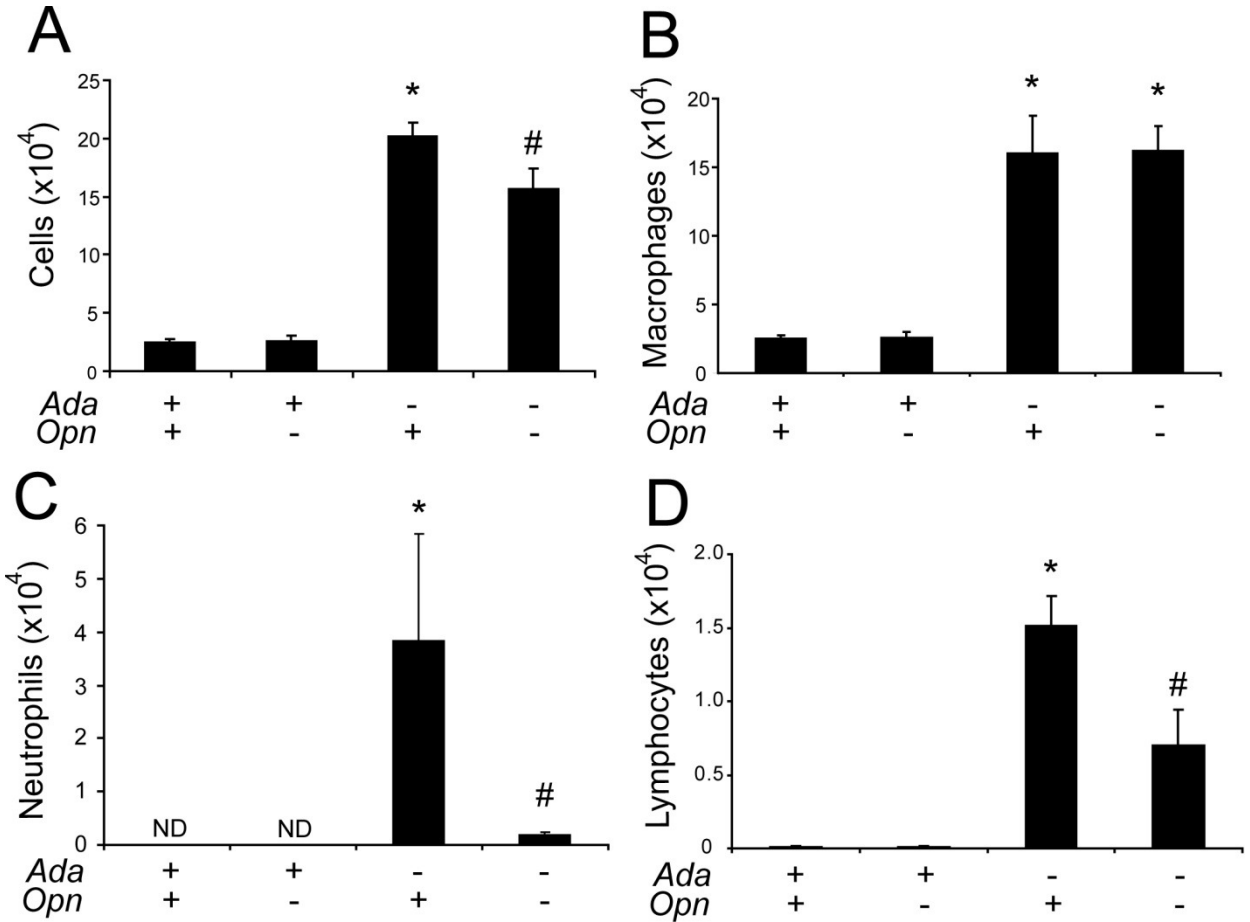


**Figure 3.6 - Airway inflammatory cells in *Ada*<sup>-/-</sup> and *Ada/Opn*<sup>-/-</sup> mice**

(A) BAL fluid was collected at postnatal day 37 and total inflammatory cells were counted. (B, C, and D) BAL cells were cytospun and stained with Diff-Quick for the determination of cellular differentials. Values given are mean cell counts  $\pm$  SEM. \* $P \leq 0.05$  versus *Ada*<sup>+</sup> mice; # $P \leq 0.05$  versus *Ada*<sup>-/-</sup> mice.  $n = 4$  (*Ada*<sup>+</sup> and *Opn*<sup>-/-</sup>),  $n = 7$  (*Ada*<sup>-/-</sup> and *Ada/Opn*<sup>-/-</sup>).



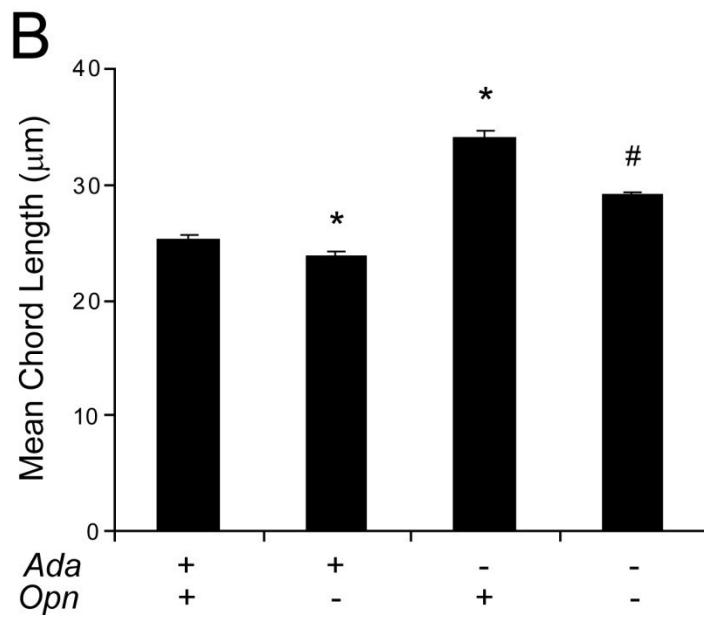
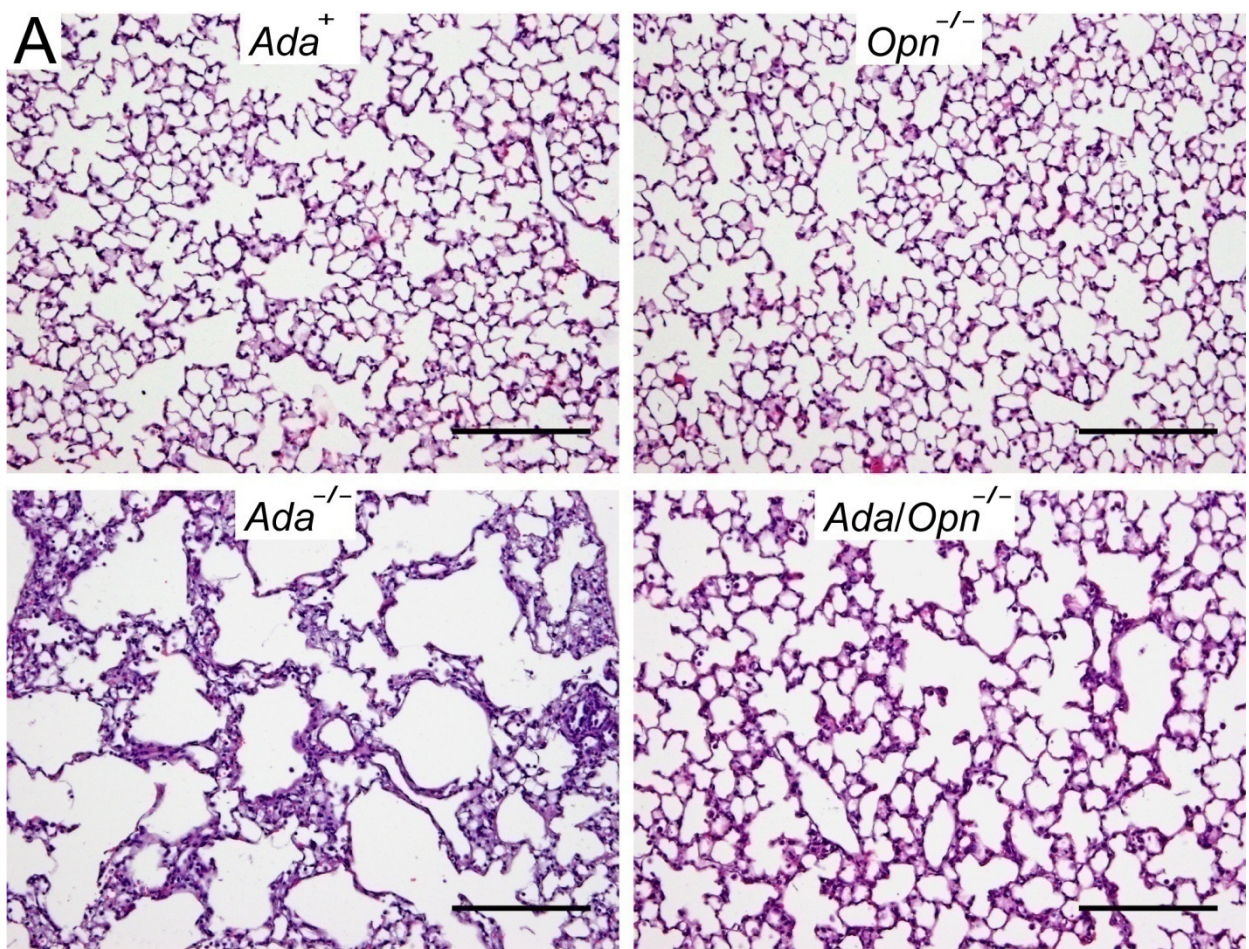


**Figure 3.7 - Alveolar air-space size in *Ada*<sup>-/-</sup> and *Ada/Opn*<sup>-/-</sup> mice**

(A) Lungs from *Ada*<sup>+</sup>, *Opn*<sup>-/-</sup>, *Ada*<sup>-/-</sup>, and *Ada/Opn*<sup>-/-</sup> mice at postnatal day 37. Scale bars: 200 μm. (B) Average alveolar air-space size was determined using Image-Pro analysis software on 8 images at 20X magnification per mouse lung. Values are given as mean cord lengths in μm ± SEM. \*P ≤ 0.05 versus *Ada*<sup>+</sup> mice; #P ≤ 0.05 versus *Ada*<sup>-/-</sup> mice. Displayed images are representative of n = 6 mice (*Ada*<sup>+</sup> and *Opn*<sup>-/-</sup>); n = 8 mice (*Ada*<sup>-/-</sup> and *Ada/Opn*<sup>-/-</sup>).

alveolar air-spaces suggesting that OPN contributes to the process of distal air-space destruction and enlargement in the *Ada*<sup>-/-</sup> model.

### **OPN increases mediators of air-space enlargement**

Matrix metalloproteases (MMPs) are heavily regarded as mediators of the process of alveolar air-space destruction leading to emphysema in patients and animal models (102-105). Multiple *in vitro* studies in cancer demonstrate that OPN increases MMP-9 activity (88-90). A previous study in the *Ada*<sup>-/-</sup> model demonstrates increases in OPN concurrent with upregulations of MMP-9, MMP-12, and the corresponding tissue inhibitor of MMPs, TIMP-1 (71). Thus, the influence of OPN on MMP expression in the *Ada*<sup>-/-</sup> model was investigated. Transcript levels of MMP-9, MMP-12, and TIMP-1 were significantly elevated in the lungs of *Ada*<sup>-/-</sup> mice (Figure 3.8). Expression of MMP-9 and TIMP-1 was significantly reduced in lungs of *Ada/Opn*<sup>-/-</sup> mice, but MMP-12 expression remained elevated. Quantification of MMP-9 immunostaining in lung sections confirmed increased levels in the lungs of *Ada*<sup>-/-</sup> mice and significant reductions in the lungs of *Ada/Opn*<sup>-/-</sup> mice (Figure 3.9B, D). These findings suggest OPN-dependent increases in MMP-9 as a mechanism of air-space enlargement.

### **OPN-dependent *in vivo* neutrophil recruitment**

Neutrophils are characteristically elevated in the lungs of *Ada*<sup>-/-</sup> mice (71) and patients with COPD (107, 108). Also, neutrophils are a significant source of destructive MMPs and serine proteases thought to contribute to the pathogenesis of COPD (105). Immunostaining for a neutrophil marker in lungs of *Ada*<sup>-/-</sup> mice displays extensive staining within the alveolar air-spaces and interstitium (Figure 3.9A), a similar pattern shown in MMP-9 immunostaining (Figure 3.9B). Quantification of staining in these sections confirms decreased neutrophils and MMP-9 protein in the alveolar air-spaces of *Ada/Opn*<sup>-/-</sup> versus *Ada*<sup>-/-</sup> mice (Figure 3.9C, D).

Many neutrophil chemotactic cytokines are upregulated in the BAL fluid of *Ada*<sup>-/-</sup> mice (71). Several studies site cytokine-like properties of OPN for numerous cell types (75) including neutrophils (109). Thus, we sought to investigate the relative contribution of OPN present in BAL fluid of *Ada*<sup>-/-</sup> mice (Figure 3.3C) to *in vivo* neutrophil chemotaxis. Intraperitoneal (IP) administration of OPN resulted in dose-dependent increases in the number of neutrophils recovered from peritoneal washes (Figure 3.10A). Similarly, BAL fluid isolated from *Ada*<sup>-/-</sup> and *Ada/Opn*<sup>-/-</sup> mice was administered IP and results demonstrated significantly fewer neutrophils recruited in the absence of OPN (Figure 3.10B).

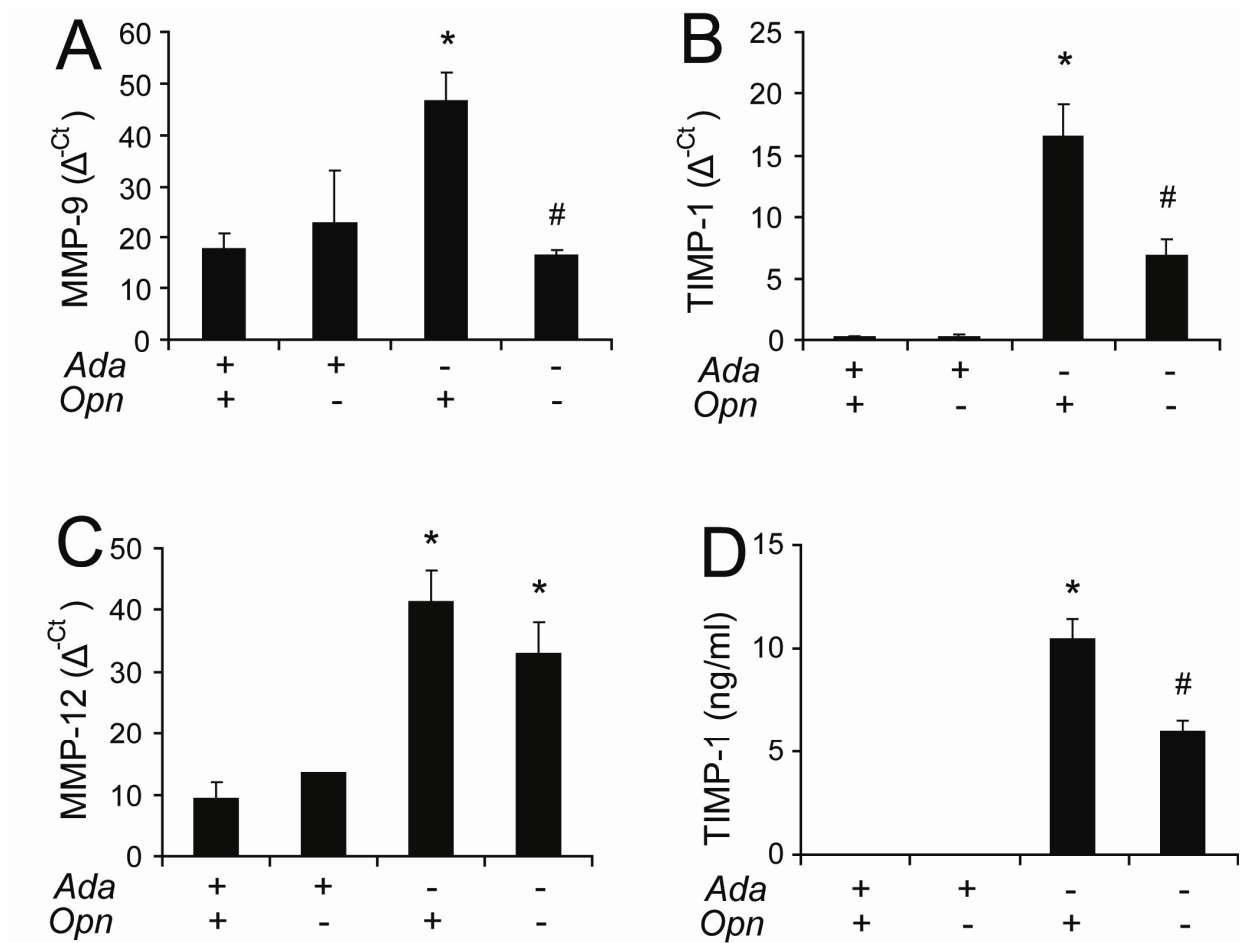


**Figure 3.8 - OPN-dependent regulation of air-space enlargement mediators**

Transcript levels of MMP-9, MMP-12, and TIMP-1 measured in whole-lung extracts from postnatal day 37 mice using quantitative RT-PCR. Transcript levels are shown for (A) MMP-9, (B) TIMP-1, and (C) MMP-12. Transcripts were measured in parallel with 18S rRNA and values are presented as mean normalized transcript levels ( $\Delta^{-Ct}$ )  $\pm$  SEM.  $n = 6$  mice ( $Ada^{-/-}$  and  $Ada/Opn^{-/-}$ );  $n = 3$  mice ( $Ada^{+}$  and  $Opn^{-/-}$ ). (D) TIMP-1 activity in airways was determined with specific ELISA (R&D Systems) on BAL fluid collected from mouse lungs. Data are mean  $\pm$  SEM.  $n = 7$  mice ( $Ada^{-/-}$  and  $Ada/Opn^{-/-}$ );  $n = 3$  mice ( $Ada^{+}$  and  $Opn^{-/-}$ ). \* $P \leq 0.05$  versus  $Ada^{+}$  mice; # $P \leq 0.05$  versus  $Ada^{-/-}$ .



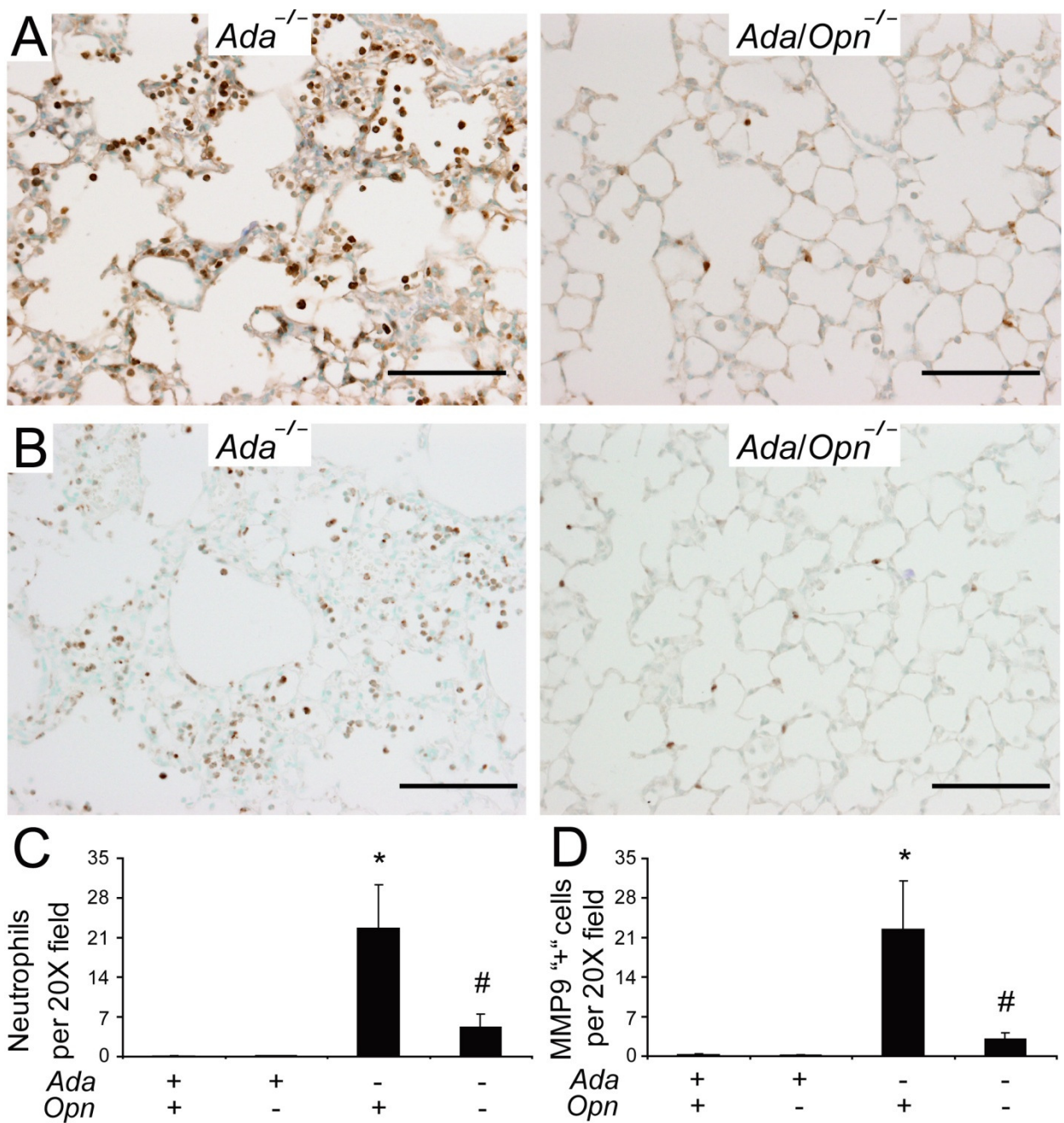


**Figure 3.9 - Lung neutrophil and MMP-9 immunolocalization**

Lung sections from *Ada*<sup>-/-</sup> and *Ada/Opn*<sup>-/-</sup> mice at postnatal day 37 were stained with (A) neutrophil specific antibody and (B) MMP-9 antibody. Scale bars: 100  $\mu$ m. (C) Neutrophils and (D) MMP-9 positive cells in lung tissue were identified and counted using Image Pro analysis software on 20 images per mouse lung. Data presented as mean number of positive staining



cells per 20X field  $\pm$  SEM. \* $P \leq 0.05$  versus  $Ada^+$ ; # $P \leq 0.05$  versus  $Ada^{-/-}$  mice.  $n = 6$  mice ( $Ada^{-/-}$  and  $Ada/Opn^{-/-}$ );  $n = 3$  mice ( $Ada^+$  and  $Opn^{-/-}$ ).

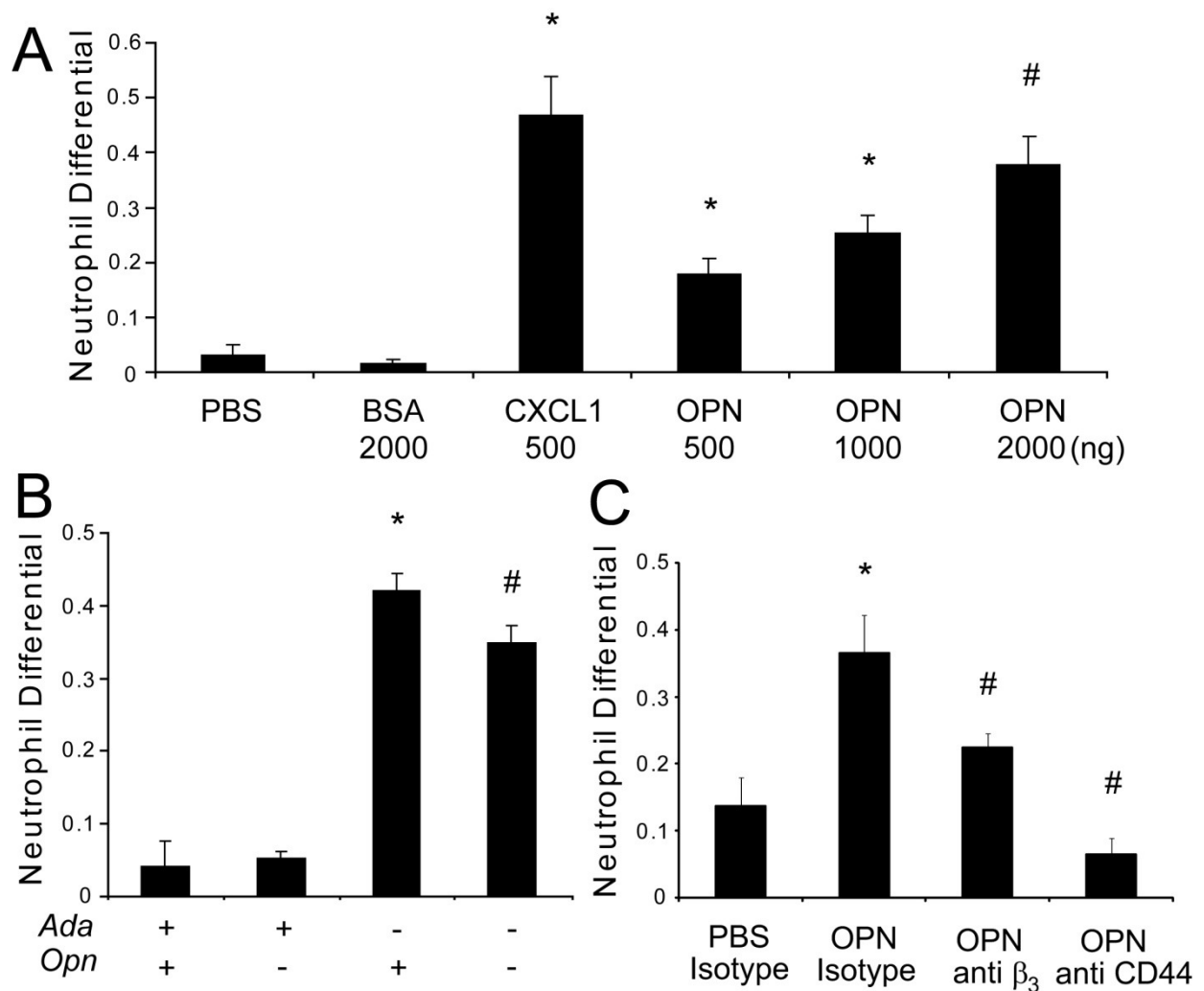


**Figure 3.10 - OPN-mediated neutrophil recruitment in an *in vivo* model**

*In vivo* neutrophil recruitment was assessed by quantification of neutrophils migrating into the peritoneal cavity following intraperitoneal (IP) administration of an agent. (A) IP injection of PBS (vehicle), BSA (negative protein control), CXCL1 (positive control), and increasing doses of OPN. Data are mean neutrophil differentials  $\pm$  SEM. \* $P \leq 0.05$  versus PBS; # $P \leq 0.05$  versus OPN 500 ng.  $n = 3$  mice (PBS, BSA, and CXCL-1);  $n = 5-7$  mice (OPN 500, 1000, and 2000 ng). (B) Peritoneal neutrophil recruitment was measured in wild type mice following IP injection of BAL fluid isolated from 4 genotypes of mice at postnatal day 37. Data are mean neutrophil differentials  $\pm$  SEM.  $n = 3$  ( $Ada^+$  and  $Opn^{-/-}$  BAL fluid);  $n = 6$  ( $Ada^{-/-}$  and  $Ada/Opn^{-/-}$  BAL fluid). (C) IP injections of OPN were preceded by IP injection of isotype control or  $\beta_3$

integrin or CD44 receptor blocking antibodies. Data are mean neutrophil differentials  $\pm$  SEM.  $n = 5$  mice (PBS + Isotype and OPN + Isotype);  $n = 6$  mice (OPN + anti-CD44);  $n = 7$  mice (OPN + anti- $\beta_3$ ).

OPN induces migration of numerous cell types including macrophages and lymphocytes through engagement of CD44 and  $\alpha_v\beta_3$  integrin receptors (84). However, OPN actions on neutrophils are not well-characterized. This *in vivo* assay was used to determine the role of CD44 and  $\beta_3$ -containing integrins in OPN-mediated neutrophil migration. IP preadministration of CD44 neutralizing Ab significantly reduced neutrophils recovered from peritoneal lavage in response to OPN (Figure 3.10C) but did not alter CXCL-1 induced neutrophil recruitment into the peritoneum (data not shown). Preadministration of  $\beta_3$  integrin blocking Ab also reduced OPN-mediated neutrophil recruitment (Figure 3.10C). These results suggest that OPN engagement of both CD44 and  $\beta_3$  integrin-containing receptors promote recruitment of neutrophils *in vivo*. These findings outline potential mechanisms involved in OPN-mediated increases in proteases present in distal air-spaces leading to the alveolar destruction seen in the *Ada*<sup>-/-</sup> model.

#### **CD44 expression, localization, and neutralization in *Ada*<sup>-/-</sup> mice**

A genome-wide microarray screen of *Ada*<sup>-/-</sup> mice displayed significant elevations in CD44 transcripts over *Ada*<sup>+</sup> littermates (73). This finding was confirmed by direct measurement of CD44 transcript levels from whole lung RNA isolates from *Ada*<sup>+</sup> and *Ada*<sup>-/-</sup> mice (Figure 3.11A). To localize the expression of CD44 to specific cell types, immunohistochemistry for CD44 was performed in lung sections. Results display ubiquitous expression of CD44 in multiple areas of the lung including bronchial airways, infiltrating inflammatory cells, and alveolar epithelial cells (Figure 3.11B). Increased immunoreactivity for CD44 was noted in the bronchial epithelium and infiltrating inflammatory cells of *Ada*<sup>-/-</sup> versus *Ada*<sup>+</sup> mouse lungs. This, coupled with previous results displaying CD44-dependent recruitment of neutrophils by OPN, suggests CD44 signaling may play a role in promoting pathology in the *Ada*<sup>-/-</sup> model.

To investigate the contribution of CD44 to lung pathology, *Ada*<sup>-/-</sup> mice maintained on PEG-ADA until postnatal day 25 were administered CD44 neutralizing Ab and endpoints were collected on postnatal day 41. In contrast to results seen in *Ada/Opn*<sup>-/-</sup> mice and *in vivo* neutrophil recruitment experiments, systemic administration of CD44 blocking Ab had no significant effect on pulmonary inflammation and neutrophilia (Figure 3.12A, C). These results

prompt repeat and alternative strategies for the investigation of CD44 in the context of pulmonary pathology.

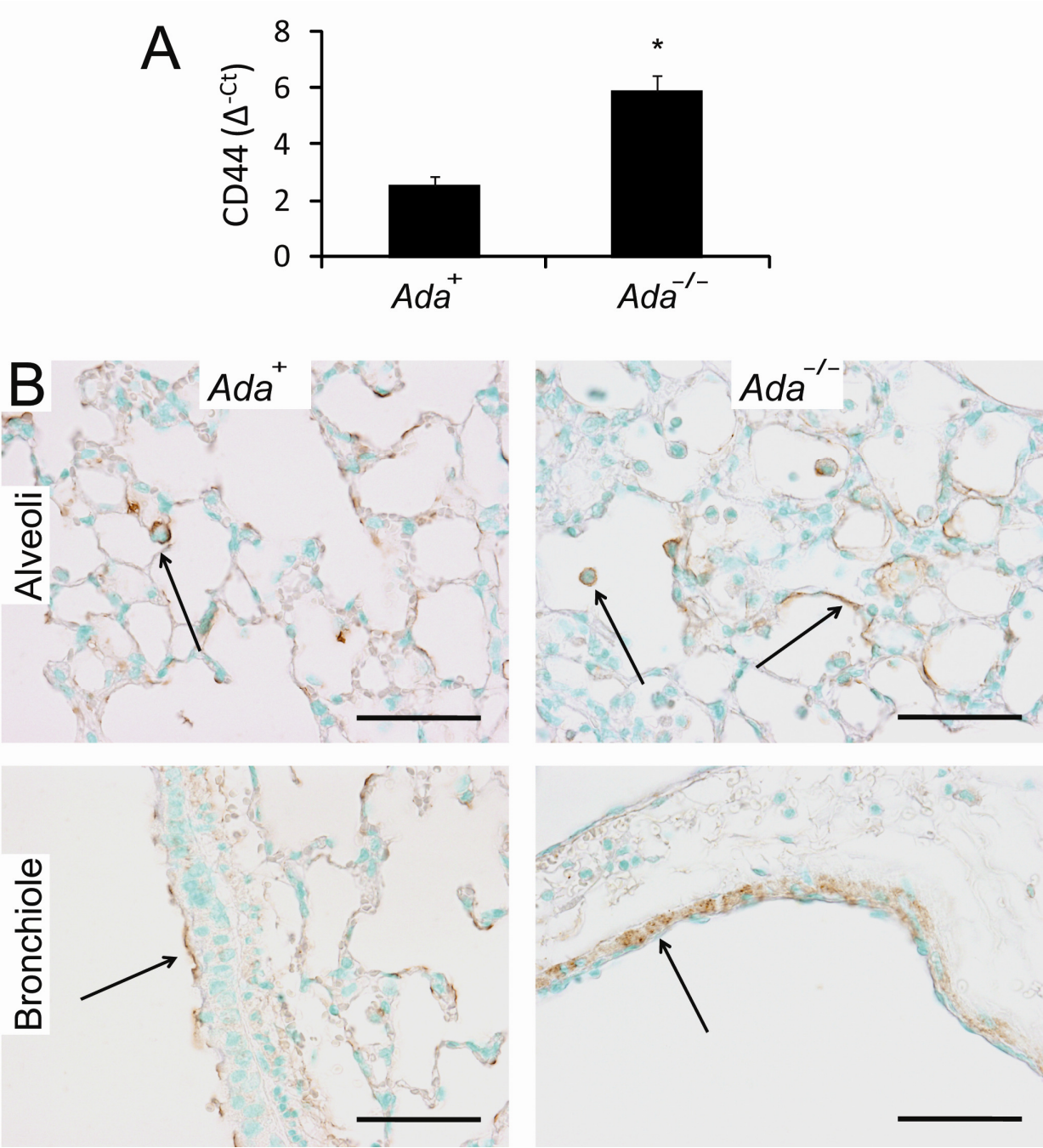
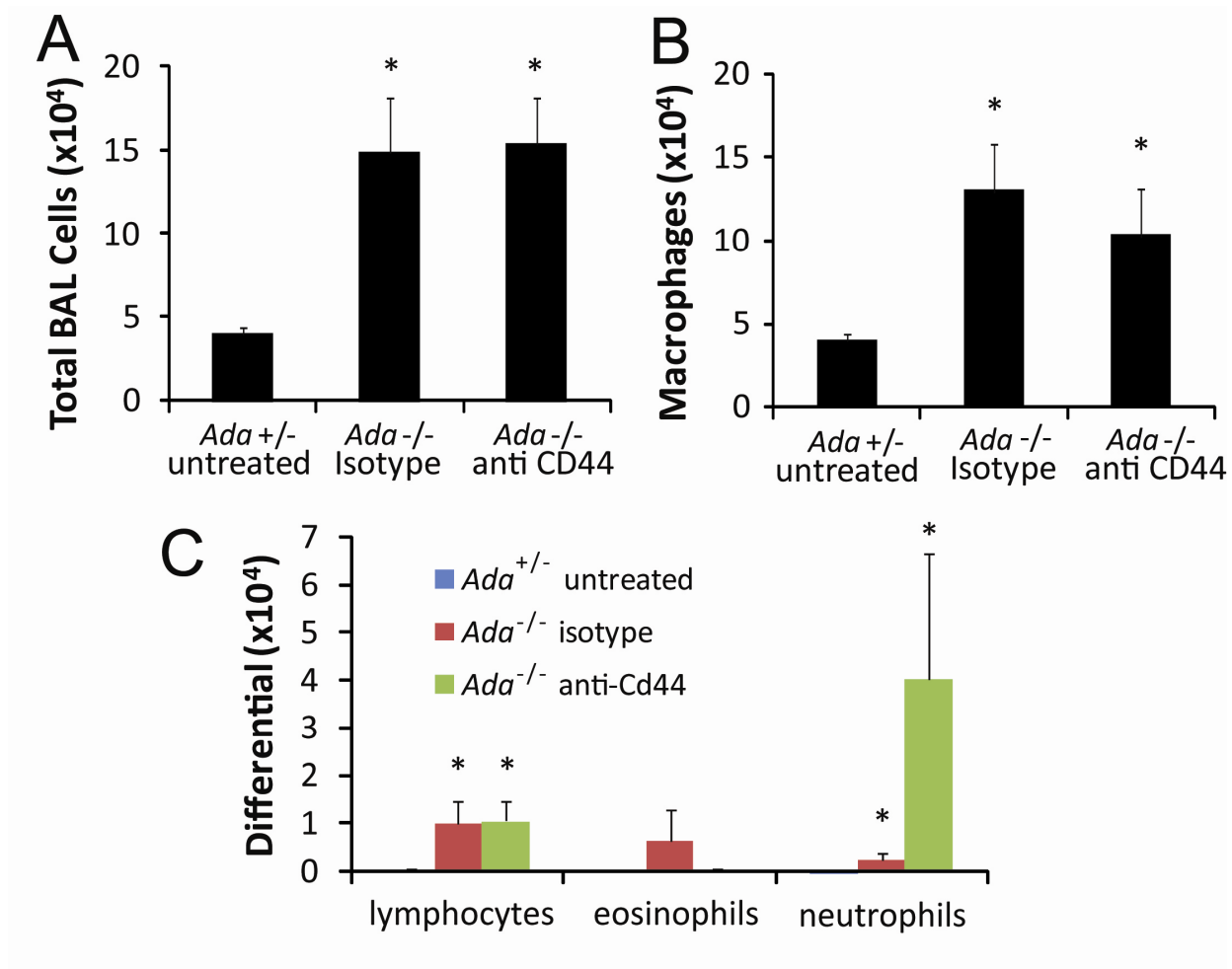


Figure 3.11 - CD44 expression in *Ada*<sup>-/-</sup> mice

(A) Transcript levels for CD44 in *Ada*<sup>+</sup> and *Ada*<sup>-/-</sup> mouse lungs at postnatal day 37. Data presented as mean transcript levels normalized to 18S rRNA ( $\Delta^{-Ct}$ )  $\pm$  SEM. \**P*  $\leq$  0.05 versus *Ada*<sup>+</sup> mice. *n* = 6 *Ada*<sup>-/-</sup> mice; *n* = 3 *Ada*<sup>+</sup> mice. (B) Lung sections processed for immunolocalization of CD44 (black arrows). Scale bars: 100  $\mu$ m.



**Figure 3.12 - CD44 neutralization in *Ada*<sup>-/-</sup> mice**

Airway inflammatory cells isolated at postnatal day 41 from *Ada*<sup>-/-</sup> mice administered systemic CD44 neutralizing antibody or isotype control versus *Ada*<sup>+</sup> littermates. (A) Total inflammatory cell counts; (B) absolute macrophage count and (C) total neutrophils, eosinophils and lymphocytes isolated in BAL fluid. Data are mean  $\pm$  SEM. \**P*  $\leq$  0.05 versus *Ada*<sup>+</sup> untreated mice. *n* = 4 *Ada*<sup>+</sup> untreated mice; *n* = 8 *Ada*<sup>-/-</sup> isotype; *n* = 9 *Ada*<sup>-/-</sup> anti-CD44.

### ***OPN and the regulation of proinflammatory cytokines***

In the setting of lung pathology, *Ada*<sup>-/-</sup> mice exhibit increased levels of cytokines and chemokines, many of which are regulated by the A<sub>2B</sub>R (71) and promote the recruitment of neutrophils. To investigate if OPN-dependent recruitment of inflammatory cells is indirect through the upregulation of cytokines, their transcript levels were measured in whole lung RNA extracts from mice at postnatal day 37. Results show characteristic increases in expression of proinflammatory cytokines in the lungs of *Ada*<sup>-/-</sup> versus *Ada*<sup>+</sup> mice, but no significant differences between *Ada*<sup>-/-</sup> and *Ada/Opn*<sup>-/-</sup> transcripts (Figure 3.13). Although a trend decrease in CXCL-1 transcripts was observed in *Ada/Opn*<sup>-/-</sup> versus *Ada*<sup>-/-</sup> mice (data not shown), there was no difference in protein levels of CXCL-1 between the two genotypes. These findings suggest that OPN does not significantly influence the levels of adenosine-regulated proinflammatory cytokines. These data demonstrate that OPN promotes the recruitment of neutrophils through engagement of cell surface receptors and not via the regulation of other proinflammatory cytokines.

### ***OPN and peripheral blood neutrophilia***

To examine if reductions in lung neutrophilia in the absence of OPN were due to a fundamental defect in granulopoiesis, circulating leukocytes were obtained and quantified in the peripheral blood of wild type and *Opn*<sup>-/-</sup> mice. The numbers of neutrophils and other leukocyte populations were the same as wild type mice (Figure 3.14), suggesting neutrophil development is normal in *Opn*<sup>-/-</sup> mice.

### ***OPN and alveolarization***

Developing lungs undergo secondary septation during the process of alveogenesis from postnatal days 5 to 10 in *Ada*<sup>+</sup> mice (30). To determine if reduced alveolar air-space size in *Ada/Opn*<sup>-/-</sup> mice at postnatal day 37 was due to OPN-dependent alterations in alveogenesis, airspace size was quantified from H&E-stained lung sections isolated from *Ada*<sup>+</sup> and *Opn*<sup>-/-</sup> mice on postnatal day 10. Results demonstrate no significant differences in air-space size between these two genotypes (Figure 3.15) suggesting OPN does not play a critical role in secondary septation of the air-spaces. Further, *Ada*<sup>-/-</sup> mice display adenosine-dependent defects in alveogenesis in the absence of inflammation resulting in increased size of alveolar

air-spaces (30). Results of this study demonstrate significantly increased alveolar air-space size in both *Ada*<sup>-/-</sup> and *Ada/Opn*<sup>-/-</sup> mice at postnatal day 10 (Figure 3.15). These results

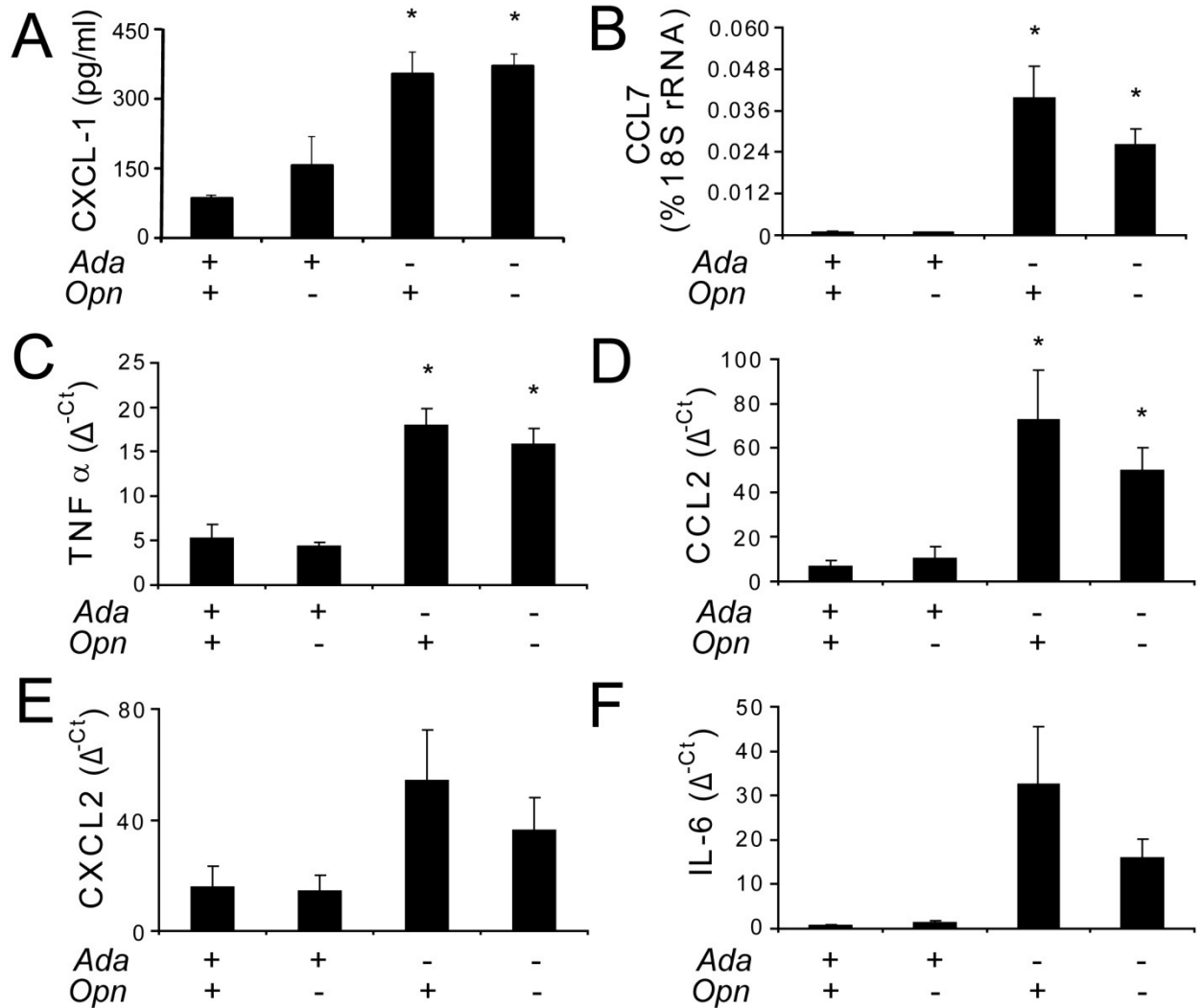


**Figure 3.13 - OPN-dependent regulation of proinflammatory cytokines**

(A) Protein levels of CXCL1 in BAL. Transcript levels are shown for (B) CCL7, (C) TNF  $\alpha$ , (D) CCL2, (E) CXCL2, and (F) IL-6. Transcripts for CCL7 were measured in parallel with 18S rRNA and values are presented as mean %18S rRNA  $\pm$  SEM. Remaining transcripts were normalized to 18S rRNA and are presented as mean normalized transcript levels ( $\Delta$ -Ct)  $\pm$  SEM.  $n = 4$  mice (*Ada*<sup>+</sup> and *Opn*<sup>-/-</sup>);  $n = 6$  mice (*Ada*<sup>-/-</sup> and *Ada/Opn*<sup>-/-</sup>). \* $P \leq 0.05$  versus *Ada*<sup>+</sup> mice.

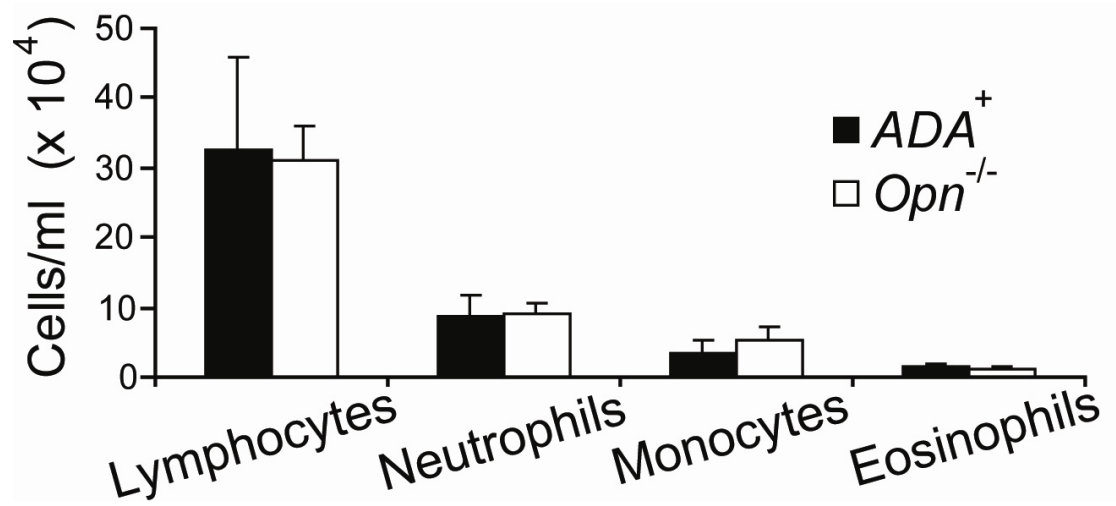


**Figure 3.14 - Quantification of blood leukocytes in *Opn*<sup>-/-</sup> mice**

Peripheral blood leukocytes were isolated and counted from *Ada*<sup>+</sup> and *Opn*<sup>-/-</sup> mice at postnatal day 37. Data presented are mean cell counts  $\pm$  SEM.  $n = 4$  mice per genotype.



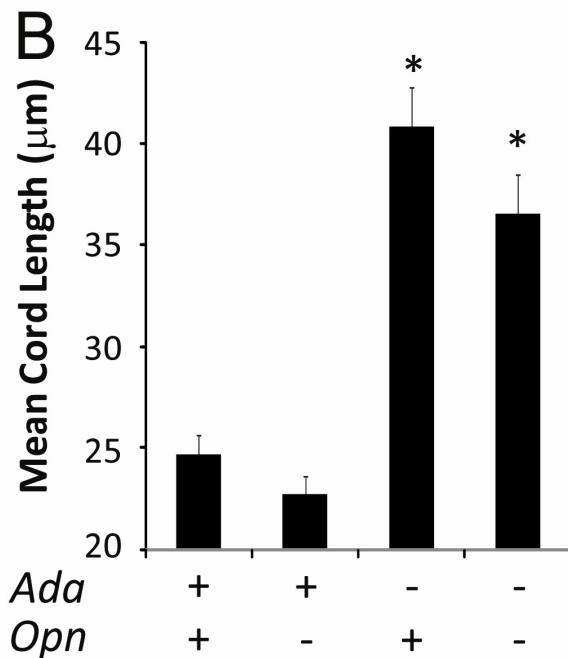
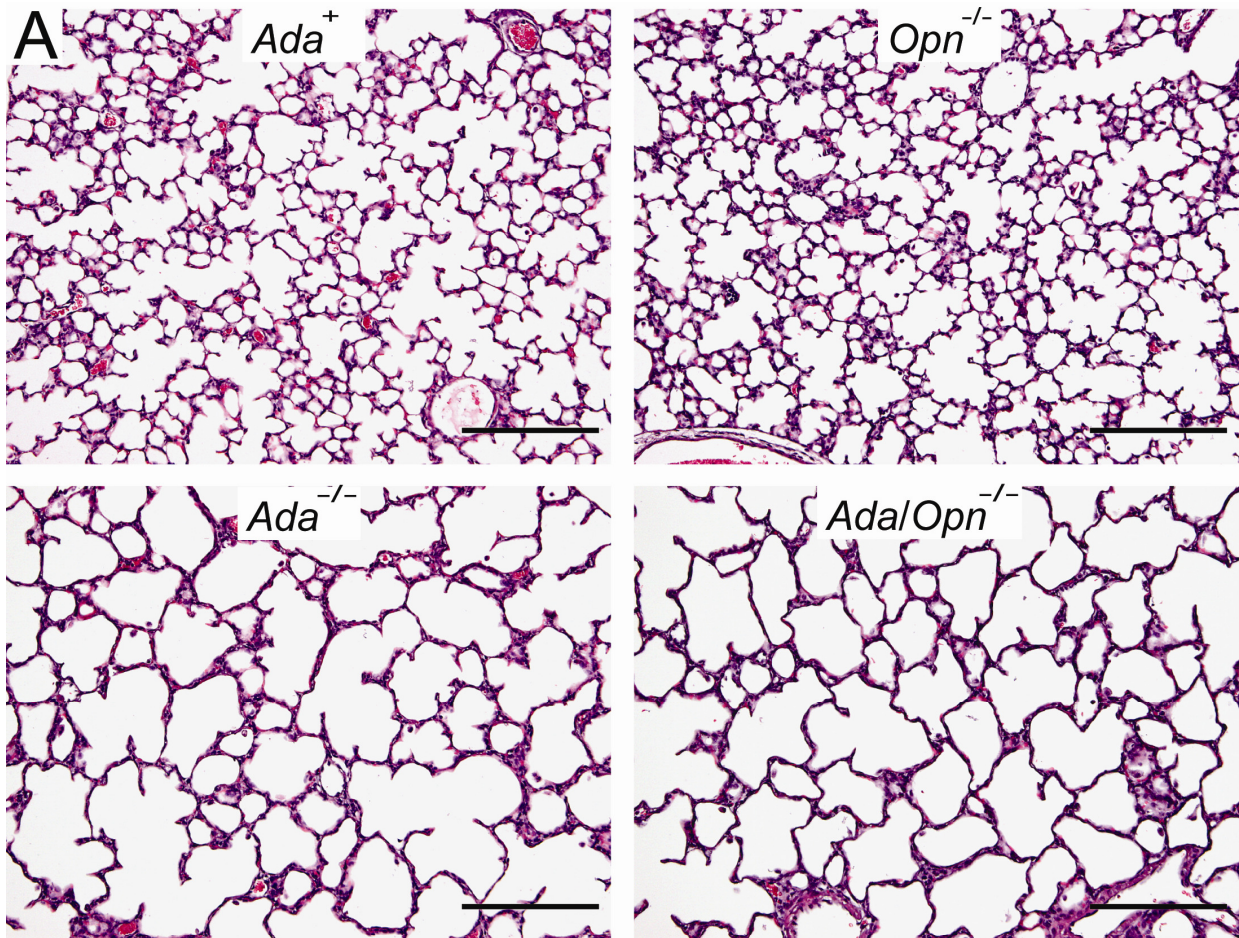


**Figure 3.15 - OPN and alveolarization**

(A) Lungs from *Ada*<sup>+</sup>, *Opn*<sup>-/-</sup>, *Ada*<sup>-/-</sup>, and *Ada/Opn*<sup>-/-</sup> mice at postnatal day 10. Scale bars: 200 μm. (B) Average alveolar airway size was determined using Image-Pro analysis software on 16 images at 10X magnification per mouse lung. Values are given as mean cord lengths in μm ± SEM. \**P* ≤ 0.05 versus *Ada*<sup>+</sup> mice. Displayed images are representative of *n* = 8 mice (*Ada*<sup>+</sup> and *Opn*<sup>-/-</sup>); *n* = 10 *Ada*<sup>-/-</sup> mice; *n* = 6 *Ada/Opn*<sup>-/-</sup> mice.



indicate that OPN does not contribute to normal or pathologic development of the alveolar air-spaces.

### ***OPN-mediated angiogenesis in $Ada^{-/-}$ mice***

Previous work has shown that symptomatic  $Ada^{-/-}$  mice display increased pulmonary angiogenesis (28). Enhanced angiogenesis has also been described in association with air-space destruction seen in COPD and ARDS (99). Furthermore, OPN has been shown to promote the process of angiogenesis (76, 81). To determine the contribution of OPN to angiogenesis in the  $Ada^{-/-}$  model, tracheal vascularity was utilized as a measure of lung angiogenesis (29) in  $Ada^{-/-}$  and  $Ada/Opn^{-/-}$  mice. Results demonstrate a significant reduction in vascularity of tracheas isolated from  $Ada/Opn^{-/-}$  mice (Figure 3.16) suggesting OPN contributes to lung angiogenesis, an indicator of the development of pulmonary pathology in this model.

### ***Mucus metaplasia in $Ada/Opn^{-/-}$ mice***

Patients with COPD, especially the chronic bronchitis subtype, exhibit mucus metaplasia in the large airways. Previous studies have demonstrated increased mucus cell metaplasia in  $Ada^{-/-}$  mice in parallel with increased adenosine levels and emphysema (22, 30). Furthermore, OPN is suggested to contribute to mucus metaplasia in a model of allergic airway disease (96). Therefore, the contribution of OPN to mucus metaplasia in the  $Ada^{-/-}$  model was investigated. Results of PAS staining (Figure 3.17A) and subsequent scoring (Figure 3.17B) established no significant changes in large airway mucus between  $Ada^{-/-}$  and  $Ada/Opn^{-/-}$  mice. These findings suggest that OPN does not contribute to mucus metaplasia in the  $Ada^{-/-}$  model.

### ***OPN-dependent airway remodeling and fibrosis***

Patients and animal models including  $Ada^{-/-}$  mice exhibiting alveolar air-space enlargement also display features consistent with pulmonary fibrosis (13, 14, 26). In addition,  $Opn^{-/-}$  mice are protected from the effects of tissue fibrosis in various animal models (97, 98, 110, 111). Therefore, experiments were performed to determine the contribution of OPN to pulmonary fibrosis in  $Ada^{-/-}$  mice. Lungs of  $Ada^{-/-}$  mice were noted to exhibit characteristic increases in collagen production indicated by  $\alpha_1$  procollagen transcripts, increased collagen deposition detected by Masson's Trichrome staining, and elevated soluble collagen in the airways. These mice simultaneously display  $\alpha$  SMA staining in the distal air-spaces indicating increased numbers of myofibroblasts (Figure 3.18A-D). Surprisingly,  $Ada/Opn^{-/-}$  displayed no

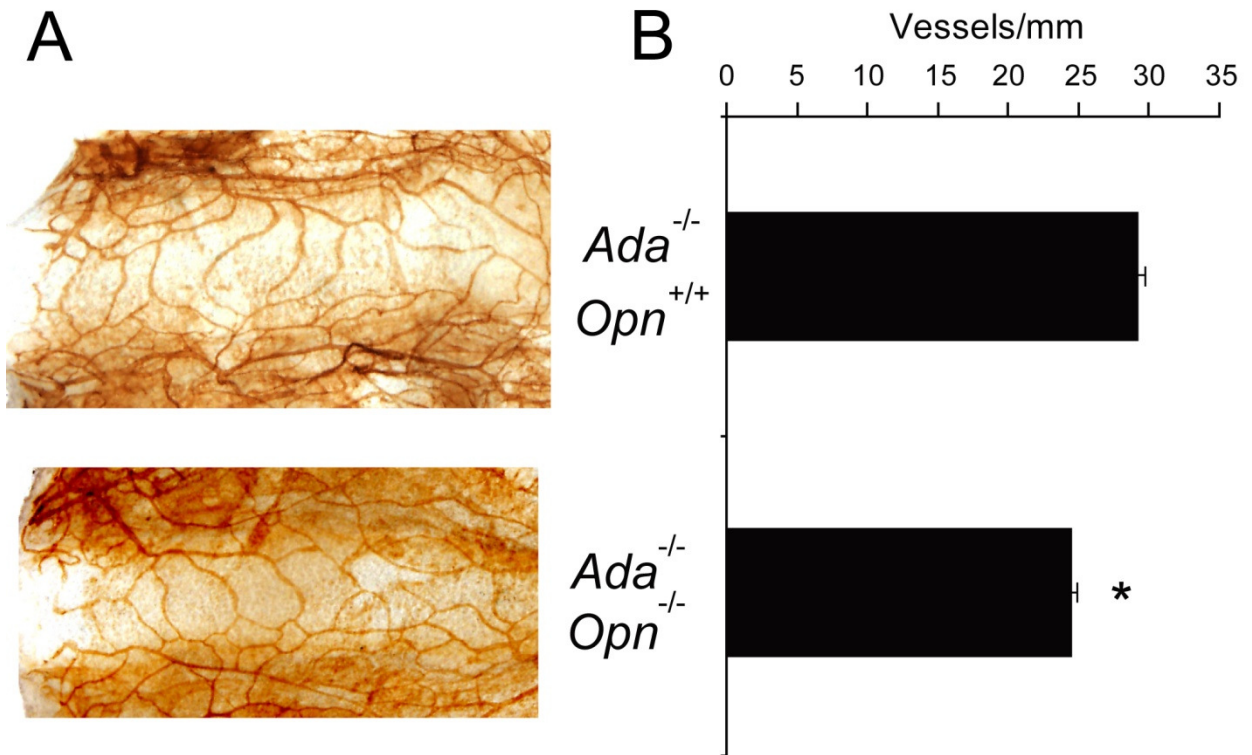


**Figure 3.16 - Angiogenesis and OPN in the *Ada*<sup>-/-</sup> model**

(A) Tracheas were removed from postnatal day 37 mice and analyzed by whole mount CD31 immunostaining for visualization of vessels. Images shown are representative of  $\geq 6$  per genotype. (B) Vascularity was quantified by counting number of vessels intersecting a line drawn the length of a cartilage ring. At least 8 cartilage rings per sample were analyzed. Data presented as mean number of vessels per mm  $\pm$  SEM. \* $P \leq 0.05$  versus *Ada*<sup>-/-</sup>.  $n = 6$  mice (*Ada*<sup>-/-</sup>).  $n = 7$  mice (*Ada/Opn*<sup>-/-</sup>).

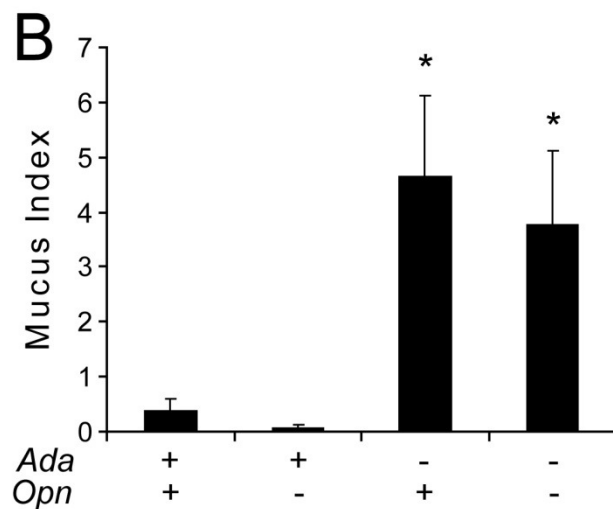
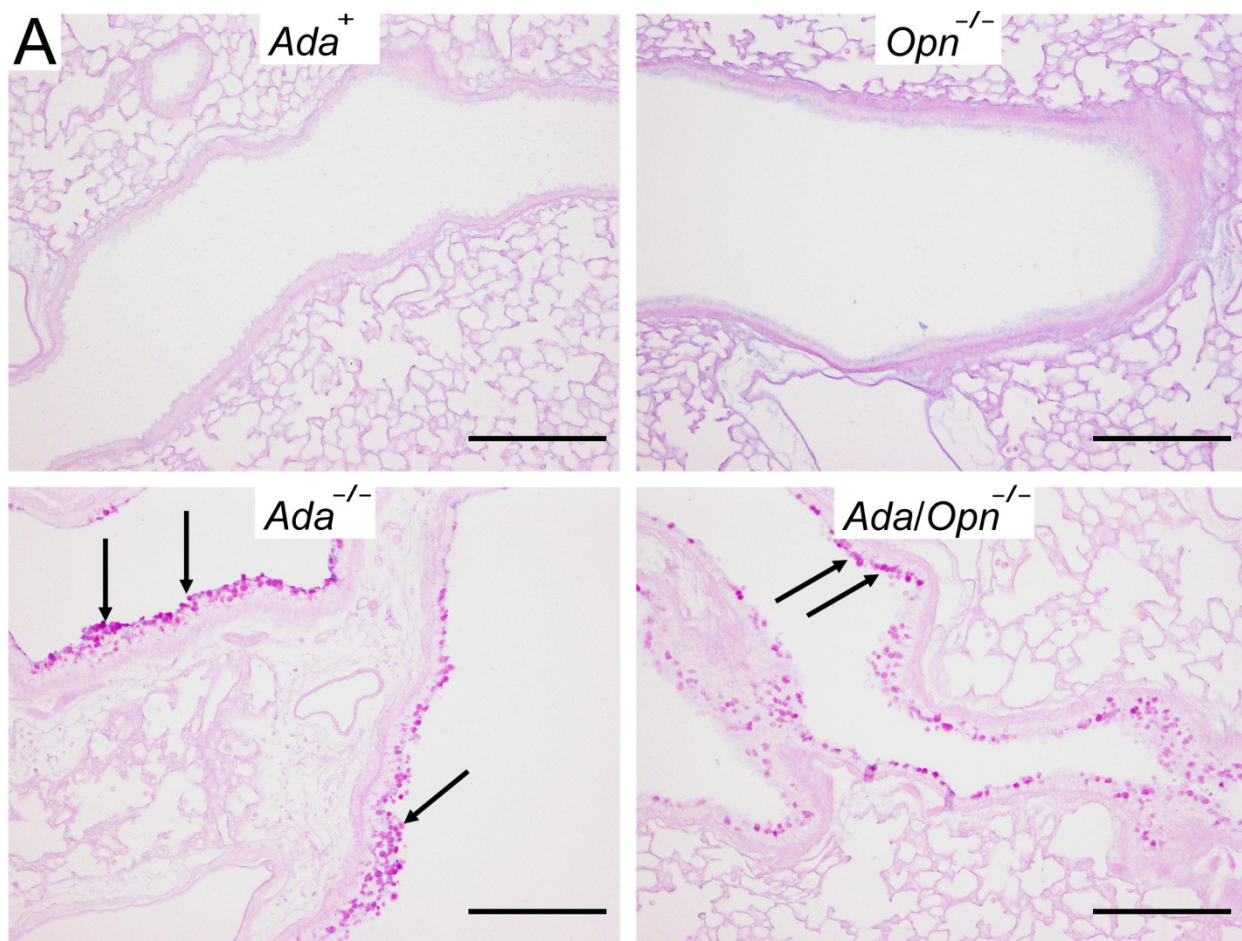


**Figure 3.17 - Role of OPN in mucus production in the *Ada*<sup>-/-</sup> model**

(A) Mouse lungs were stained with Periodic Acid-Schiff (PAS) to assess for mucus present in the airways (arrows). Scale bars: 200  $\mu$ m. (B) Mucus staining was quantified using Image Pro analysis software on composite images of all large airways per mouse lung section. Data are mean mucus index  $\pm$  SEM. \* $P \leq 0.05$  versus *Ada*<sup>+</sup>.  $n = 4$  mice (*Ada*<sup>+</sup> and *Opn*<sup>-/-</sup>);  $n = 6$  (*Ada*<sup>-/-</sup> and *Ada/Opn*<sup>-/-</sup>).



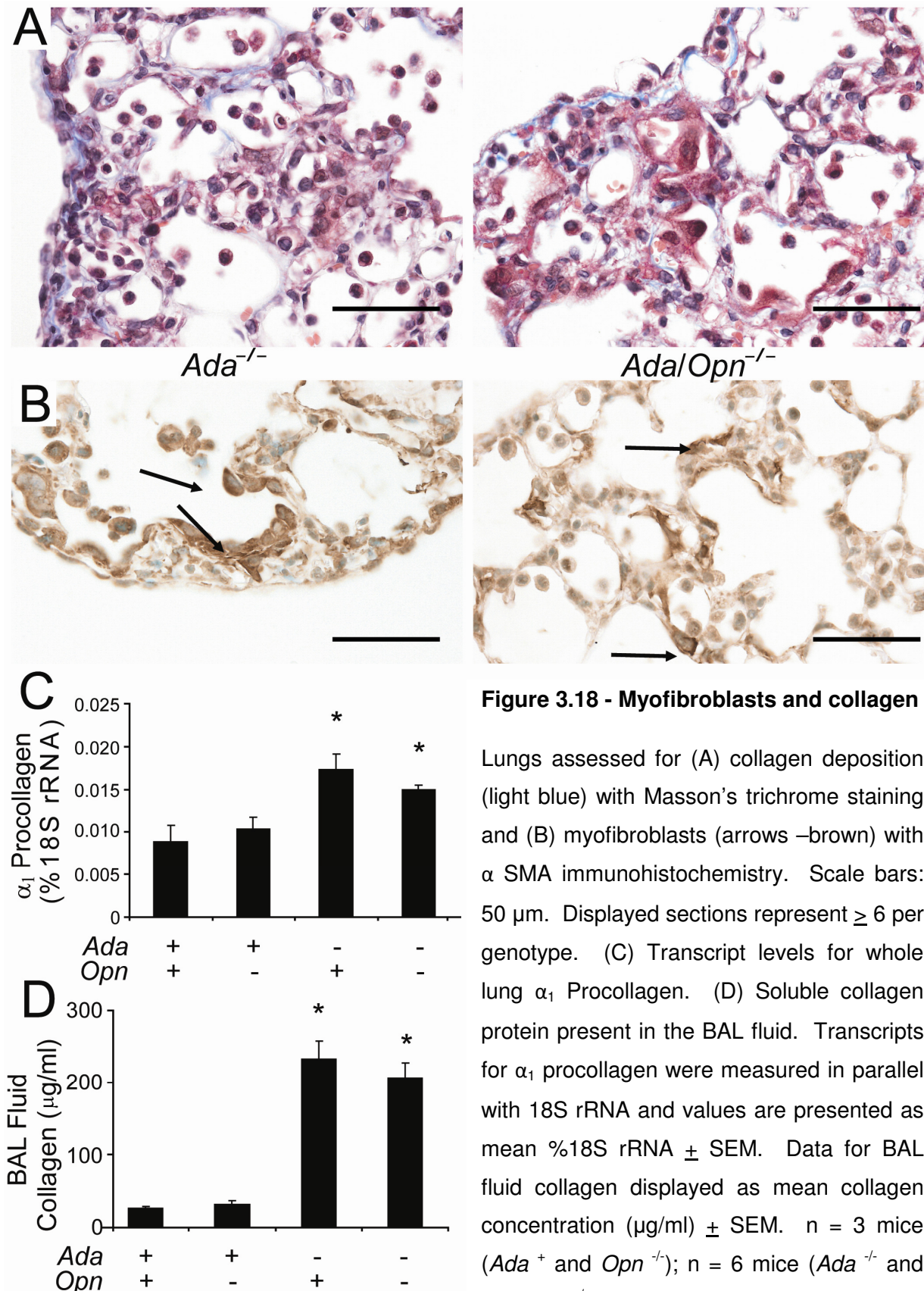


**Figure 3.18 - Myofibroblasts and collagen**

Lungs assessed for (A) collagen deposition (light blue) with Masson's trichrome staining and (B) myofibroblasts (arrows –brown) with  $\alpha$  SMA immunohistochemistry. Scale bars: 50  $\mu$ m. Displayed sections represent  $\geq 6$  per genotype. (C) Transcript levels for whole lung  $\alpha_1$  Procollagen. (D) Soluble collagen protein present in the BAL fluid. Transcripts for  $\alpha_1$  procollagen were measured in parallel with 18S rRNA and values are presented as mean %18S rRNA  $\pm$  SEM. Data for BAL fluid collagen displayed as mean collagen concentration ( $\mu$ g/ml)  $\pm$  SEM.  $n = 3$  mice (*Ada*<sup>+</sup> and *Opn*<sup>-/-</sup>);  $n = 6$  mice (*Ada*<sup>-/-</sup> and

changes in these endpoints suggesting that OPN is not required for the development of pulmonary fibrosis in the *Ada*<sup>-/-</sup> model.

Profibrotic mediators including TGF- $\beta$ <sub>1</sub>, uPA, MMP-2 and PAI-1 were also examined. Consistent with histologic endpoints of fibrosis, transcripts for TGF- $\beta$ <sub>1</sub>, uPA, and MMP-2 were significantly elevated in the lungs of both *Ada*<sup>-/-</sup> and *Ada/Opn*<sup>-/-</sup> mice (Figure 3.19 A-C). However, while the lungs of *Ada*<sup>-/-</sup> mice displayed significant increases in PAI-1, expression in *Ada/Opn*<sup>-/-</sup> was significantly reduced (Figure 3.19D) suggesting OPN influences lung PAI-1 levels.

Finally, the production of fibronectin, an ECM protein, is regulated by adenosine signaling (112) and is increased in association with inflammation and air-space destruction seen in conditions such as COPD (113) and ARDS (99). Increased fibronectin deposition in distal air-spaces is also associated with pulmonary fibrosis. Production and deposition of fibronectin was elevated in *Ada*<sup>-/-</sup> mice, but these endpoints were substantially reduced in lungs of *Ada/Opn*<sup>-/-</sup> mice (Figure 3.20A, B) suggesting OPN-dependent regulation of fibronectin expression and/or deposition. Taken together, while it appears that OPN is not necessary for the development of major indices of pulmonary fibrosis in the lungs of *Ada*<sup>-/-</sup> mice, OPN does regulate other mediators and endpoints commonly associated with its progression.

### ***OPN expression, localization, and association with severity of COPD in humans***

*Ada*<sup>-/-</sup> mice exhibit features consistent with COPD including pulmonary inflammation and alveolar air-space destruction and remodeling in parallel with increased OPN expression (71) within alveolar macrophages. A microarray screen of alveolar macrophages isolated from smokers identified elevated expression of OPN that correlated with degree of airway obstruction (101). However, the levels of OPN in COPD patients with emphysema have not been examined. Immunolocalization of OPN expression in patients with COPD was localized to infiltrating cells within the alveolar air-spaces (Figure 3.21A) consistent with findings in the *Ada*<sup>-/-</sup> model. While OPN staining was present in lungs of Stage 0 COPD patients, relatively little was present on infiltrating cells. To quantify differences in OPN expression in patients with COPD, transcript levels were measured in whole lung RNA extracts from patients with Stage 4 COPD and Stage 0. Results demonstrate minimal differences in the expression of OPN in the whole lungs of patients with Stage 4 versus Stage 0 (Figure 3.21B). However, quantification of OPN positive cells in lung sections revealed dramatic increases in Stage 4 patients versus

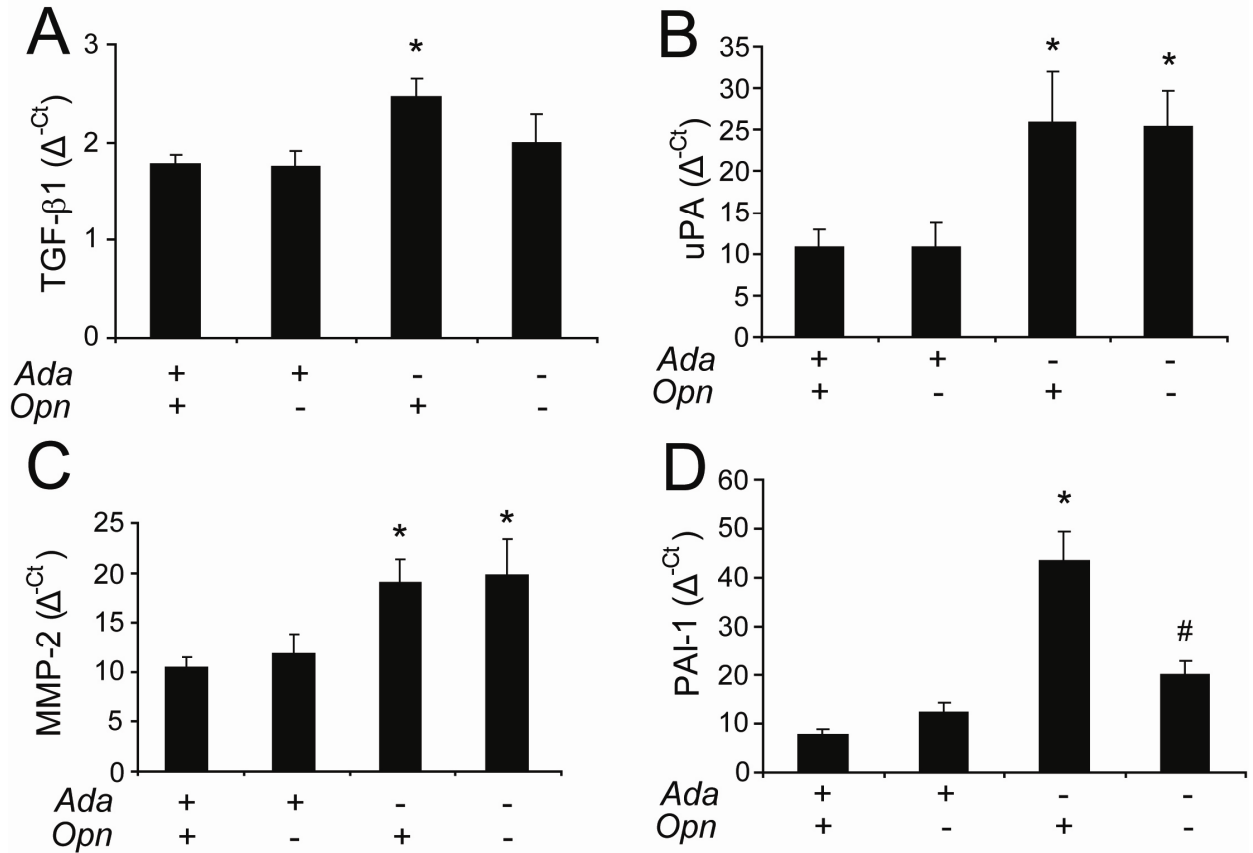


**Figure 3.19 - Profibrotic mediators**

Transcript levels of mediators of airway remodeling and fibrosis were measured using quantitative RT-PCR. Transcript levels are shown for (A) TGF- $\beta$ <sub>1</sub>, (B) uPA, (C) MMP-2, and (D) PAI-1. Transcripts were normalized to 18S rRNA and are presented as mean normalized transcripts ( $\Delta$ -Ct)  $\pm$  SEM.  $n = 3$  mice ( $Ada^{+/+}$  and  $Opn^{-/-}$ );  $n = 6$  mice ( $Ada^{-/-}$  and  $Ada/Opn^{-/-}$ ). \* $P \leq 0.05$  versus  $Ada^{+/+}$  mice. # $P \leq 0.05$  versus  $Ada^{-/-}$  mice.

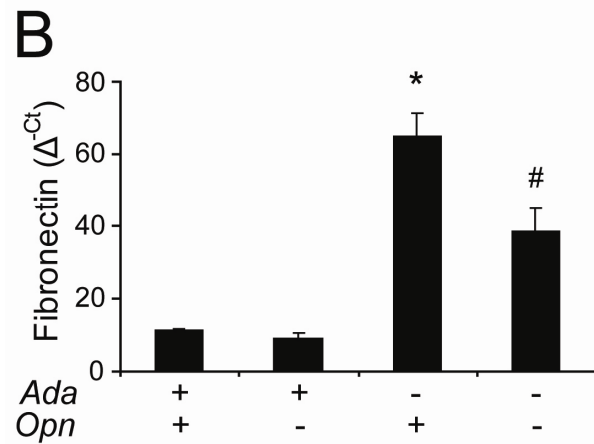
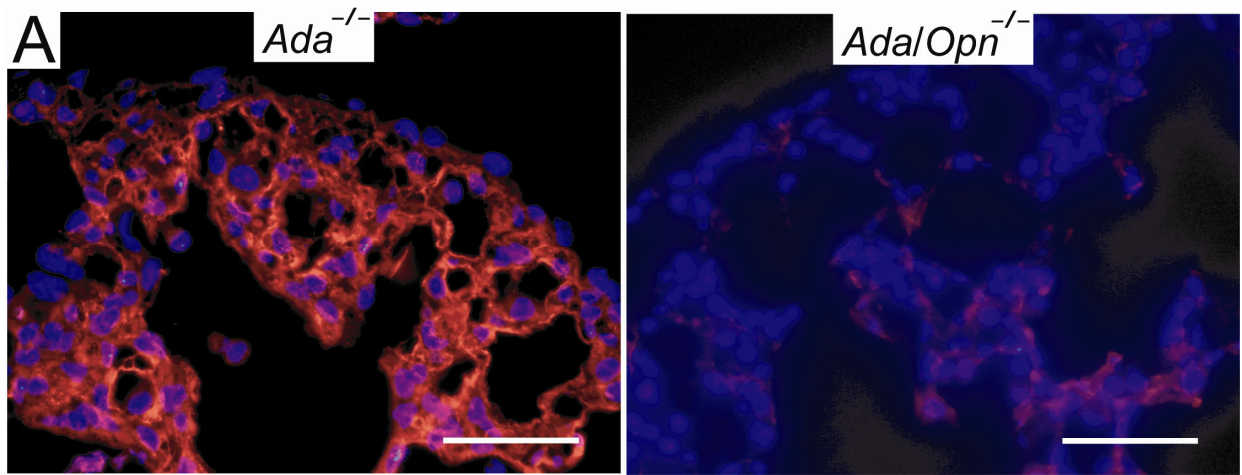


**Figure 3.20 - Fibronectin**

(A) Fibronectin immunofluorescence on lung sections at postnatal day 37 and corresponding (B) whole lung fibronectin transcript levels. Scale bars: 100  $\mu$ m. Fibronectin transcripts were normalized to 18S rRNA and are presented as mean normalized transcript levels ( $\Delta C_t$ )  $\pm$  SEM.  $n = 3$  mice ( $Ada^+$  and  $Opn^{-/-}$ );  $n = 6$  mice ( $Ada^{-/-}$  and  $Ada/Opn^{-/-}$ ). \* $P \leq 0.05$  versus  $Ada^+$  mice. # $P \leq 0.05$  versus  $Ada^{-/-}$  mice.



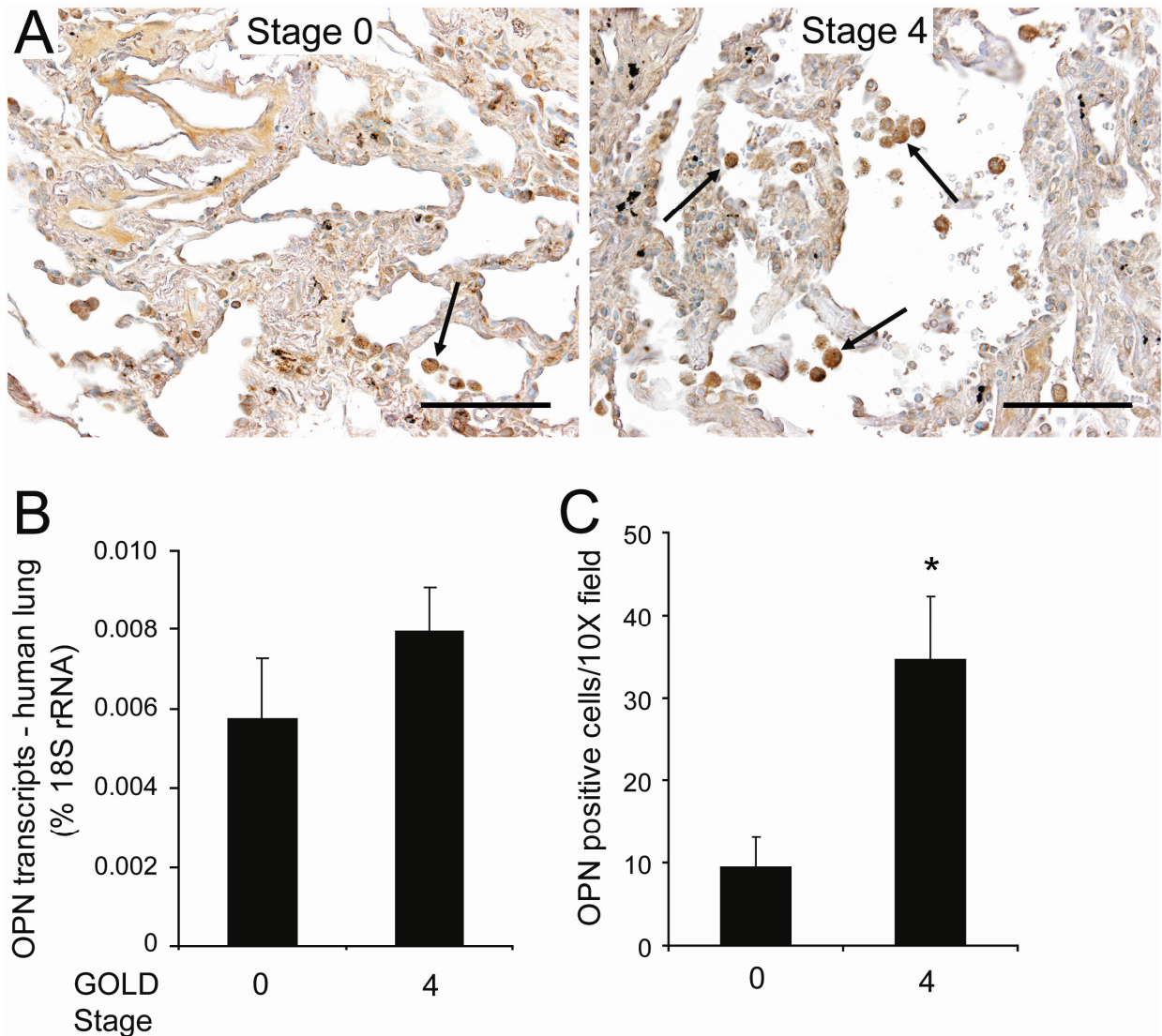


**Figure 3.21 - OPN expression in patients with COPD**

(A) Immunolocalization of OPN expression within infiltrating cells present in alveolar airways (arrows) of patients with COPD stage 0 and stage 4 using GOLD criteria. Scale bars: 100  $\mu$ m. (B) Transcript levels of OPN in patients at stage 0 vs. 4. Transcripts for OPN were measured in parallel with 18S rRNA and values are presented as mean %18S rRNA  $\pm$  SEM.  $n = 4$  (Stage 0);  $n = 9$  (Stage 4). (C) OPN positive staining cells within alveolar airways were quantified on  $\geq 12$  images per patient lung. Data presented as mean number of positive staining cells per 10X field  $\pm$  SEM.  $n = 4$  (Stage 0);  $n = 10$  (Stage 4). \* $P \leq 0.05$  versus Stage 0.



Stage 0 (Figure 3.21C). These results indicate increased OPN-positive infiltrating inflammatory cells in patients with COPD, similar to the *Ada*<sup>-/-</sup> model. Finally, number of OPN-positive cells in patient samples was associated with degree of airway obstruction measured by forced vital capacity (FVC), forced expiratory volume in one second (FEV<sub>1</sub>), and peak expiratory flow rate (PEFR) (Figure 3.22). Collectively, the results of this study describe the importance of increased OPN in the lungs leading to the development of emphysema in patients with COPD.

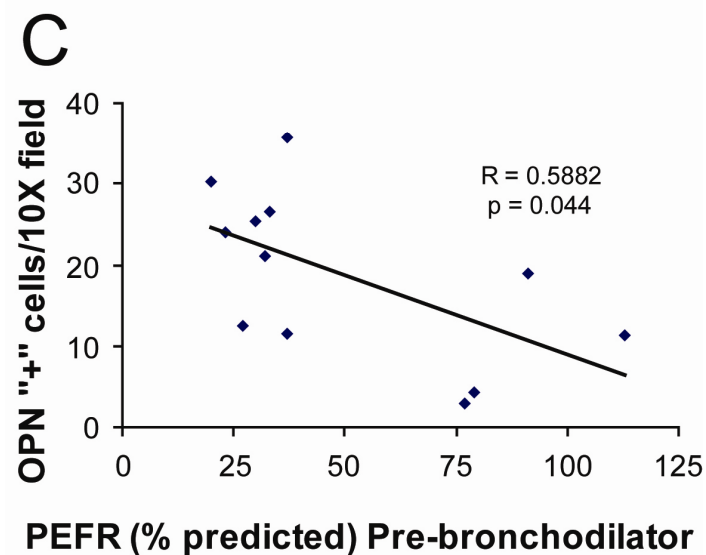
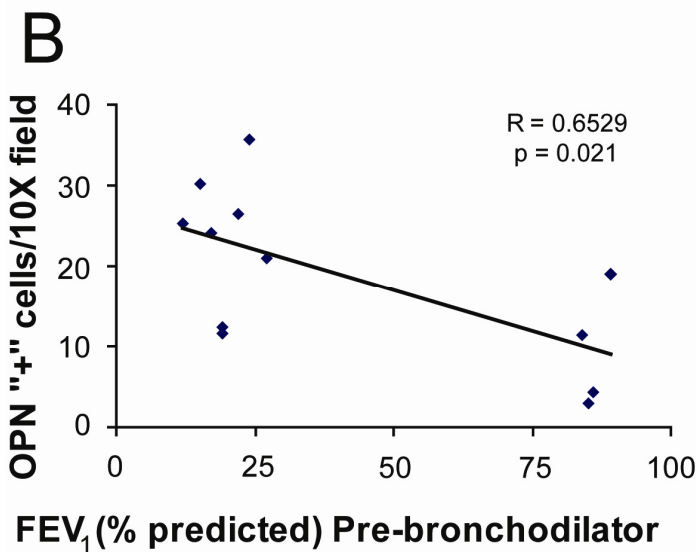
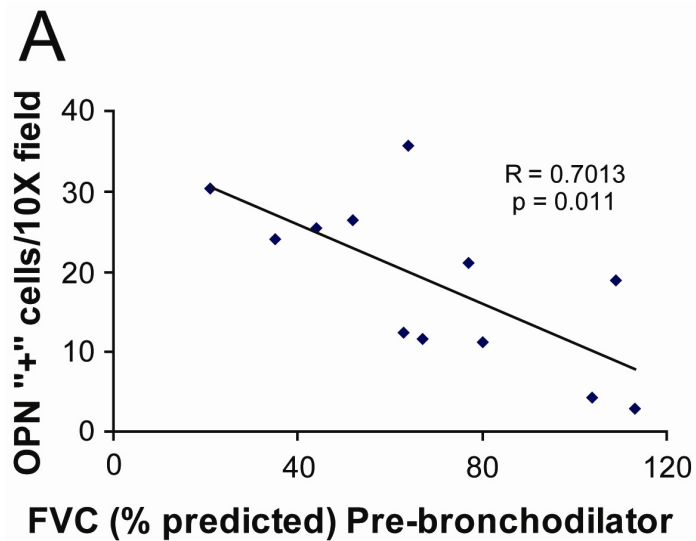


**Figure 3.22 - OPN expression associates with clinical indicators of COPD**

Association of number of OPN positive staining cells with disease severity represented by (A) forced vital capacity (FVC), (B) forced expiratory volume in one second (FEV<sub>1</sub>), and (C) peak expiratory flow rate (PEFR). n = 4 (Stage 0); n = 8 (Stage 4).

### **Chapter 3 - Discussion**

A well-established model displaying the tissue destructive effects of chronic adenosine elevations is the *Ada*<sup>-/-</sup> mouse (30, 114). These mice exhibit a pulmonary phenotype consisting of pulmonary inflammation, alveolar air-space destruction, mucus metaplasia, and pulmonary fibrosis. Recent studies have suggested that signaling through the A<sub>2B</sub>R represents a major mechanism involved in disease progression in this model (71). Furthermore, these studies also revealed that these mice will concurrently exhibit A<sub>2B</sub>R-dependent upregulations in OPN, a protein implicated in various pathologic conditions which include inflammation and fibrosis. Therefore, it was hypothesized that OPN contributes to the pulmonary phenotype in *Ada*<sup>-/-</sup> mice. To test this, *Ada/Opn*<sup>-/-</sup> mice were generated and pulmonary endpoints were examined. Genetic removal of *Opn* in *Ada*<sup>-/-</sup> mice dramatically reduced features of chronic lung disease including pulmonary inflammation and alveolar air-space enlargement. Most endpoints consistent with pulmonary fibrosis were unchanged in *Ada/Opn*<sup>-/-</sup> lungs. The results of this study demonstrate that OPN regulates the process of inflammation and alveolar air-space enlargement in the setting of elevated adenosine levels (Figure 3.23). Similarities between *Ada*<sup>-/-</sup> mice and humans with chronic lung disease demonstrate that the *Ada*<sup>-/-</sup> mouse is a useful model to guide the development of therapeutic targets for these conditions.

*Ada*<sup>-/-</sup> mouse lungs display an inflammatory cell infiltrate consisting of alveolar macrophages, lymphocytes, and neutrophils (19, 26). OPN has well-described chemotactic properties for these cell types (84, 86, 87, 93, 109). Consistent with this, these results demonstrate that genetic removal of OPN in *Ada*<sup>-/-</sup> mice reduced pulmonary neutrophilia (Figure 3.6C). These changes were found to be independent of OPN-mediated changes in proinflammatory cytokines (Figure 3.13) and alterations in peripheral blood neutrophilia (Figure 3.14). Furthermore, these results demonstrate using an *in vivo* assay of neutrophil recruitment that OPN is a significant contributor to neutrophil chemotaxis (Figure 3.10B) among several cytokines upregulated in *Ada*<sup>-/-</sup> mouse lungs. OPN-mediated chemotaxis of several cell types is dependent on OPN binding to cell surface receptors CD44 (75, 83, 85, 86) and  $\alpha_v\beta_3$  (80, 82, 115). This *in vivo* assay demonstrated that OPN-mediated neutrophil recruitment can be inhibited by blocking interactions with these receptors (Figure 3.10C). Thus, these receptors may contribute to OPN-dependent neutrophil chemotaxis in the lungs of *Ada*<sup>-/-</sup> mice.

*Ada*<sup>-/-</sup> mice develop alveolar air-space enlargement resembling histological findings of patients with emphysema (30, 71). A major observation of this study was that *Ada/Opn*<sup>-/-</sup> mice

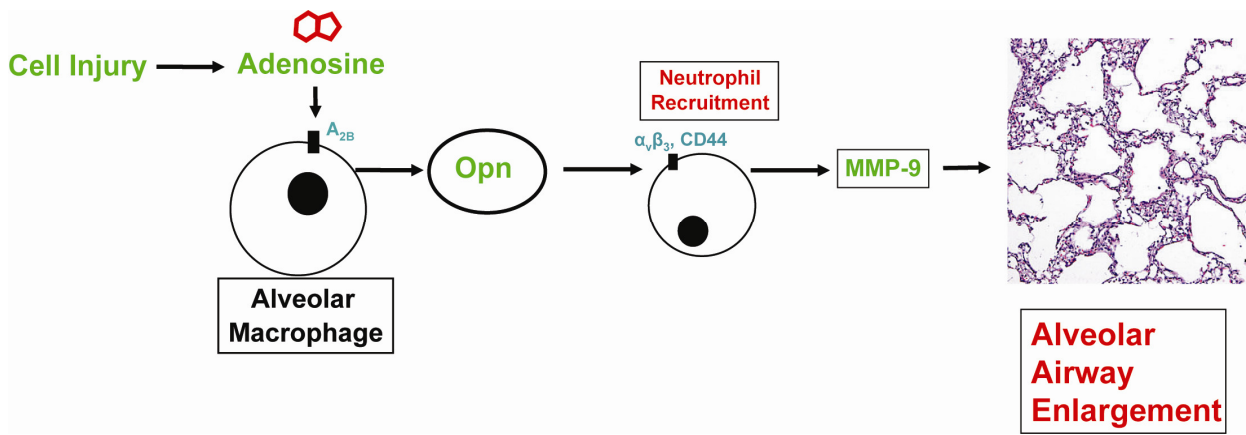


**Figure 3.23 - Schematic representation of OPN-mediated air-space enlargement**

Repeated tissue injury results in chronic elevations in extracellular adenosine levels. As a result, A<sub>2B</sub> adenosine receptors on macrophages are engaged promoting the upregulation and secretion of OPN. This promotes the recruitment of neutrophils via chemotaxis through engagement of cell surface receptors CD44 and α<sub>v</sub>β<sub>3</sub> integrin. Increased neutrophils in the distal airways release proteases including MMP-9 leading to the destruction and enlargement of alveolar air-spaces.

had dramatically reduced size of alveolar air-spaces compared to *Ada*<sup>-/-</sup> mice (Figure 3.7). Microarray analysis of alveolar macrophages isolated from smokers identified upregulations in OPN and found it was the only protein that correlated with severity of airway obstruction (101). Results of our studies demonstrate that the majority OPN immunolocalization in human COPD lung samples is present in alveolar macrophages (Figure 3.21) and this expression is associated with severity of airway obstruction (Figure 3.22). Given these findings and the report that adenosine levels are elevated in patients with COPD (31), our findings suggest that adenosine-dependent regulation of OPN may be a major driving mechanism of emphysema.

Our studies indicate that OPN<sup>-/-</sup> mice exhibit slightly reduced air-space size at postnatal day 37 versus *Ada*<sup>+</sup> mice. Additionally, there are reports that OPN is down-regulated in lungs of rats during secondary septation (116) and OPN is up-regulated in models exhibiting defective alveolarization (116, 117). Collectively, this suggests that reduced OPN expression in air-spaces at stages of secondary septation is associated with alveolar air-space development resulting in smaller average air-space size. However, *Opn*<sup>-/-</sup> mice display no significant changes in average air-space size compared to *Ada*<sup>+</sup> mice at postnatal day 10 (Figure 3.15). These results confirm that OPN does not significantly influence developmental alterations in air-space size and support conclusions that OPN contributes to pathologic enlargement of alveolar air-spaces.

A<sub>2B</sub>R signaling has been shown to contribute to the pathogenesis of emphysema in the *Ada*<sup>-/-</sup> model (71). This is in association with increases in recruitment of neutrophils and macrophages as well as upregulations of MMP-9, MMP-12, TIMP-1 and OPN. These results indicate that OPN is a significant mediator of alveolar air-space destruction downstream of A<sub>2B</sub>R signaling given that *Ada/Opn*<sup>-/-</sup> mice are protected from A<sub>2B</sub>R-mediated air-space enlargement and display reductions in neutrophils and MMP-9 (Figure 3.9). Though these findings do not address or rule out the contribution of alveolar macrophages or MMP-12 to the development of emphysema in this model, they do suggest that OPN-dependent changes in air-space size are a result of pulmonary neutrophilia and increased activity of MMP-9. This is consistent with reports (88, 89) on mechanisms OPN-mediated malignant transformation describing OPN signaling through the  $\alpha_v\beta_3$  integrin receptor leading to increased activation of MMP-9. Furthermore, elevations in OPN are described in other disease processes such as ARDS (99, 118) and bronchiolitis obliterans (100) which display influx of neutrophils and MMP-9 in association with alveolar air-space destruction and remodeling. Also, neutrophils have a

well-recognized role in the pathogenesis of emphysema (119). Taken together, this supports the model that A<sub>2B</sub>R-dependent upregulations of OPN result in increased chemotaxis of neutrophils leading to MMP-9 mediated alveolar air-space destruction.

Finally, in addition to enhanced OPN expression and air-space destruction, *Ada*<sup>-/-</sup> mice and patients with COPD and ARDS all display associated increases in pulmonary angiogenesis (99). The finding of reduced angiogenesis in *Ada/Opn*<sup>-/-</sup> mice is supported by the established role of OPN and the  $\alpha_v\beta_3$  receptor in the process of angiogenesis (76, 81). These results display additional evidence for reduced lung pathology in the absence of OPN and potentially suggest an additional role of OPN-dependent angiogenesis in adenosine-mediated lung pathology.

Overall, these findings clearly indicate OPN is a physiologically relevant mediator of neutrophil chemotaxis and outline a mechanism for OPN-driven emphysema in the lung. An attempt to display contribution of CD44 signaling to pulmonary neutrophilia and emphysema in the *Ada*<sup>-/-</sup> model was inconclusive (Figure 3.12). However, it is well-established that the putative OPN receptors CD44 and  $\alpha_v\beta_3$  are an integral part of OPN-driven inflammatory and malignant pathogenesis and pharmacologic therapies targeting these receptors for these conditions have been developed (120, 121). Only recently are these receptors and OPN realized to function in a similar fashion to drive the pathogenesis of acute and chronic lung disease. Hence, it is clear that further investigation of CD44 and  $\alpha_v\beta_3$  in the pathogenesis of COPD and other chronic lung diseases is warranted.

Other phenotypic features consistent with COPD in *Ada*<sup>-/-</sup> mice include mucus metaplasia (30). It has been reported previously that engagement of the A<sub>3</sub> adenosine receptor is responsible for mucus metaplasia in *Ada*<sup>-/-</sup> mice (22). However, recent studies in models of allergic airway disease demonstrated that genetic removal of OPN protected mice from inflammation and mucus production (96, 106). Our findings indicate that while genetic removal of OPN attenuated pulmonary inflammation, mucus production was unchanged (Figure 3.17). This suggests that elevated adenosine levels engage other pathways leading to mucus metaplasia in this model.

Another feature of *Ada*<sup>-/-</sup> mice is the development of pulmonary fibrosis (26) characterized by increased collagen production and deposition in association with myofibroblasts within fibrotic foci in the distal air-spaces (122). In conjunction with these pathologic changes are elevated profibrotic mediators including TGF- $\beta_1$ , MMP-2, PAI-1, and

uPA. Several recent publications report that *Opn*<sup>-/-</sup> mice are protected from tissue fibrosis (97, 98, 110, 111) and there is suggestion that OPN directs the differentiation of fibroblasts into myofibroblasts (123). While genetic removal of *Opn* in *Ada*<sup>-/-</sup> mice largely resolved features of emphysema, major indices of pulmonary fibrosis were unchanged. Specifically, *Ada*<sup>-/-</sup> and *Ada/Opn*<sup>-/-</sup> mice both exhibited increased soluble collagen, collagen production and deposition within fibrotic foci represented by increased  $\alpha$  SMA staining within the distal air-spaces (Figure 3.18). Furthermore, there were no differences in major profibrotic mediators TGF- $\beta$ <sub>1</sub>, MMP-2, and uPA associated with the genetic removal of *Opn* in *Ada*<sup>-/-</sup> mice (Figure 3.19A-C). These results suggest that OPN is not required for the development of pulmonary fibrosis in the *Ada*<sup>-/-</sup> model.

In contrast, expression of PAI-1, a protease inhibitor implicated in the pathogenesis of fibrosis (124), was reduced in *Ada/Opn*<sup>-/-</sup> mice (Figure 3.19D). This is consistent with reports that elevated systemic concentrations of PAI-1 are reduced in *Opn*<sup>-/-</sup> mice (125). While the genetic removal of *Opn* in *Ada*<sup>-/-</sup> mice did not affect the number of myofibroblasts or production and deposition of collagen, significant reductions were observed in fibronectin expression and deposition (Figure 3.20). Consistent with OPN-dependent changes in air-space enlargement, increased detection of extracellular matrix proteins, including collagen and fibronectin, are associated with inflammation-driven alveolar destruction seen in animal models (126) and in patients with COPD (113), ARDS (99), and bronchiolitis obliterans (127). These results suggest that OPN selectively drives the expression of fibronectin in the lungs of *Ada*<sup>-/-</sup> mice. Similarly, it may be interpreted that fibronectin expression is relatively sensitive to changes in inflammation-mediated alveolar air-space damage and that overriding profibrotic mechanisms driving the production of collagen exist independent of inflammation and OPN expression. These findings provide important insight into the potential disconnect between inflammation and the onset of fibrosis. In summary, despite evidence revealing OPN is not required for the development of fibrosis in this model, we observed OPN may contribute to select features and may be a beneficial therapeutic target for pulmonary fibrosis at certain stages of disease.

In conclusion, results of this study demonstrate *in vivo* OPN-mediated recruitment of neutrophils, protease activation, and angiogenesis. These findings are consistent with the hypothesis that OPN contributes to the pulmonary phenotype in *Ada*<sup>-/-</sup> mice. This body of work was the first report of OPN-dependent alveolar air-space destruction and enlargement. Furthermore, this work was the first to demonstrate elevated OPN expression in patients with the emphysema subtype of COPD. Drugs targeting the A<sub>2B</sub> adenosine receptor, CVT-6883,

and neutrophil-recruiting chemokines and their receptors are currently in different phases of clinical trials for the treatment of COPD/emphysema (128, 129). The results of this study will guide the school of thought that A<sub>2B</sub>R signaling and neutrophil trafficking are important in the onset and progression of this condition. This will aid future neutrophil-targeted and A<sub>2B</sub>R-based therapeutics for the treatment of COPD. Finally, given the ability of OPN to regulate multiple processes promoting the pathogenesis of COPD, this study introduces OPN as an attractive biomarker candidate to follow disease progression or a therapeutic target in the treatment of these patients.



# **Chapter 4**

## **Cadherin 11 and pulmonary fibrosis**

## **Chapter 4 - Introduction**

### **Pulmonary fibrosis**

Pulmonary fibrosis is a histopathologic feature of chronic lung diseases of the interstitium affecting the large and small airways and distal air-spaces of at least 200,000 Americans (15, 16). Particularly severe forms, such as idiopathic pulmonary fibrosis (IPF) carry a mean survival rate of 3-5 years (130) and the only available treatment is lung transplantation. Changes associated with fibrosis include distorted lung architecture and excessive, dysregulated deposition of collagen which impairs gas exchange. Repeated, often insidious tissue injury leading to chronic inflammation is thought to be the origin of fibrosis. In fact, many similarities exist between pathways and cell types activated during normal wound healing and fibrosis. Full understanding of how these pathways shift away from normal healing toward fibrosis will ultimately further knowledge of its pathogenesis and hopefully lead to adequate management of these devastating conditions.

Normal wound healing is a temporal process encompassing the recruitment and activation of several different cell types (8, 131). Epithelial and endothelial cell damage recruits platelets to the site of injury providing the initial fibrin clot, hemostasis, and the release of cytokines, chemokines and growth factors. These factors induce chemotaxis, permeabilization and regional vasodilation to facilitate inflammatory cell influx. These cells secrete antimicrobial agents and remove invading organisms, damaged host tissue, and foreign debris. Angiogenic factors are also secreted stimulating the migration endothelial cells and neovascularization. Inflammatory cells also secrete profibrotic factors such as PAI-1, IL-13, PDGF, IL-6, and TGF- $\beta$  that promote the activation, migration, and differentiation of various cell types and the formation of myofibroblasts. These cells secrete ECM and promote contraction of tissue at the wound site to facilitate closure and re-epithelialization. Proper degradation of deposited ECM by matrixmetalloproteases and departure of myofibroblasts from the repair site are necessary steps to finalize the wound healing process.

For reasons poorly understood, in the setting of chronic inflammation and repeated tissue injury, there is a shift toward excessive production of profibrotic mediators leading to enhanced formation and survival of myofibroblasts (8, 18). This ultimately promotes progressive accumulation of collagen and the development of fibrosis. Investigation into aberrations in the wound healing process and the regulation of myofibroblast biology is an area of intense investigation in hopes of developing therapeutic targets to halt and/or reverse the

progression of fibrosis. Recent studies demonstrate that a subset of the myofibroblast population in pulmonary fibrosis arises from bone marrow progenitor cells known as fibrocytes (132, 133). These cells express collagen and localize to the lung in response to injury. Pharmacologic and adoptive transfer studies have demonstrated that fibrocytes contribute to the pathogenesis of pulmonary fibrosis. Other proposed sources of myofibroblasts arise from differentiation of resident cell types in the lung in response to changes in the tissue milieu following long-standing injury.

### **TGF- $\beta$ in pulmonary fibrosis**

As previously mentioned, numerous cytokines, chemokines, and growth factors are released from resident and inflammatory cells following injury. During the acute stages of inflammation, TGF- $\beta$  interestingly serves an anti-inflammatory role during clearance of apoptotic cells (134, 135). However, in scenarios of sustained tissue injury and prolonged release of TGF- $\beta$ , there is a shift from anti-inflammatory to a profibrotic role (136-138). Elevations in TGF- $\beta$  are reported in patients with IPF (139) and animal models of pulmonary fibrosis. TGF- $\beta$  over-expression worsens fibrosis and blocking TGF- $\beta$  interactions with its receptor prevents fibrosis in animal models. Naturally, tissue injury increases production of TGF- $\beta$  prior to measurable increases in extracellular matrix. Furthermore, TGF- $\beta$  is sufficient to promote the differentiation (140) and survival of myofibroblasts and is a potent stimulator of extracellular matrix production and deposition (141). Finally, TGF- $\beta$  stimulation of alveolar epithelial cells increases production of mesenchymal markers such as vimentin, N cadherin, type I collagen, and  $\alpha$  smooth muscle actin and decreases expression of epithelial cell markers. These findings demonstrate that TGF- $\beta$  induces pulmonary fibrosis by increasing myofibroblasts in alveolar airways through differentiation of fibroblasts and epithelial to mesenchymal transition.

### **Epithelial to mesenchymal transition (EMT)**

Epithelial cells characteristically have cell polarity and cell-to-cell adhesion creating barriers or surfaces for absorption. In contrast, mesenchymal cells have diminished cell-to-cell contact, reduced polarity, and have a propensity for migration and invasion. The transition between these two cell types, EMT, is a regulated process occurring in normal and pathologic scenarios. This phenotypic change in cells is required in all organisms for migration of cells in developing tissue structure in embryos. Cancer cells undergoing malignant transformation destabilize cell-to-cell junctions and acquire a more invasive, mesenchymal phenotype to

facilitate migration and metastasis away from primary tumors. Epithelial cells adjacent to wounded tissue acquire migratory and mesenchymal characteristics consistent with EMT to facilitate wound closure (142, 143). Similarly, lineage-tracing in transgenic mice also indicates that hepatocytes undergo EMT during liver fibrosis (144), as do the alveolar epithelial cells during the pulmonary fibrosis induced by TGF- $\beta$  (145) contributing to the population of myofibroblasts in fibrotic foci (146).

Epithelial and mesenchymal cells characteristically display differential expression of proteins which function to promote the aforementioned phenotypic differences between the two cell types. Regulation of proteins involved in stabilization of epithelial cell-to-cell junctions and reorganization of the actin cytoskeleton are key processes in the transition of epithelial cells to a mesenchymal phenotype. Cadherins are a family of proteins which play a direct role in these functions facilitating EMT. Results outlined later in this chapter will demonstrate a novel role for cadherin 11 (CDH11) in promoting pulmonary fibrosis through the regulation of EMT.

### **Cadherins and EMT**

Cadherins are a group of transmembrane glycoproteins known for mediating calcium-dependent homophilic cell-to-cell adhesion at points of cell-cell contact known as adherens junctions (147). The cadherin cytoplasmic tail is a highly conserved region which interacts with  $\beta$ -catenin. In conjunction,  $\alpha$  catenin may bind with  $\beta$  catenin providing a functional link between cadherins and the actin cytoskeleton. Through this, cadherins are regulators of cell shape, polarization, cell junction stability, and tissue architecture (147). During embryogenesis, cadherins dictate patterns of cell differentiation, morphogenesis, migration and invasion. Similar cadherin-dependent functions play a critical role in certain pathologies exhibiting EMT such as cancer. The most widely studied of these are E cadherin (Cadherin 1) and N cadherin (Cadherin 2).

E cadherin, typically found in epithelial cells, is localized to adherens junctions and plays a pivotal role in the structural maintenance of the epithelial cell lining in a variety of tissues. N cadherin is the prototypical mesenchymal-type cadherin typically expressed in motile and invasive cell types including fibroblasts, epithelial cells undergoing EMT, and invasive cancers (148). Disruption of E cadherin function through down-regulation or knockdown of cancer cells *in vitro* leads to diminished cell-to-cell contact, disruption of typical epithelial cell organization, and increased migratory and invasive capacity (149, 150). It follows that poorly differentiated, invasive cancers characteristically show reduced expression of E cadherin. In contrast expression of N cadherin correlates with migratory and invasive capacity of cancers *in vivo* and

*in vitro* (151). Thus, these genetic reprogramming events are hallmarks of EMT-dependent tumor progression. It follows that loss of E cadherin (152-154) and gain of N cadherin (145, 155) in cells of epithelial origin translate to EMT in fibrosis of multiple organs including the lung.

### **Cadherin 11 (CDH11)**

CDH11 is another mesenchymal cadherin and expression is associated with mesenchymal morphogenesis, motility, and invasion. Namely, during development increased CDH11 expression correlates with cell migration and outgrowth (156). CDH11 is also preferentially expressed in migratory and invasive breast cancer cell lines (157). Finally, CDH11 is present on fibroblast-like synoviocytes in the joint (158) and promotes the invasive behavior of these cells in a model of rheumatoid arthritis (159) contributing to its overall pathogenesis (23). These findings suggest that CDH11 influences a specific invasive and mesenchymal phenotype in cells and if extrapolated to lung epithelial cells, is consistent with the process of EMT. However, the role of this specific cadherin in the process of lung EMT has not been investigated.

In addition, there is evidence to suggest that CDH11 may also be important in the differentiation of myofibroblasts. CDH11 is increased at sites of wound healing (160) suggesting its role in the physiology of myofibroblasts during repair of injured tissue. This was corroborated with the detection of increased CDH11 in subcutaneous and lung fibroblasts stimulated with TGF- $\beta$  to differentiate into myofibroblasts. Further, CDH11 is increased in biopsies taken from fibrotic skin of patients with scleroderma versus normal tissue (161, 162). Thus, CDH11 is upregulated during normal wound healing and pathologic skin fibrosis, yet its role in pulmonary fibrosis has not been examined.

These findings led to **the hypothesis that cadherin 11 contributes to the pathogenesis of pulmonary fibrosis**. To address this, utilizing both genetic and pharmacologic approaches, we examined the contribution of CDH11 to the standard bleomycin model of pulmonary fibrosis. Further, we examined the expression of CDH11 in various samples obtained from patients with IPF. CDH11 expression was demonstrated in two cell types in lungs of the bleomycin model and patients with IPF: alveolar macrophages and hyperplastic airway epithelial cells. In addition, the contribution of CDH11 to EMT was examined in an *in vitro* model. The results of this study demonstrate that both of these cell types contribute to CDH11-dependent pulmonary fibrosis through the regulation of EMT and TGF- $\beta$  production.

## **Chapter 4 - Results**

### **Expression and localization of CDH11 in patients with ILD**

To address the role of CDH11 in pulmonary fibrosis, *Cdh11* transcripts and CDH11 protein were examined in IPF patients with severe airway restriction versus IPF patients with normal lung function (Figure 4.1A,B). Immunolocalization was performed to determine cell types expressing CDH11 in lungs of patients with IPF. The cell type expressing CDH11 identified in both mild (Figure 4.1C) and severe IPF patients (Figure 4.1E) was the alveolar macrophage, while only severe IPF patients displayed expression in hyperplastic alveolar epithelial cells (AECs) adjacent to fibrotic foci (Figure 4.1D). These results indicate an association of CDH11 expression with disease severity. Further, CDH11 immunolocalization in hyperplastic AECs and alveolar macrophages directed subsequent studies of these cell types to ascertain the potential function of CDH11 in fibrosis.

### **Expression and localization of CDH11 in bleomycin model of pulmonary fibrosis**

The intratracheal bleomycin model is the most commonly utilized animal model to study mechanisms of pulmonary fibrosis. To examine the contribution of CDH11 to this model, initial characterization included RNA, protein levels, and immunolocalization for CDH11 in wild type mice given intratracheal saline and bleomycin. While results of whole lung *Cdh11* mRNA expression demonstrate no differences at day 21 between saline and bleomycin (Figure 4.2A), western blot indicates increased protein levels of CDH11 in mice given bleomycin (Figure 4.2B). Similar to findings in patients with IPF, immunohistochemistry on lungs from mice given bleomycin displays CDH11 in hyperplastic AECs and alveolar macrophages (Figure 4.2D). These results demonstrate similarities between this mouse model and humans and support analysis of these cell types in addressing the mechanism of CDH11-dependent fibrosis.

### **Immunofluorescence detection of CDH11 on alveolar macrophages**

Findings in lung sections of patients with IPF and mice given bleomycin indicate immunolocalization of CDH11 to alveolar macrophages. This is the first indication of CDH11 expression on any cell of hematopoietic origin. Therefore, to carefully examine CDH11 expression on alveolar macrophages, cytopins obtained from BAL fluid of a patient with ILD were incubated with N cadherin Ab (Figure 4.3B), two CDH11 Abs recognizing different

domains (Figure 4.3C,D), and a corresponding isotype control (Figure 4.3A). Results demonstrate very low baseline levels of fluorescence in the N cadherin cytospin versus isotype

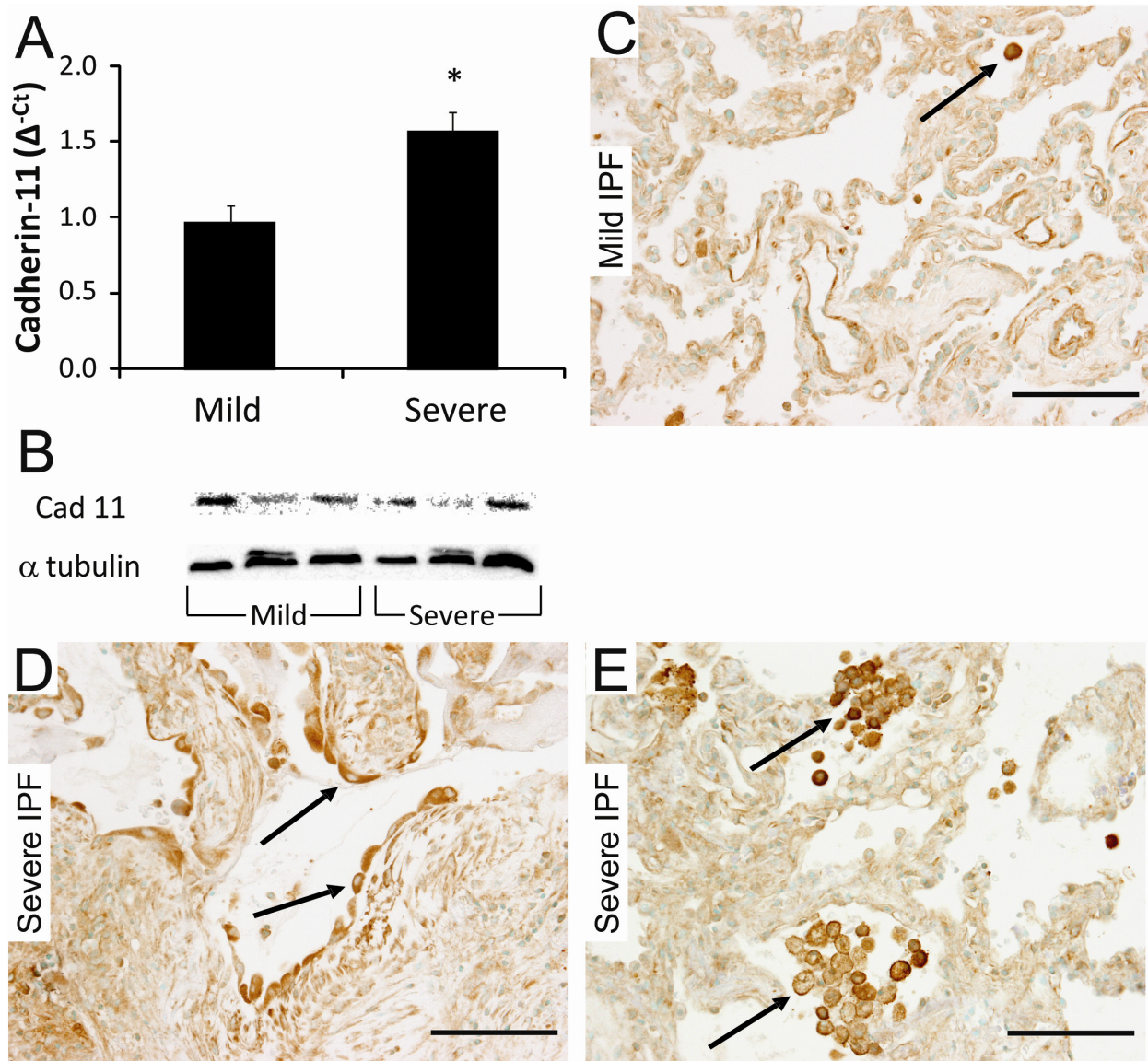


**Figure 4.1 - Cadherin 11 expression and immunolocalization in human IPF patients**

(A) Quantitative RT-PCR measuring *Cdh11* transcripts present in RNA isolates from biopsies taken from IPF patients with mild and severe airway restriction. Transcripts for *Cdh11* were measured in parallel with PPIA and values are presented as mean normalized transcript levels ( $\Delta^{-Ct}$ )  $\pm$  SEM.  $n = 10$  (mild IPF);  $n = 10$  (severe IPF). \* $P \leq 0.05$  versus mild IPF. Immunolocalization for CDH11 in representative lung sections of (C) mild IPF and (D,E) severe IPF patients. Arrows denote staining present in (C,E) alveolar macrophages and (D)

hyperplastic alveolar epithelial cells. Scale bars = 100  $\mu\text{m}$ . Displayed sections are representative of n = 10 (mild IPF) and n = 10 (severe IPF).



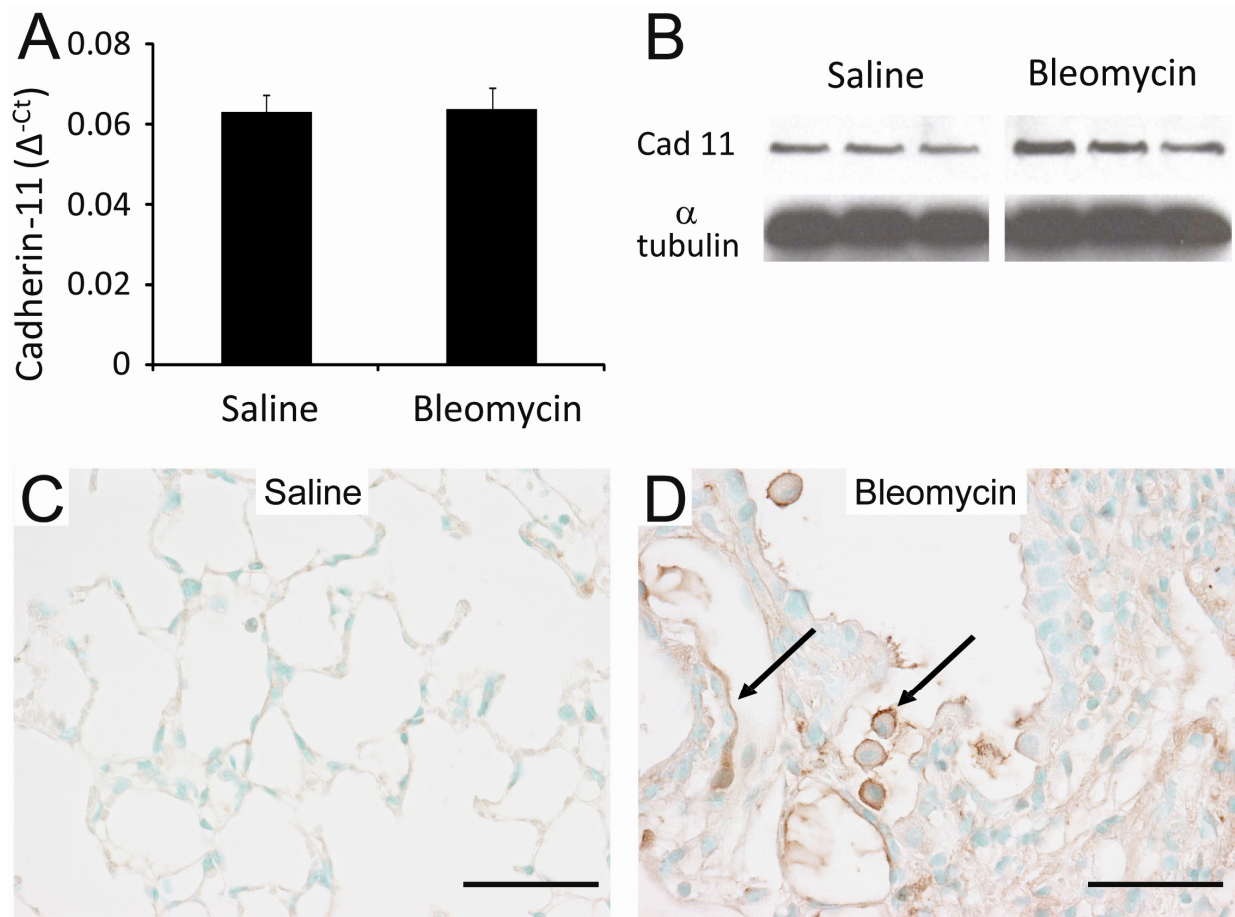


**Figure 4.2 - Cadherin 11 expression and localization in bleomycin-induced fibrosis**

(A) Quantitative RT-PCR measuring *Cdh11* transcripts present in whole lung RNA isolates from mice at day 21 after intratracheal saline and bleomycin. Transcripts for *Cdh11* were measured in parallel with PPIA and values are presented as mean normalized transcript levels ( $\Delta^{-Ct}$ )  $\pm$  SEM.  $n = 5$  (saline);  $n = 5$  (bleomycin). (B) Western blot for CDH11 from lung homogenates isolated from mice given bleomycin and saline. Immunolocalization for CDH11 in representative lung sections of (C) saline (D) bleomycin-treated mice. Arrows denote staining present in alveolar macrophages and hyperplastic alveolar epithelial cells. Scale bars = 50  $\mu$ m. Displayed sections are representative of  $n = 12$  (saline) and  $n = 20$  (bleomycin).

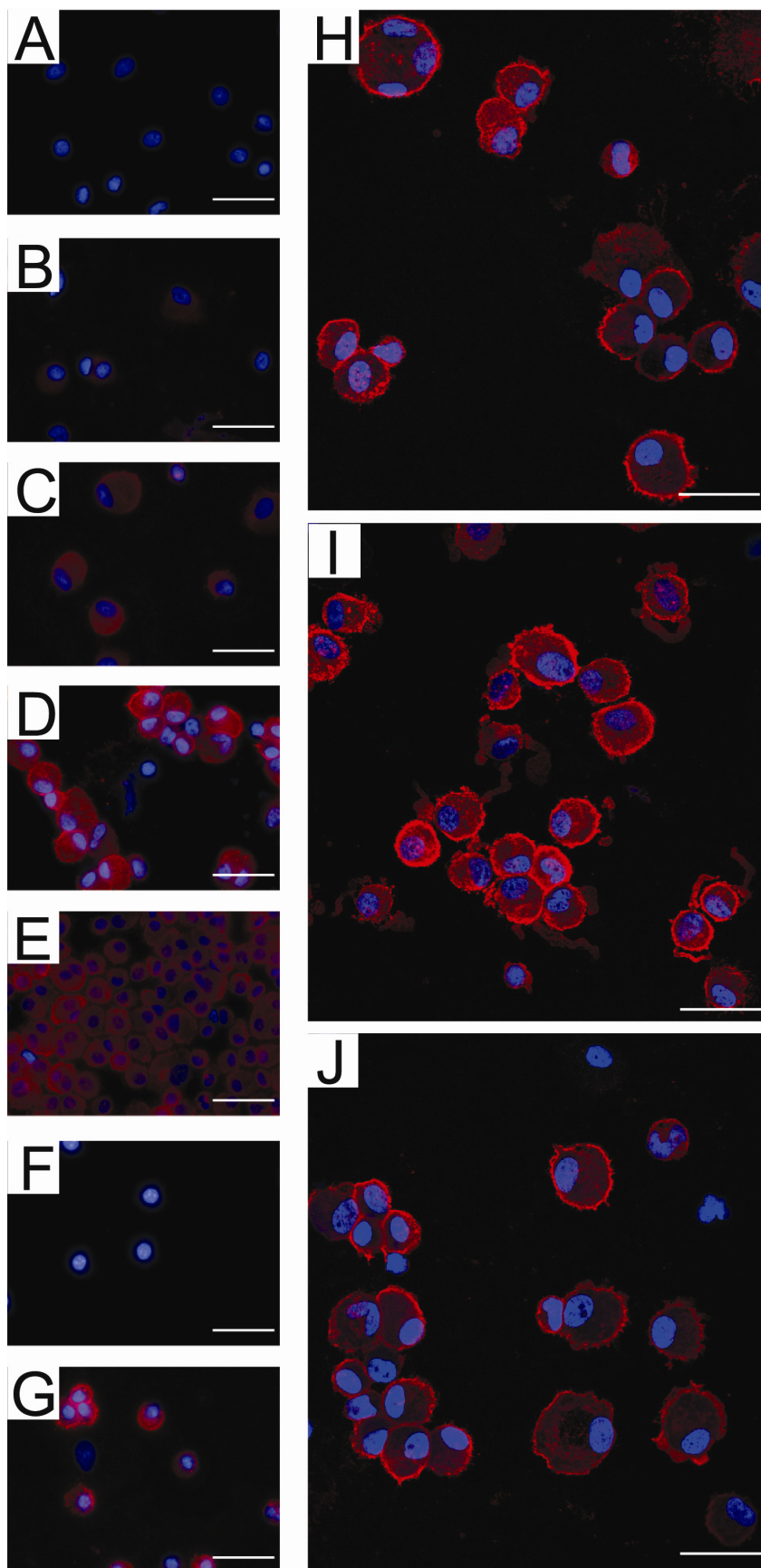


**Figure 4.3 - CDH11 immunolocalization on alveolar macrophages**

Immunofluorescence detection of CDH11 on BAL cytopins. Cells isolated from a patient with ILD (scleroderma) stained with (A) isotype control, (B) N-cadherin, (C) CDH11 (invitrogen), and (D) CDH11 (23C6) antibodies. (E) Cells from a patient with IPF stained with CDH11 (23C6) antibody. Cells from mouse given bleomycin stained with (F) isotype control and (G) CDH11 (23C6) antibodies. Confocal imaging of cells stained with CDH11 (23C6) antibody isolated from a patient with (H) ILD (scleroderma), (I) IPF, and (J) mouse given bleomycin. Scale bars = 50 μm.

control, but increased fluorescence in cytopspins stained with both CDH11 Abs further suggesting alveolar macrophages specifically express CDH11. In a similar manner, cytopspins obtained from a patient with IPF (Figure 4.3E) and from mice given bleomycin (Figure 4.3G) demonstrate immunofluorescence activity for CDH11 on alveolar macrophages. Detailed examination of alveolar macrophages isolated from BAL taken from patients with ILD (Figure 4.3H), IPF (Figure 4.3I), and mice given bleomycin (Figure 4.3J) demonstrates specific expression of CDH11 on alveolar macrophages localized to the cell membrane by confocal microscopy. These results strongly suggest CDH11 expression on alveolar macrophages.

### **Contribution of CDH11 to features of pulmonary fibrosis**

CDH11 confers a mobile, invasive phenotype to key cell types involved in pathologies such as cancer and rheumatoid arthritis. In addition, CDH11 is upregulated in skin biopsies exhibiting fibrosis and in fibroblasts stimulated to differentiate into myofibroblasts. Results above indicate increased CDH11 expression in lungs of patients with IPF and mice with bleomycin-induced fibrosis. To examine the contribution of CDH11 to pulmonary fibrosis, intratracheal bleomycin was administered to mice lacking *Cdh11* (*Cdh11*<sup>-/-</sup>). All endpoints were assessed at 21 days after bleomycin installation. Results of H&E staining display no detectable difference in pulmonary histology between wild type (WT) and *Cdh11*<sup>-/-</sup> mice given saline (Figure 4.4). Examination of lung sections from WT mice given bleomycin displays standard histopathologic features consistent with pulmonary fibrosis including inflammation, fibrotic foci disrupting normal alveolar architecture (Figure 4.4), and increased collagen (Figure 4.5A) and myofibroblasts (Figure 4.5B) in the alveolar air-spaces. These histologic endpoints are substantially reduced in *Cdh11*<sup>-/-</sup> mice (Figure 4.4, 4.5). Quantifiable endpoints consistent with pulmonary fibrosis such as soluble collagen (Figure 4.6A) and Ashcroft scoring (Figure 4.6B) display typical increases in wild type mice given bleomycin versus saline and significant reductions in these endpoints in *Cdh11*<sup>-/-</sup> mice given bleomycin. Collectively, these results suggest that CDH11 contributes to the pathogenesis of pulmonary fibrosis.

### **Systemic delivery of CDH11 blocking Ab improves established pulmonary fibrosis**

Our results display that *Cdh11*<sup>-/-</sup> mice demonstrate reduced fibrosis in response to bleomycin challenge. Well-documented studies indicate pulmonary fibrosis in the bleomycin model is established at least seven days after bleomycin installation (163). Therefore, to



determine if mice with established fibrosis can be successfully treated by targeting CDH11, wild type mice were administered one of two systemic CDH11 blocking Abs (clone 23C6 or 13C2)

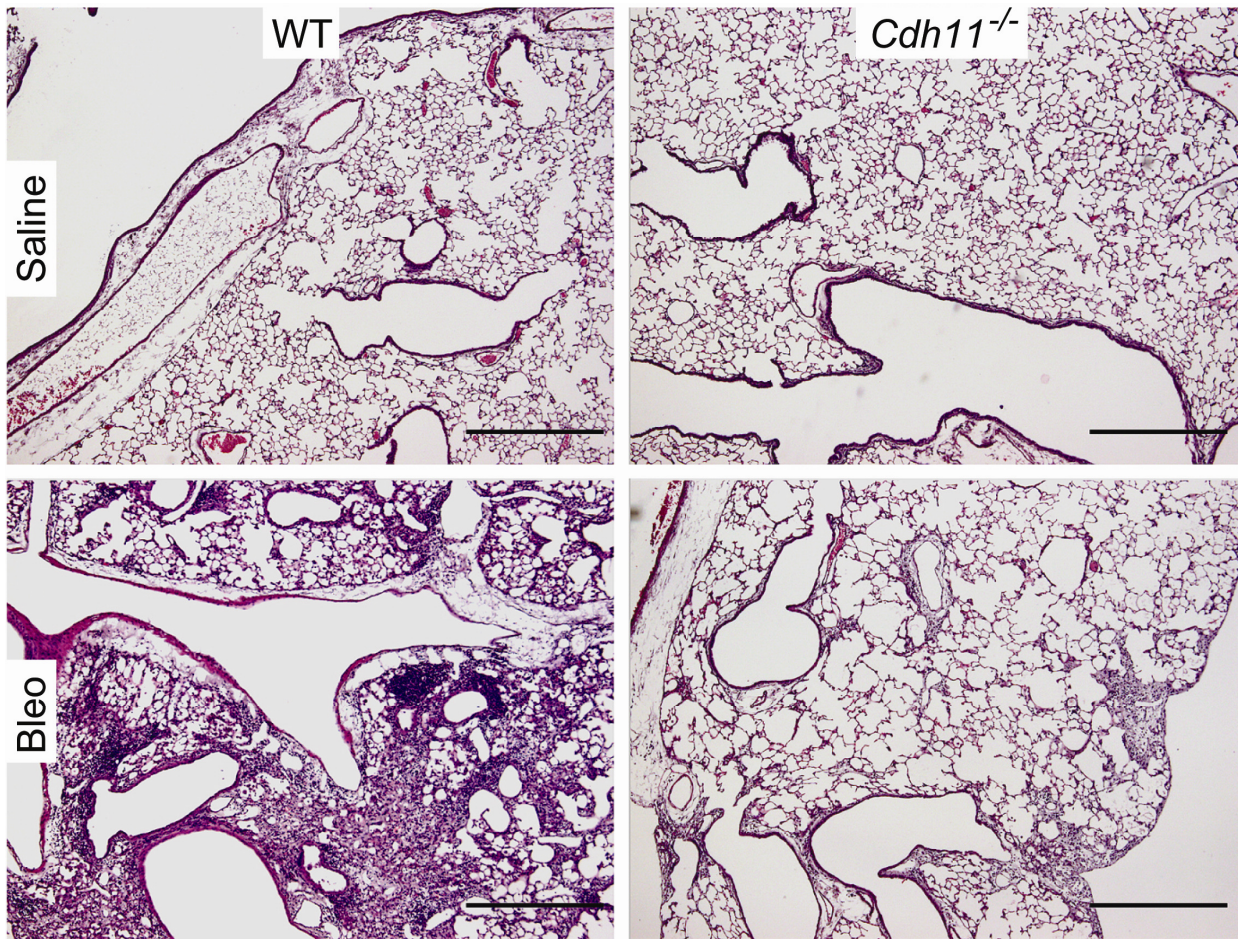


**Figure 4.4 - Cadherin 11-dependent histopathology**

Histopathologic changes in bleomycin-induced pulmonary fibrosis associated with the genetic removal of *Cdh11*. Lungs were taken from mice 21 days after 3.5U bleomycin installation and processed for sectioning and H&E staining. Scale bars = 500  $\mu$ m. Sections are representative of n = 6 WT saline, n = 6 *Cdh11*<sup>-/-</sup> saline, n = 13 WT bleomycin, n = 11 *Cdh11*<sup>-/-</sup> bleomycin.



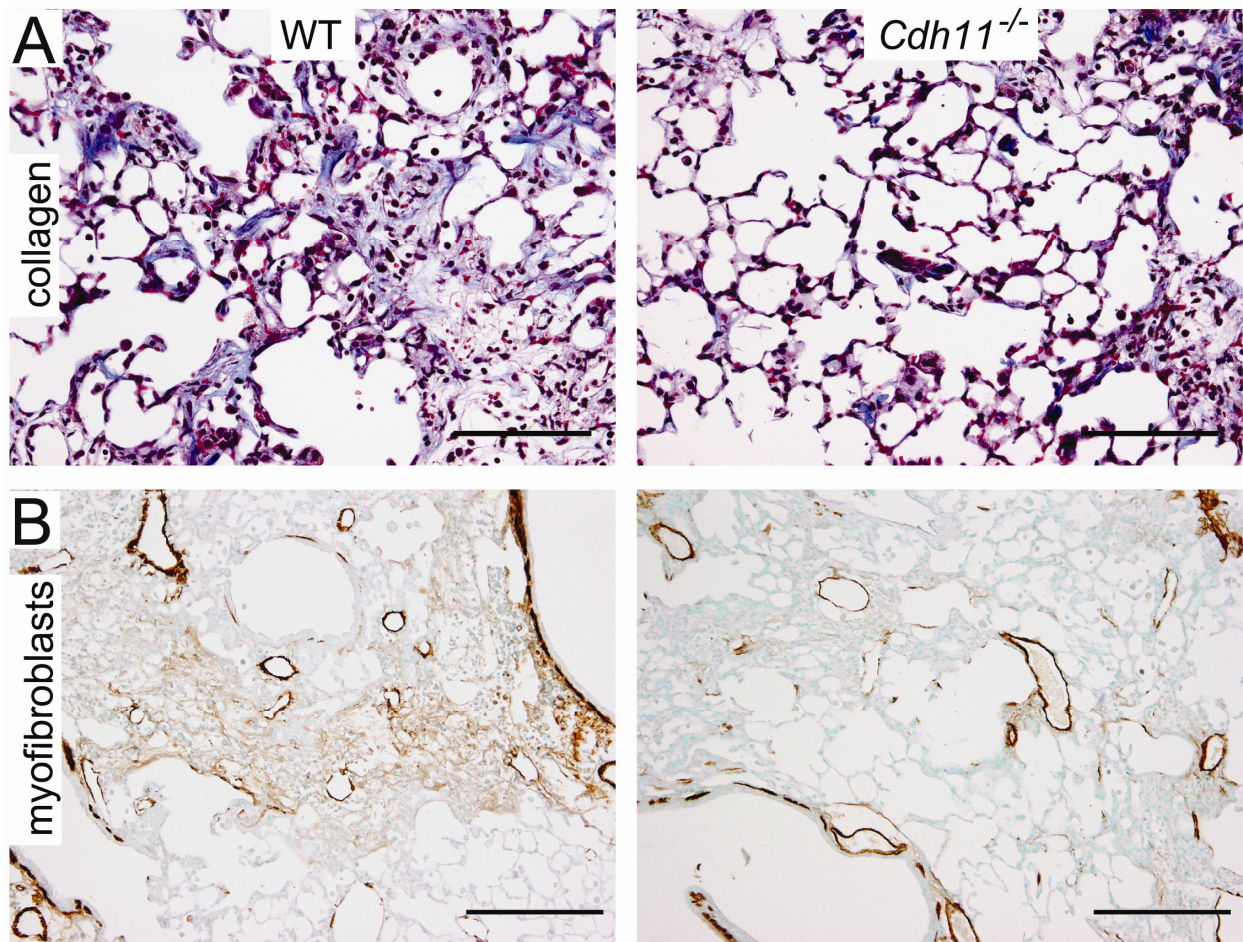


**Figure 4.5 - Histologic evidence of CDH11-dependent myofibroblast formation and collagen deposition**

WT and *Cdh11*<sup>-/-</sup> mouse lungs given bleomycin stained for (A) collagen deposition (Masson's Trichrome stain) and (B) myofibroblasts (α SMA immunohistochemistry). Scale bars = 200 μm. Sections are representative of n = 13 WT bleomycin, n = 11 *Cdh11*<sup>-/-</sup> bleomycin.

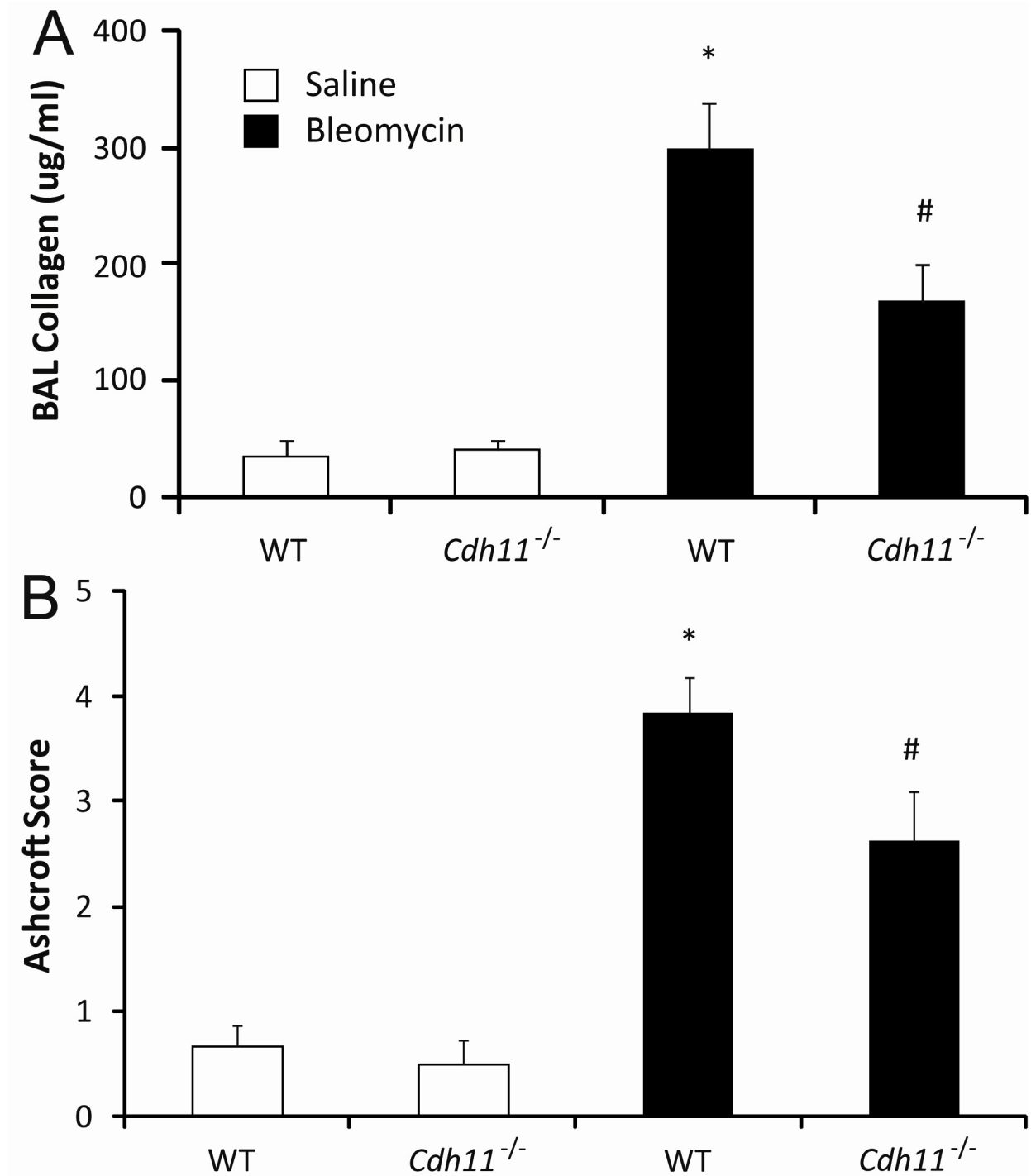


**Figure 4.6 - Quantifiable fibrotic endpoints associated with genetic removal of *Cdh11***

Fibrosis was quantified by determination of (A) BAL collagen via colorimetric assay and (B) Ashcroft scoring on H&E stained lung sections. Scores were determined on 20 images per

mouse lung. n = 6 WT saline, n = 6 *Cdh11*<sup>-/-</sup> saline, n = 13 WT bleomycin, n = 11 *Cdh11*<sup>-/-</sup> bleomycin. \*P ≤ 0.05 versus WT saline; #P ≤ 0.05 versus WT bleomycin.

beginning 10 days after bleomycin installation (Figure 2.1). Lung sections stained with H&E (Figure 4.7), masson's trichrome (Figure 4.8A), and  $\alpha$  SMA immunohistochemistry (Figure 4.8B) all demonstrate markedly reduced histopathology in mice receiving bleomycin plus 23C6 or 13C2 versus mice receiving isotype control Ab. Similarly, soluble collagen levels in mice treated with CDH11 Abs were significantly reduced (Figure 4.8C). These results confirm findings in *Cdh11*<sup>-/-</sup> mice that CDH11 contributes to pulmonary fibrosis and demonstrates systemic delivery of CDH11 blocking Ab successfully treats established disease.

### **CDH11 contributes to EMT in AECs**

Hyperplasia is a suggested characteristic of AECs undergoing the profibrotic process of EMT, *in vivo* (154, 164, 165). Furthermore, results demonstrate CDH11 on hyperplastic AECs in IPF patients (Figure 4.1D) and mice given bleomycin (Figure 4.2D) suggesting CDH11 is an indicator or promoter of EMT. To confirm CDH11 expression in AECs undergoing EMT, A549 cells were stimulated with TGF- $\beta$  *in vitro* and endpoints consistent with EMT were measured. TGF- $\beta$ -stimulated A549 cells demonstrate a trend decrease in E cadherin (Figure 4.9A) expression and expected increases in N cadherin (Figure 4.9B) and collagen production (Figure 4.9C). Results demonstrate a parallel increase in *Cdh11* expression (Figure 4.9D) consistent with findings *in vivo* of CDH11 immunolocalization on hyperplastic AECs (Figures 4.1C, 4.2D).

To determine the contribution of CDH11 to EMT, lung AECs were incubated with siRNA specific for *Cdh11* transcripts and subsequently stimulated with TGF- $\beta$ . Findings display *Cdh11* message was knocked down with approximately 75% efficiency (Figure 4.10A). *Cdh11* knockdown showed a slight reversal of TGF- $\beta$ -induced decrease in E cadherin (Figure 4.10B) and increased N cadherin expression (Figure 4.10C). However, *Cdh11* knockdown substantially reduced TGF- $\beta$ -induced collagen expression (Figure 4.10D). In addition, knockdown prevented the development of mesenchymal morphology in TGF- $\beta$ -stimulated AECs (Figure 4.11). These results display CDH11 contributes to pulmonary fibrosis by regulating the process of EMT in AECs.

### **Role of CDH11 in pulmonary inflammation**



Particularly in the intratracheal bleomycin model, pulmonary inflammation precedes and contributes to the development of pulmonary fibrosis (163). Additionally, inflammatory cells are a source of numerous profibrotic mediators, including TGF- $\beta$ . To determine the effect of CDH11 on pulmonary inflammation, inflammatory cells recovered (Figure 4.12) from BAL fluid

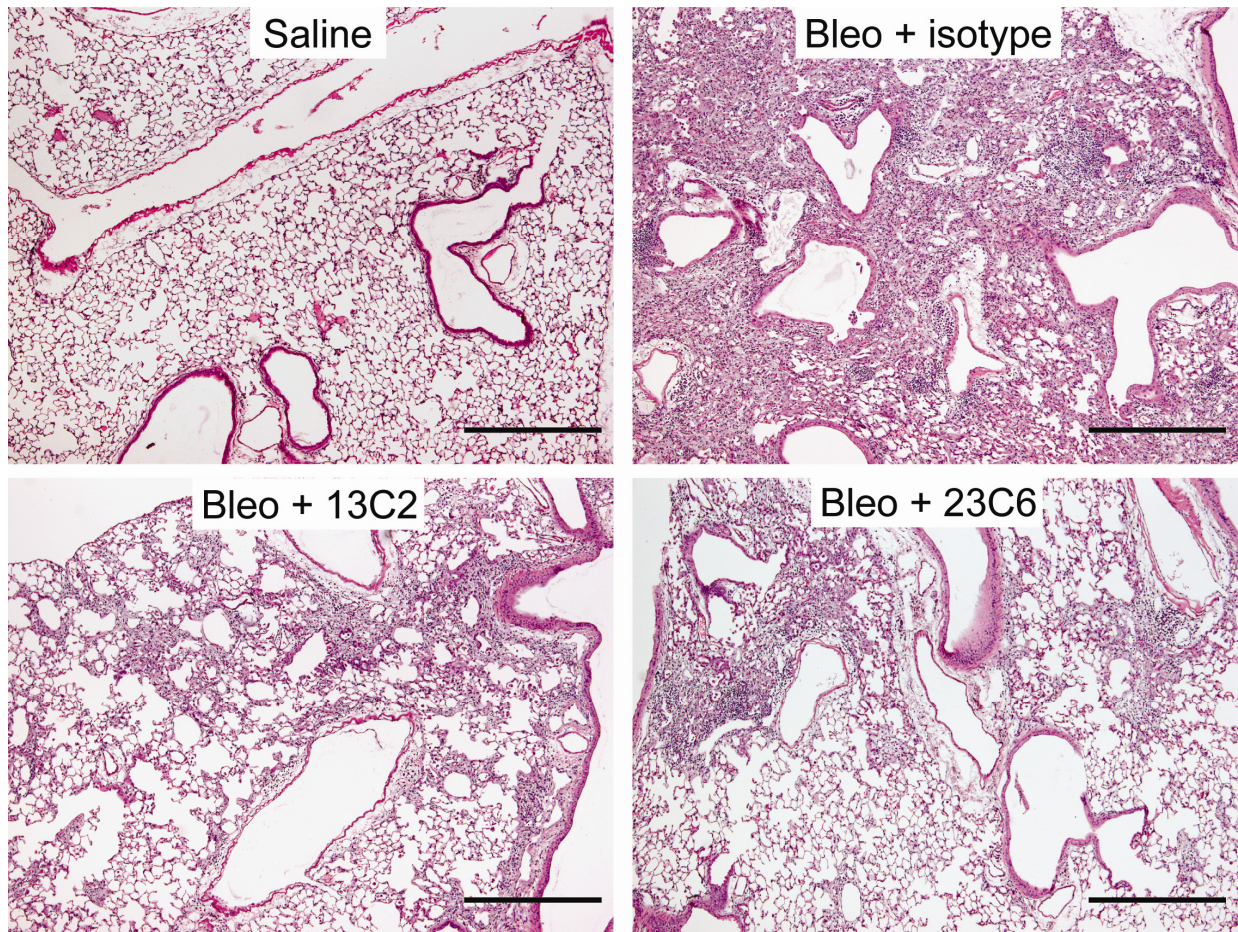


**Figure 4.7 - CDH11 blocking antibody improves established pulmonary fibrosis**

Histopathologic changes in bleomycin-induced pulmonary fibrosis associated with systemic delivery of CDH11 blocking antibody. Mice received antibody every other day beginning 10 days after bleomycin exposure. Lungs were then taken at day 21 and processed for sectioning and H&E staining. Scale bars = 500  $\mu$ m. Sections are representative of n = 6 saline, n = 7 Bleo + isotype, n = 8 Bleo + 13C2, and n = 6 Bleo + 23C6.



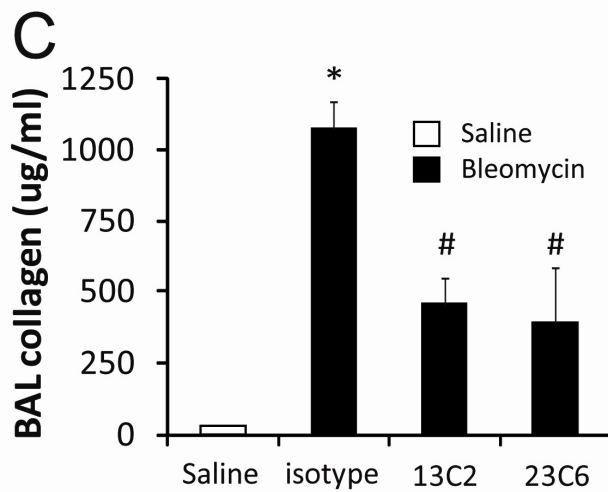
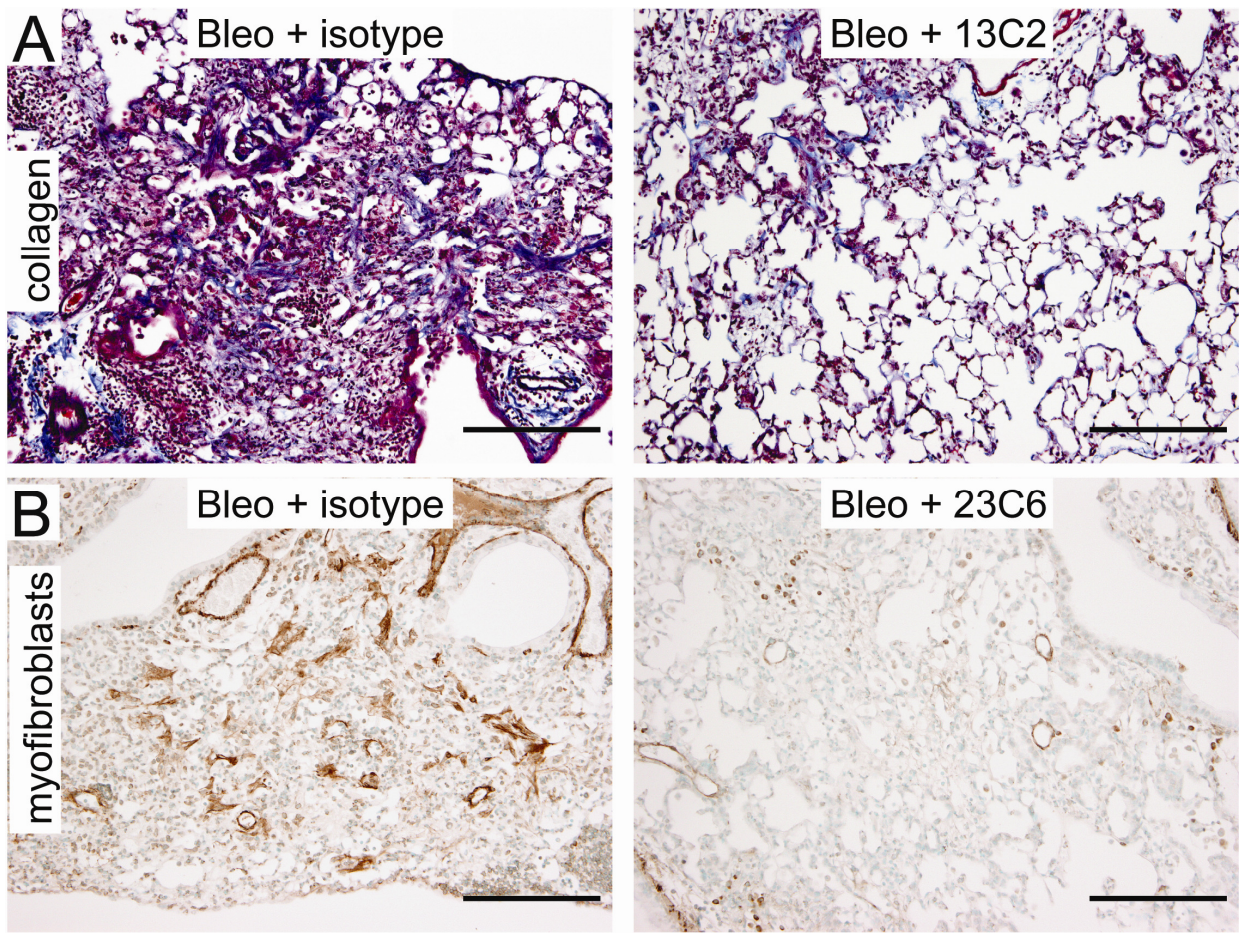


**Figure 4.8 - CDH11 blocking antibody reduces lung myofibroblasts and collagen**

Mouse lungs given bleomycin plus systemic antibody were processed and stained for (A) collagen deposition (Masson's Trichrome stain) and (B) myofibroblasts ( $\alpha$ -SMA immunohistochemistry). Scale bars = 200  $\mu$ m. (C) Soluble collagen in BAL fluid quantified with colorimetric assay.  $n = 6$  saline,  $n = 7$  Bleo + isotype,  $n = 8$  Bleo + 13C2, and  $n = 6$  Bleo + 23C6. \* $P \leq 0.05$  versus saline; # $P \leq 0.05$  versus bleomycin + isotype.

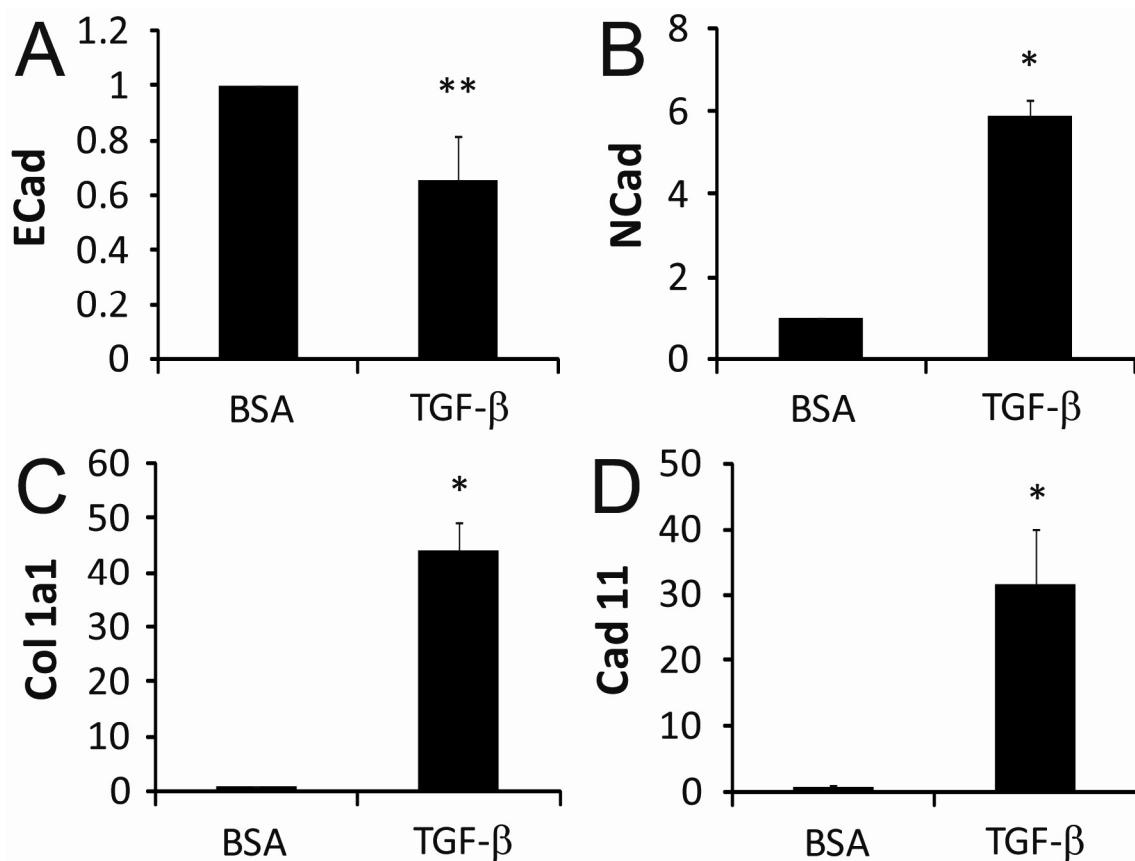


**Figure 4.9 - TGF- $\beta$ -induced EMT and *Cdh11* expression in A549 lung epithelial cells**

A549 lung epithelial cells were stimulated with TGF- $\beta$  (10 ng/ml) and at 24 hours, RNA was isolated and fold change transcripts (vs. BSA) were determined for (A) E cadherin, (B) N cadherin, (C)  $\alpha_1$  pro-collagen, and (D) cadherin 11. \* $P \leq 0.05$  versus BSA. \*\* $P = 0.06$  versus BSA. Data representative of 3 separate experiments. Experiments performed by Sandeep K. Agarwal.

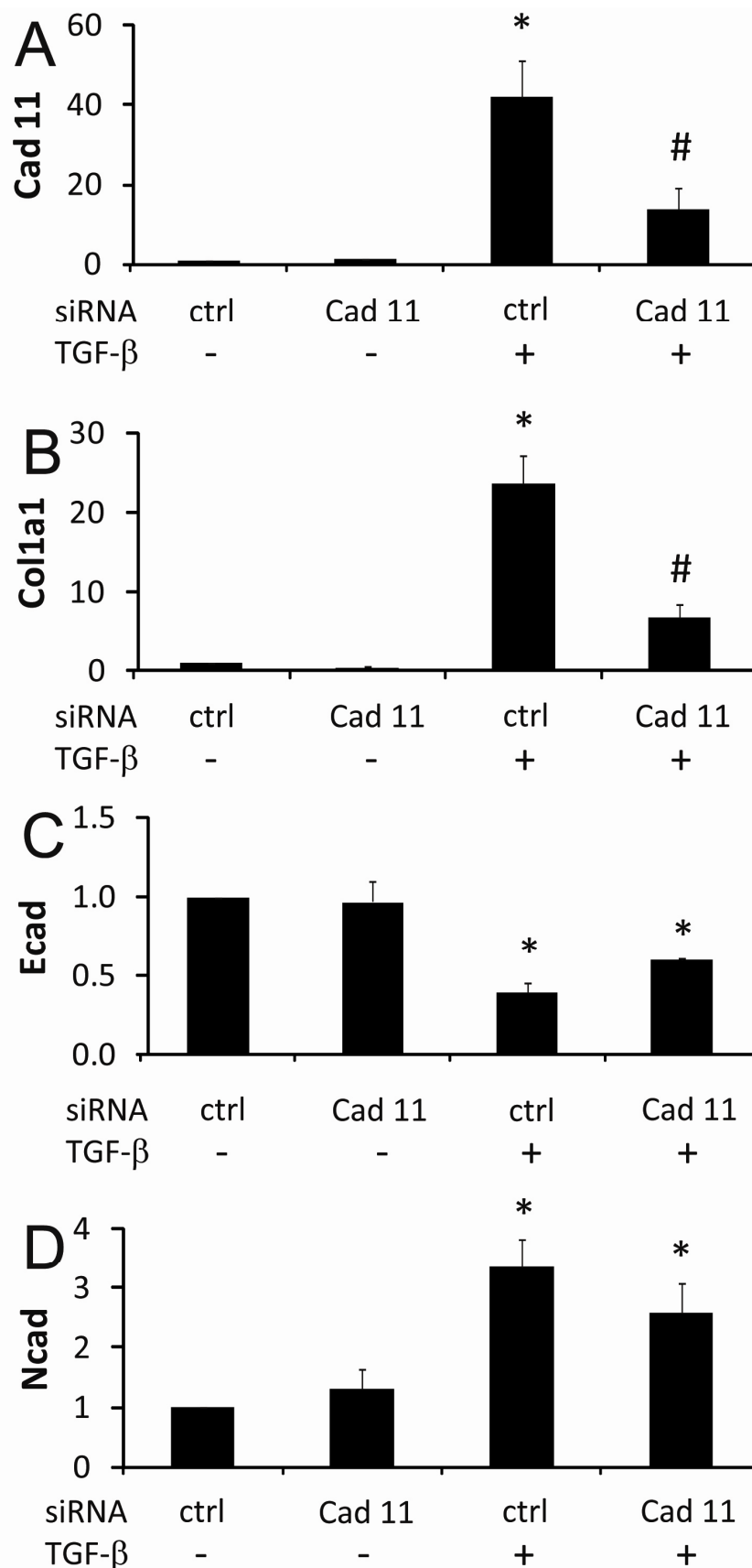


**Figure 4.10 – *Cdh11* knockdown prevents TGF- $\beta$ -induced EMT of lung epithelial cells**

A549 lung epithelial cells were transfected with *Cdh11* or control siRNA, subsequently stimulated with TGF- $\beta$  and at 24 hours, RNA was isolated and fold change transcripts (vs. BSA + control siRNA) were determined for (A) E cadherin, (B) N cadherin, (C)  $\alpha_1$  pro-collagen, and (D) cadherin 11. Data representative of 3 separate experiments. Experiments performed by Sandeep K. Agarwal.



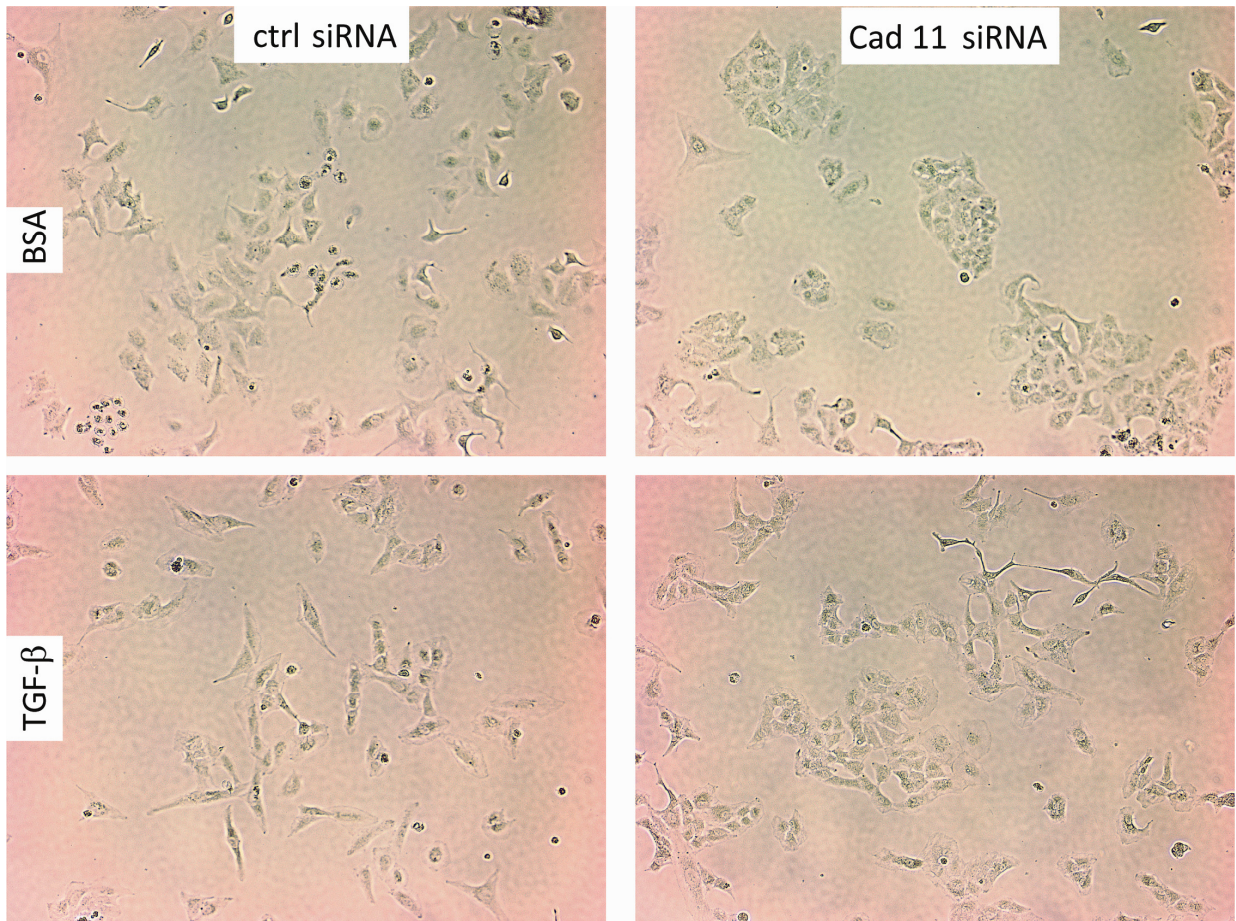


**Figure 4.11 - *Cdh11* knockdown prevents TGF- $\beta$ -induced transition to mesenchymal morphology in lung epithelial cells**

A549 lung epithelial cells were transfected with *Cdh11* or control siRNA and subsequently stimulated with TGF- $\beta$ . At 24 hours cell morphology was assessed using phase contrast microscopy. Experiments performed by Sandeep K. Agarwal.

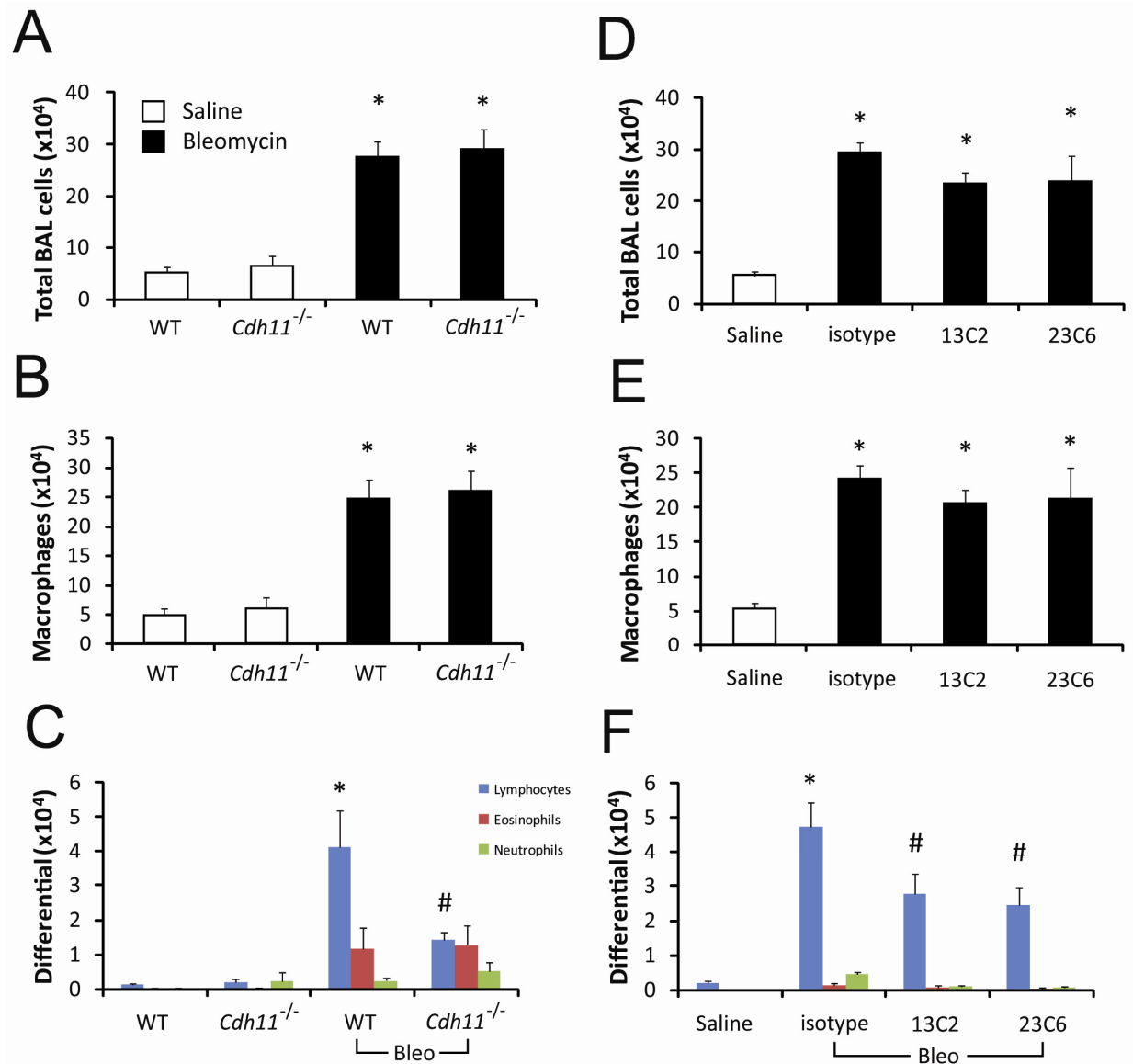


**Figure 4.12 - Contribution of CDH11 to pulmonary inflammation**

(A,D) BAL fluid was collected at day 21 after IT bleomycin and total inflammatory cells were counted. (B, C, E, and F) BAL cells were cytospun and stained with Diff-Quick for the determination of cellular differentials.  $n = 12$  WT saline,  $n = 6$  *Cdh11*<sup>-/-</sup> saline,  $n = 13$  WT bleomycin,  $n = 11$  *Cdh11*<sup>-/-</sup> bleomycin.  $n = 7$  Bleo + isotype,  $n = 8$  Bleo + 13C2, and  $n = 6$  Bleo + 23C6. Values given are mean cell counts  $\pm$  SEM. \* $P \leq 0.05$  versus Saline; # $P \leq 0.05$  versus bleomycin.

were isolated and counted. Results display characteristic increases in macrophages, eosinophils, lymphocytes and neutrophils in mice given bleomycin versus saline. Although pulmonary lymphocyte numbers were reduced in *Cdh11*<sup>-/-</sup> and anti-CDH11 treated mice given bleomycin, pulmonary inflammation was otherwise unchanged. These results suggest that CDH11-dependent profibrotic effects are largely independent of pulmonary inflammation.

### **CDH11-dependent regulation of TGF- $\beta$**

TGF- $\beta$  is a well-recognized profibrotic mediator due, in part, to its ability to induce EMT and the differentiation of myofibroblasts resulting in excess collagen production. Also, TGF- $\beta$  is elevated in bronchoalveolar lavage fluid from mice given bleomycin and patients with pulmonary fibrosis. To determine CDH11-dependent effects on TGF- $\beta$ , BAL fluid levels of soluble TGF- $\beta$  were determined in *Cdh11*<sup>-/-</sup> and anti-CDH11 treated mice given bleomycin. Results demonstrate typical increases in BAL TGF- $\beta$  from WT mice given bleomycin (Figure 4.13A,B). In contrast, *Cdh11*<sup>-/-</sup> mice and anti-CDH11 treated mice given bleomycin displayed markedly reduced levels of BAL TGF- $\beta$ . Further, *Cdh11*<sup>-/-</sup> mice demonstrated significantly lower levels of TGF- $\beta$  at baseline compared to WT mice given saline (Figure 4.13A). Localization studies demonstrate that the majority of TGF- $\beta$  is produced in the alveolar macrophage (166, 167). To isolate and quantify TGF- $\beta$  at its source in the model, total protein was isolated from inflammatory cells pelleted from BAL fluid. Findings display expected increases in cell pellet TGF- $\beta$  isolated from mice given bleomycin, but significant decreases in *Cdh11*<sup>-/-</sup> and anti-CDH11 treated mice given bleomycin (Figure 4.13C,D). These results suggest CDH11 present on alveolar macrophages (Figure 4.1E, 4.2D) regulates the expression of TGF- $\beta$ .

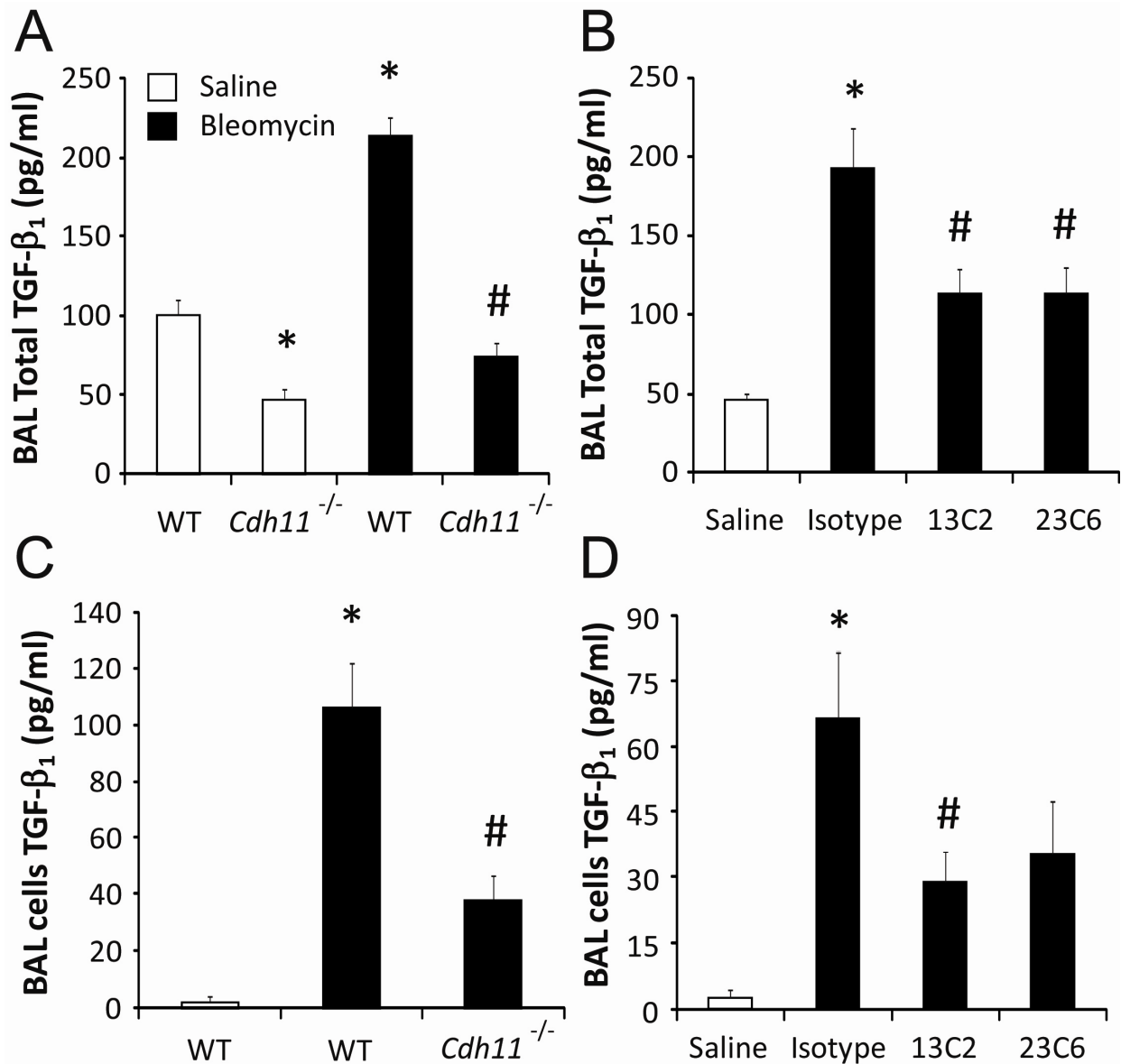


**Figure 4.13 - CDH11-dependent regulation of TGF- $\beta$**

BAL fluid was collected from both cohorts at day 21 after IT bleomycin. TGF- $\beta$  levels were quantified in (A,B) BAL supernatants and (C,D) protein lysates from BAL cell pellet utilizing a standard TGF- $\beta$  ELISA.  $n = 6$  WT,  $n = 6$  *Cdh11*<sup>-/-</sup> saline,  $n = 13$  WT bleomycin,  $n = 11$  *Cdh11*<sup>-/-</sup> bleomycin.  $n = 6$  saline,  $n = 7$  Bleo + isotype,  $n = 8$  Bleo + 13C2, and  $n = 6$  Bleo + 23C6. Values given are mean  $\pm$  SEM. \* $P \leq 0.05$  versus WT saline; # $P \leq 0.05$  versus bleomycin  $\pm$  isotype.



## **Chapter 4 - Discussion**

Differentiation of lung fibroblasts and EMT are two processes implicated in the formation of myofibroblasts, the cardinal cell type contributing to the pathogenesis of pulmonary fibrosis (8, 17, 131). However, a complete understanding of mechanisms driving these processes is yet to be achieved. The presence of CDH11 on cell types of varying origin contributes to a mesenchymal morphology and invasive phenotype characteristic of epithelial cells undergoing EMT. Furthermore, CDH11 is upregulated during the process of myofibroblast differentiation (160) and in biopsies from patients exhibiting skin fibrosis (161). Therefore, we hypothesized that CDH11 contributes to pulmonary fibrosis. To test this, expression and localization of CDH11 in human IPF samples were examined. Further, *Cdh11*<sup>-/-</sup> and wild type mice given systemic CDH11 blocking antibody were exposed to intratracheal bleomycin and pulmonary endpoints consistent with fibrosis were examined. Findings (Figure 4.14) represent the first demonstration of CDH11 expression on hyperplastic AECs and alveolar macrophages (Figures 4.1-3), key cell types implicated in the pathogenesis of human IPF. We are also first to report the CDH11-dependent regulation of EMT (Figures 4.9-11) and the production of TGF- $\beta$  (Figure 4.13), two pivotal processes in the pathogenesis of IPF. It follows that *Cdh11*<sup>-/-</sup> (Figures 4.4-6) and mice given CDH11 antibody (Figures 4.7,8) showed marked reductions in endpoints consistent with fibrosis including the formation of myofibroblasts and the deposition of collagen. Thus, agents targeting CDH11 warrant consideration for the treatment of patients with IPF and other fibroproliferative diseases.

A review (163) by Moeller et. al clearly characterizes two distinct phases of the intratracheal bleomycin model of pulmonary fibrosis. First an 'inflammatory phase', from day zero to day seven after bleomycin installation, characterized by massive influx of inflammatory cells and expression of proinflammatory cytokines and chemokines. The second is a 'fibrotic phase' characterized by profibrotic mediators such as TGF- $\beta$  and production and deposition of extracellular matrix proteins such as fibronectin and collagen. Studies containing agents administered before or during the inflammatory phase are deemed 'preventative' because observed effects are before fibrosis is established and largely dampen pulmonary inflammation. This review emphasizes the lack of studies containing agents administered in the second phase, or those that aim to treat existing pulmonary fibrosis.

Currently, prevention of IPF is impractical due to subclinical pathology occurring in the vast majority of patients. In other words, in many patients, fibrotic foci destroy a substantial portion of alveolar air-spaces before gas exchange is hindered beyond the body's capacity of

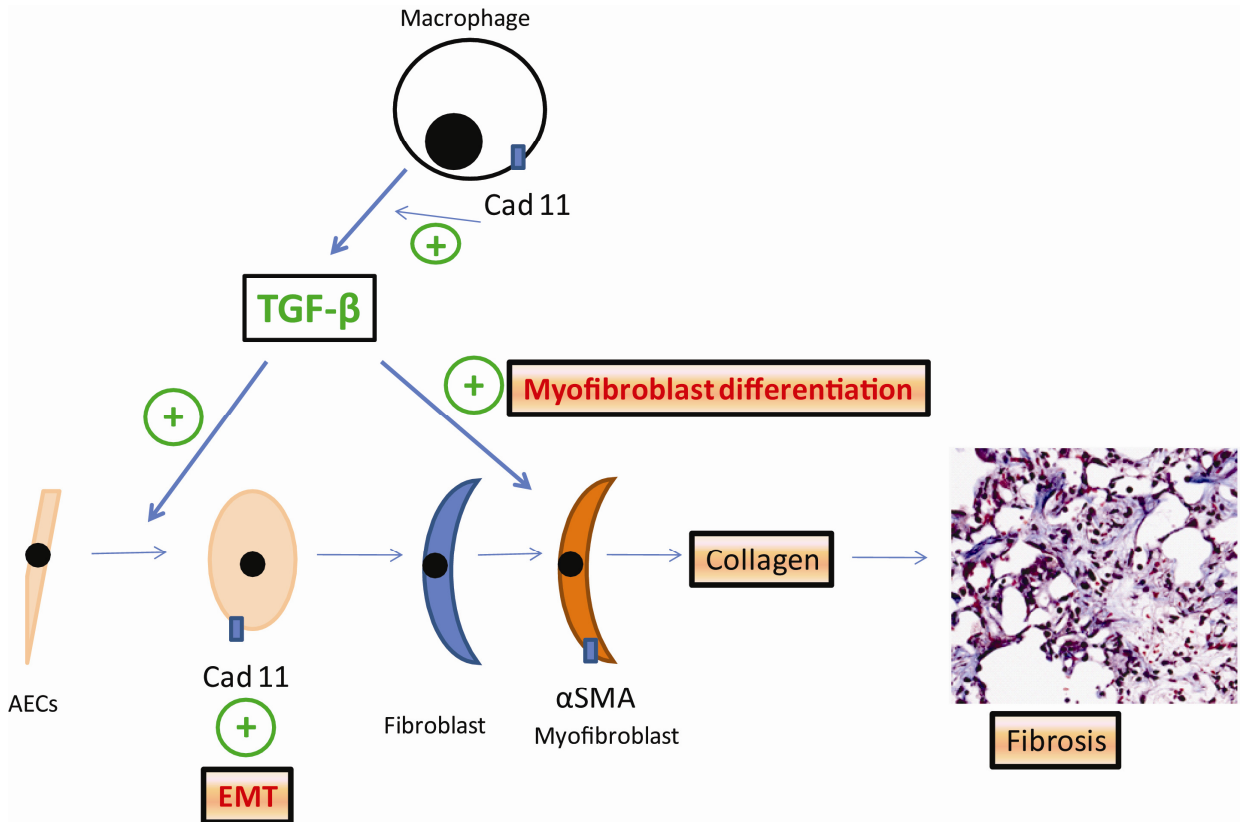


**Figure 4.14 - Working model of cadherin 11-dependent pulmonary fibrosis**

*In vivo* and *in vitro* studies demonstrate that CDH11 present on hyperplastic epithelial cells contributes to the process of EMT leading to production of collagen. Additionally, we are the first to demonstrate CDH11 expression on a hematopoietic cell, the alveolar macrophage. Data suggests that CDH11 on alveolar macrophages regulates the production of TGF- $\beta$  from this source leading to further stimulation of collagen production through the regulation of EMT and differentiation of myofibroblasts.

compensation. At that point, it still may be months or years before patients acknowledge that their notoriously non-specific symptoms of shortness of breath and fatigue have an underlying cause worthy of a visit to the doctor. Furthermore, it is obvious that immunomodulatory and anti-inflammatory agents do not alter disease progression or improve the grim survival rates in these patients (168). Finally, the side effect profile accompanying the use of these agents is reason enough for investigation of new therapies. Hence, while interesting, agents targeting inflammation or studies otherwise designed to prevent pulmonary fibrosis in animal models have little utility with regard to advancing patient care for IPF. Therefore, one aim of this study was to investigate the feasibility of specifically treating established pulmonary fibrosis by targeting CDH11.

Mice given bleomycin and subsequently treated ten days later with CDH11 blocking Ab displayed substantial reductions in typical pulmonary fibrotic endpoints (Figures 4.7,8). Although reductions in lymphocytes were observed, this treatment effect was otherwise independent of any changes in inflammatory cell counts (Figure 4.12). While this may be attributable to the strategic delivery of CDH11-targeted therapy after the 'inflammatory phase', *Cdh11*<sup>-/-</sup> mice receiving bleomycin displayed virtually identical inflammatory cell counts and differentials. This suggests that observed anti-fibrotic effects resulting from pharmacologic inhibition of CDH11 are a direct result of targeting EMT and TGF- $\beta$  as opposed to affecting these endpoints indirectly through inflammation. This emphasizes the promise and novelty of CDH11 as a therapeutic target for pulmonary fibrosis.

CDH11 is associated with a mesenchymal phenotype in cells during development and in various forms of pathology including cancer and rheumatoid arthritis. Though referred to as a marker of EMT (169-172), the role of CDH11 in promoting this process has not been investigated. We report CDH11 expression on AECs in the bleomycin model of pulmonary fibrosis and patients with IPF (Figures 4.1,2). Hyperplastic AECs are found in fibrotic regions in patients with IPF (154, 164, 165), commonly express epithelial and mesenchymal markers, and thus, are suggested to represent a transitional epithelial cell undergoing EMT. Though its significance to human pathology is still under investigation, the contribution of epithelial cells to fibroblast and myofibroblast populations in the lung is well documented (145, 146, 173). *In vitro* studies of epithelial cells stimulated to undergo EMT demonstrate substantial upregulations in CDH11 (Figure 4.9) consistent with *in vivo* findings in the bleomycin model (Figure 4.2) and patients with IPF (Figure 4.1). Results demonstrate that CDH11 permits the process of TGF- $\beta$ -

induced EMT of epithelial cells (Figures 4.10,4.11) suggesting a mechanism of reduced fibrosis in mice where CDH11 is genetically and pharmacologically targeted.

Patients with ILD, including IPF, and mice given bleomycin demonstrate CDH11 on alveolar macrophages (Figures 4.1-4.3), the principle source of TGF- $\beta$  in clinical and experimental pulmonary fibrosis. TGF- $\beta$  induces differentiation of myofibroblasts and stimulates epithelial cells to undergo EMT. Targeting TGF- $\beta$  has demonstrated success in experimental pulmonary fibrosis and was recently FDA-approved for treatment of IPF. The heralded critical regulatory step of (patho)biologic TGF- $\beta$  activity is the activation of TGF- $\beta$  protein through cleavage of the LAP protein fragment by various proteases (174-176). However, we demonstrate for the first time that CDH11 dramatically regulates the expression of TGF- $\beta$  in bleomycin induced fibrosis from alveolar macrophages (Figure 4.13). In the context of TGF- $\beta$  activity in pathologic scenarios, regulation of substrate availability upstream of protein cleavage would influence its overall activity as evidenced by our study demonstrating paralleled reductions in fibrotic endpoints *in vivo*. These endpoints include known TGF- $\beta$ -mediated fibroproliferative processes such as myofibroblast production and EMT. Given the extensive regulation of TGF- $\beta$  by CDH11, the results of this study are of value as knowledge of pathologic mechanisms centered about TGF- $\beta$  continues to expand.

There are likely numerous initiating stimuli driving the CDH11-dependent expression of TGF- $\beta$  from alveolar macrophages. However, while TGF- $\beta$  promotes several factors important in the progression of fibrosis, CDH11-dependent EMT and a significant impact on TGF- $\beta$  production suggests that CDH11 is important in the initiation and maintenance of the fibrotic phase of disease. Given the classic cadherin function of homophilic interaction, once expressed on the surface of hyperplastic AECs, CDH11 may be free to interact with CDH11 on macrophages. This would support a feed-forward model of perpetual TGF- $\beta$  production and further propagation of EMT and myofibroblast formation (Figure 4.13). Because the functions of CDH11 and TGF- $\beta$  are closely linked via interactions of at least these two different cell types, targeting CDH11 and TGF- $\beta$  in combination may represent a powerful approach in the treatment of pulmonary fibrosis.

There is extensive potential for the influence of cadherins on profibrotic intracellular signaling pathways. It is well recognized that cadherin-dependent formation of adherens junctions regulates the actin cytoskeleton through Rho GTPases (177). Of note, activation of Rho GTPases is increased in fibroblasts of patients with IPF and promotes their migratory phenotype (178). Furthermore, increased activation of Rho GTPase was detected during TGF-

$\beta$ -dependent myofibroblast differentiation *in vitro* (179). These studies support the *in vivo* evidence of CDH11-dependent formation of myofibroblasts (Figures 4.5, 4.8) and suggest direct influence of CDH11 on fibroblast migration and myofibroblast differentiation through the action of Rho GTPases. While myofibroblast formation in our study is most likely the result of CDH11-directed upregulations in TGF- $\beta$  (Figure 4.13), other investigations indicate this may also be mediated by Rho activity. Interestingly, one study found that Rho GTPase activation in macrophages positively regulates TGF- $\beta$  translation (180). In addition, inhibition of signaling downstream of Rho activity reduced experimental kidney fibrosis in association with reduced expression of TGF- $\beta$  (181). These studies provide insight into potential mechanisms of CDH11-dependent regulation of TGF- $\beta$  expression and further suggest details of CDH11-mediated fibrosis.

Alternatively, previous studies indicate the role of the Wnt pathway in promoting endpoints consistent with pulmonary fibrosis such as EMT (165), lung fibroblast proliferation, and ECM production (182). Other reports demonstrate increased nuclear localization of  $\beta$ -catenin in type II AECs and fibroblasts of patients with IPF (165, 183, 184) indicative of increased Wnt signaling. Classically, the cadherin cytoplasmic tail is bound to  $\beta$ -catenin through intermediary interaction with  $\alpha$ -catenin. Interestingly, a recent study demonstrates that cadherin-bound  $\beta$ -catenin is released upon adherens junction dissociation and becomes part of the intracellular pool available to signal within the canonical Wnt/ $\beta$ -catenin pathway (185). Epithelial cadherins, especially E cadherin, are critical in maintaining epithelial cell-to-cell junctions through adherens junctions. Loss of these adherens junctions, mainly through downregulation of E cadherin, is a fundamental and critical step in the process of EMT. As demonstrated previously (Figures 4.9-4.11), CDH11 promotes EMT in lung epithelial cells. Therefore, CDH11-dependent transition to mesenchymal morphology may mobilize intracellular  $\beta$ -catenin pools increasing substrate for the profibrotic Wnt intracellular signaling pathway.

Finally, cadherins can associate with numerous tyrosine kinase receptors and influence their downstream intracellular signaling pathways which have been suggested to promote pulmonary fibrosis (186-189). E cadherin can associate with and influence activity of the EGF receptor even in the absence of its ligand, EGF (190). CDH11 (191) and N cadherin (192) interact with and promote the downstream signaling pathways of the FGF receptor during neurite outgrowth. Finally, interaction between VE-cadherin and VEGF receptor increases the half life of the receptor (193). In addition, similar to CDH11, these receptors are expressed on AECs and alveolar macrophages in the context of experimental and clinical pulmonary fibrosis.

Therefore, conceivable mechanisms of CDH11-dependent EMT and regulation of TGF- $\beta$  involve potentiation of profibrotic signaling through tyrosine kinase receptor pathways on AECs and alveolar macrophages.

While we are only in the beginning stages of understanding the mechanisms of CDH11-driven fibrosis, the results of this study clearly demonstrate promise to have a significant impact in the management of a number of conditions in addition to IPF. The model of chronic, repetitive injury leading to dysregulated wound healing and collagen production has been applied and demonstrated in virtually every organ exhibiting fibrosis. It follows that the processes of EMT and myofibroblasts differentiation play a central role in the pathogenesis of these conditions.

Organ fibrosis is a substantial health problem worldwide and represents primary pathology or a complicating factor in a significant fraction of health-related deaths in the United States (2). Cirrhosis of the liver, a fibroproliferative condition potentially arising from alcoholism or infectious hepatitis, is the tenth leading cause of health-related death in the United States. Kidney diseases of varying etiology such as diabetes (5<sup>th</sup>-leading cause of death), chronic nephritic and nephrotic inflammatory conditions (8th), and hypertensive renal disease (11th) may all exhibit renal fibrosis as an end-stage/complicating factor. Similarly, fibrosis arises in the heart from a number of etiologies, but the vast majority occurs after myocardial infarct which is the leading cause of death in the United States. Furthermore, organ fibrosis is a complicating feature of a number of existing therapeutic regimens such as chemotherapy and radiation in the treatment of malignancies. We have clearly demonstrated CDH11 as a key regulator of EMT and myofibroblast differentiation thus underscoring the potential of CDH11-targeted therapy to have a momentous impact in the management of human disease.

Finally, CDH11 has an established role in promoting malignancy. As mentioned previously, the role of cadherins in the process of EMT-dependent malignant transformation has been well-established. Findings in this study exhibiting the role of CDH11 in promoting EMT will contribute to the overall understanding of this process in malignant transformation and metastasis. As parallels between mechanisms of malignancy and fibrosis continue to be realized, results demonstrated in this thesis will aid the investigation of CDH11 as a potential marker or therapeutic target for cancer, the second leading cause of death in the United States.

In summary, results of this study suggest that CDH11 on AECs and alveolar macrophages directly contribute to fibrosis through the regulation of EMT and TGF- $\beta$

production, respectively (Figure 4.14). As continuing investigation supports the role of EMT in the development of organ fibrosis, this research indicates that CDH11 is a necessary endpoint to monitor as other players in these conditions are considered. We have also established that consideration must be given to CDH11 as research continues to understand the role of TGF- $\beta$  in the development of fibrosis and as existing TGF- $\beta$ -targeted therapies are optimized. Understanding of detailed mechanisms regulating expression of CDH11, its ligand(s), and resulting downstream signaling pathways promoting organ fibrosis will be essential to further the development of CDH11 as a treatment option for fibroproliferative disorders.

# **Chapter 5**

## **Future directions**



## **Chapter 5 - Future Directions**

With regard to the investigation of any subject, inevitably, the ability to ask pertinent questions exceeds the capacity to adequately address them. Thus, the culmination of this dissertation leaves many unanswered questions in its wake. Nevertheless, answers to these questions are important to further the appreciation of the roles of OPN and CDH11 in human pathology.

### **Characterize the contribution of $\alpha_v\beta_3$ integrin to the *Ada*<sup>-/-</sup> pulmonary phenotype**

This dissertation demonstrates that OPN contributes to pathologic air-space enlargement in a model of adenosine-mediated lung injury. Results also suggested that features of this phenotype were mediated by OPN-dependent recruitment of neutrophils through interactions with CD44 and  $\alpha_v\beta_3$ . An attempt to ascertain the contribution of CD44 to the *Ada*<sup>-/-</sup> phenotype produced inconclusive results. This could reflect the need for optimization of the experimental design, or might suggest that OPN-CD44 interaction does not significantly contribute to the overall *Ada*<sup>-/-</sup> phenotype. Because OPN- $\alpha_v\beta_3$  interactions in different scenarios contribute to an array of human pathology, future studies should investigate the role of  $\alpha_v\beta_3$  in the *Ada*<sup>-/-</sup> pulmonary phenotype utilizing similar neutralization strategies and pulmonary endpoints outlined in chapter 3.

### **OPN-dependent regulation of adhesion molecules**

Results in this thesis demonstrate that OPN interactions with its two putative receptors promote the recruitment of neutrophils, *in vivo*. These results were found to be independent of changes in lung proinflammatory cytokines or granulopoiesis associated with the genetic removal of *Opn*. While this suggests a direct OPN interaction with these receptors on the surface of neutrophils, additional mechanisms need to be investigated and/or ruled out. Elevated adenosine levels in the *Ada*<sup>-/-</sup> model are associated with increased expression of adhesion molecules, such as P-selectin, E-selectin, VCAM and ICAM, responsible for promoting the recruitment of neutrophils from the bloodstream to sites of tissue injury. Thus, future experiments need to address the contribution of OPN to adenosine-dependent upregulations in adhesion molecules promoting neutrophil extravasation into injured lung tissue.

## **Role of OPN in alternative models of emphysema/COPD**

Despite the demonstrations that OPN contributes to the pathogenesis of adenosine-mediated alveolar air-space enlargement and OPN expression is increased in human tissue obtained from patients with COPD, there are indications that the *Ada*<sup>-/-</sup> model does not fully represent the pathology seen in COPD. Two alternative, perhaps more well-accepted, models of emphysema include chronic cigarette smoke exposure and repeated administration of cigarette smoke extract (CSE) through various routes. Nevertheless, these models exhibit inflammation and alveolar air-space enlargement similar to the *Ada*<sup>-/-</sup> model. Therefore, to solidify the contribution of OPN to experimental emphysema, future studies may include the examination of standard endpoints consistent with emphysema in *Opn*<sup>-/-</sup> mice exposed to cigarette smoke or CSE.

## **Localization of $\beta$ catenin**

Findings in this dissertation demonstrate a pivotal role of CDH11 in promoting the process of EMT thus promoting pulmonary fibrosis. Cadherins involved in cell-to-cell adhesion at so-called adherens junctions bind intracellular proteins including  $\beta$  catenin that, under certain conditions, are involved in profibrotic intracellular signaling pathways. Upon adherens junction dissociation, as in the case of EMT, there exists evidence that cadherin-bound  $\beta$  catenin is released and is available to signal within the Wnt intracellular signaling pathway which many studies indicate promotes pulmonary fibrosis. However, CDH11-dependent localization of  $\beta$  catenin in the context of pulmonary fibrosis is not yet known. Presumably, CDH11 permitting the process of EMT in airway epithelial cells would lead to dissociation of adherens junctions thus releasing cadherin bound  $\beta$  catenin. Preliminary studies demonstrate  $\beta$  catenin localizes in cytoplasmic/perinuclear regions away from cell membrane bound CDH11 on alveolar macrophages isolated from patients with ILD (Figure 5.1). Subsequent experiments should involve immunolocalization of  $\beta$  catenin and CDH11 in AECs undergoing EMT. These studies should be performed *in vitro*, where CDH11 expression can be directly manipulated, and *in vivo* to confirm this process occurs in the overall setting of pulmonary fibrosis. If CDH11 promotes dissociation of adherens junctions in either cell type, results displaying nuclear, as opposed to cytoplasmic cell surface, localization of  $\beta$  catenin would suggest the CDH11-dependent release of  $\beta$  catenin permitting its signaling within profibrotic intracellular pathways.

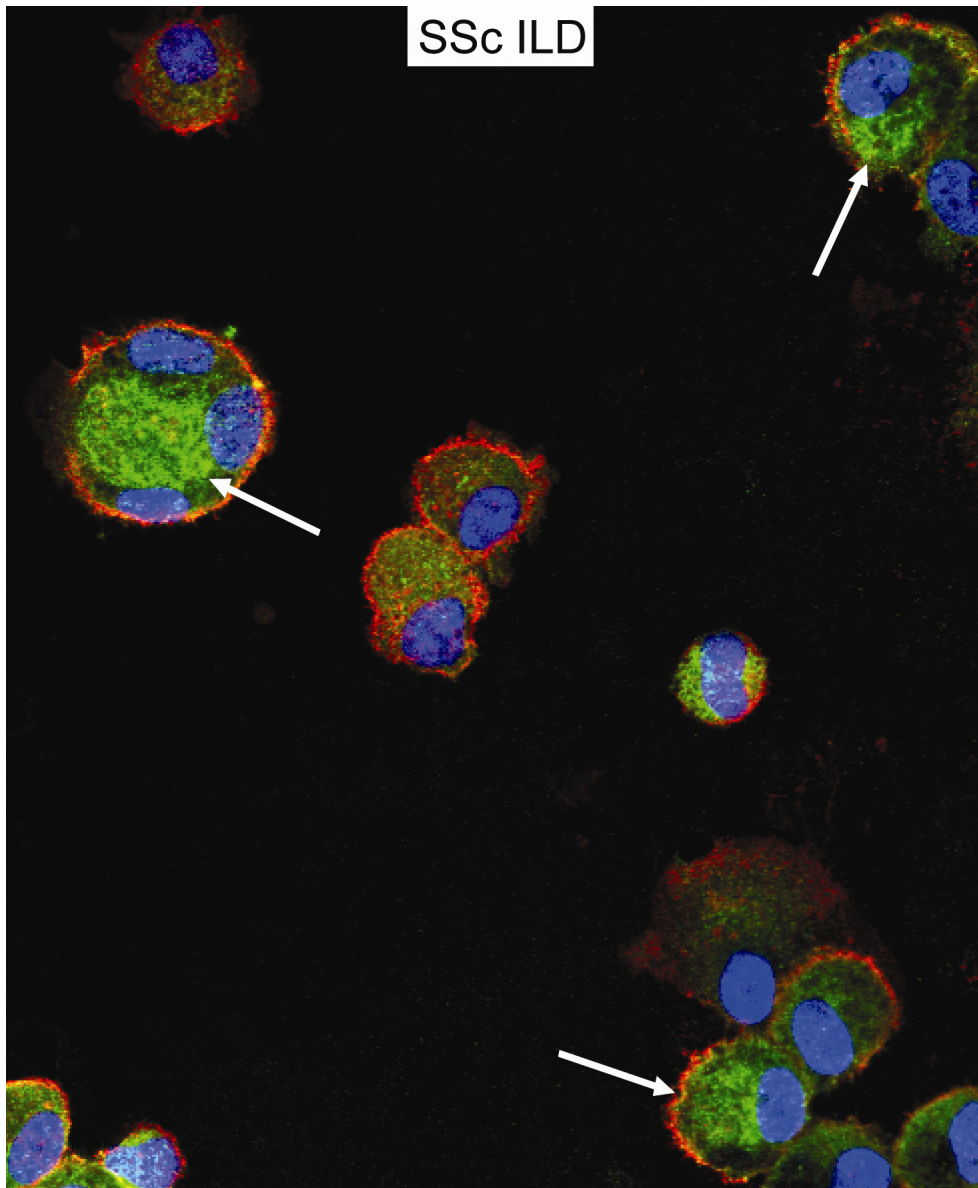


**Figure 5.1 - Dual CDH11  $\beta$ -catenin immunofluorescence on ILD macrophages**

Alveolar macrophages isolated from a patient with ILD secondary to scleroderma expresses CDH11 (red) on the cell surface and  $\beta$ -catenin (green) in cytoplasmic/perinuclear regions (white arrows).

### **CDH11-dependent expression of TGF- $\beta$ in alveolar macrophages**

TGF- $\beta$  is well-established as the quintessential profibrotic mediator. Findings in this thesis exhibit that CDH11-mediated development of pulmonary fibrosis may be a consequence of the regulation of TGF- $\beta$  expression from alveolar macrophages. While we have confirmed that changes in TGF- $\beta$  expression are not due to CDH11-mediated changes in macrophage numbers, conceivable scenarios exist independent of CDH11 on alveolar macrophages directly influencing the expression of TGF- $\beta$ . Therefore, future experiments should involve the examination of TGF- $\beta$  production in response to appropriate stimulus in the presence and absence of CDH11 on alveolar macrophages. This would involve the collection of primary alveolar macrophages from wild type and *Cdh11*<sup>-/-</sup> mice or the use of previously described *Cdh11*<sup>-/-</sup> knockdown techniques, *in vitro*. Known inducers of TGF- $\beta$  production from alveolar macrophages *in vitro* include phosphatidyl serine recognition structures and bleomycin. Discrepancies in induced *in vitro* TGF- $\beta$  production from alveolar macrophages with and without CDH11 would definitively indicate direct regulation of TGF- $\beta$  expression by CDH11.

### **CDH11-dependent clearance of 'debris' by alveolar macrophages**

Preliminary data indicates that *Cdh11*<sup>-/-</sup> mice, in parallel with a reduction in endpoints consistent with pulmonary fibrosis in response to bleomycin, exhibit an atypical morphology in alveolar macrophages isolated from BAL (Figure 5.2A). Unpublished data from Dr. Blackburn's lab reports the appearance of alveolar macrophages with basophilic inclusions in association with the resolution of fibrosis. We postulate that these inclusions, present almost exclusively in *Cdh11*<sup>-/-</sup> macrophages (Figure 5.2B), represent the phagocytosis of apoptotic cells or ECM proteins. Initial steps, such as collagen Ab or TUNEL staining, should be taken in future studies to determine the nature of these inclusions. Enhanced survival or decreased apoptosis of myofibroblasts is reported in the scientific literature as a mechanism of dysregulated wound healing leading to fibrosis. Future work should involve characterization of apoptosis within or adjacent to regions of fibrotic foci in existing tissue sections of mice given bleomycin where CDH11 is genetically and pharmacologically targeted. Subsequent studies should examine the role of CDH11 and apoptosis in fibroblasts stimulated to differentiate into myofibroblasts, *in vitro*. Alternatively, enhanced clearance of extracellular matrix in the absence of CDH11 may be explained by normalization of protease/antiprotease imbalances characteristic of pulmonary fibrosis. Investigation and quantification of proteases, such as the matrix metalloproteases, and

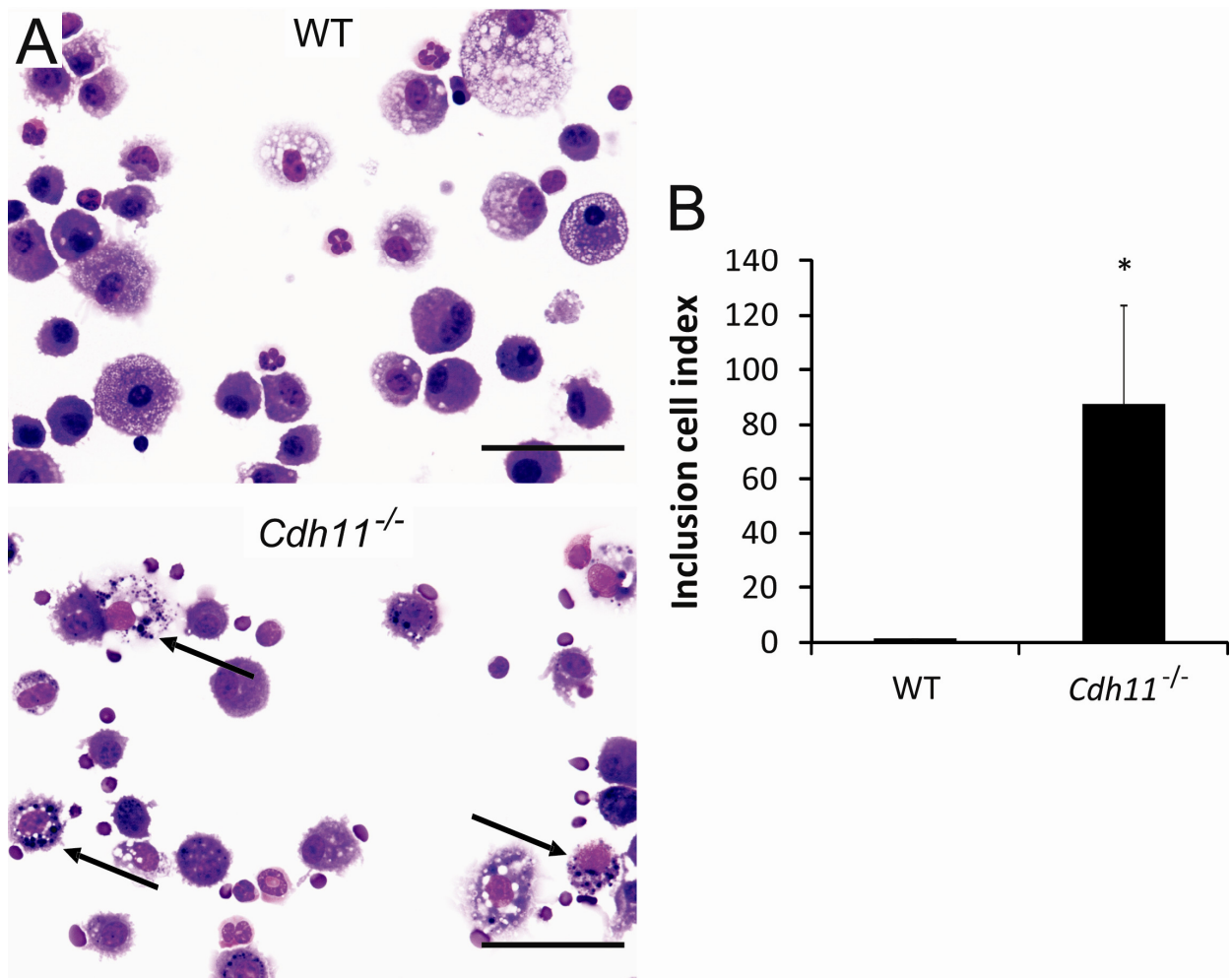


**Figure 5.2 - 'Inclusion' cells in *Cdh11*<sup>-/-</sup> alveolar macrophages**

(A) Diff-Quick-stained BAL cytopspins isolated from WT and *Cdh11*<sup>-/-</sup> mouse lungs treated with bleomycin. Arrows denote basophilic inclusions present within alveolar macrophages of *Cdh11*<sup>-/-</sup> mice. Scale bars = 50  $\mu$ m. (B) Quantification of inclusion cells present within 7 low magnification images per sample. Inclusion cell numbers were normalized to total cell number present in BAL from each sample. n = 9 (WT) and n = 7 (*Cdh11*<sup>-/-</sup>). \*P < 0.05 versus WT.

their corresponding inhibitors, TIMPs, may provide insight into the enhanced clearance of extracellular matrix and improved pathology exhibited by *Cdh11*<sup>-/-</sup> mice.

### **Further characterization of pulmonary endpoints in the bleomycin and *Ada*<sup>-/-</sup> model**

Clinical endpoints typically monitored and associated with pulmonary fibrosis and COPD are arterial oxygen saturation (SpO<sub>2</sub>) and pulmonary function tests (PFTs). PFTs identify a restrictive pattern in pulmonary fibrosis and an obstructive pattern in COPD. Recently, our lab has encountered technology enabling the measurement of these endpoints. Future studies in the both models should include full characterization of OPN and CDH11-dependent changes in lung volumes and compliance with a FlexiVent system and SpO<sub>2</sub> with the MouseOx detection system.

### **Overlap between CDH11 and OPN?**

Initially, there is reason to believe that CDH11 and OPN have overlapping pathologic mechanisms. Both have been studied in cancer and organ fibrosis. However, reports in the cancer literature suggest that CDH11 is involved with the acquisition of a mesenchymal phenotype, whereas OPN promotes the migration of tumor cells directly through interactions with cell surface receptors and indirectly via activation of extracellular matrix proteases and promoting angiogenesis. This thesis and the existing literature display that the roles of these individual proteins show striking similarity between mechanisms promoting malignant transformation and pulmonary fibrosis. However, despite our reports that CDH11 promotes features of pulmonary fibrosis similar to previous *in vivo* studies done in *Opn*<sup>-/-</sup> mice (97, 98), the mechanisms of fibrosis appear to occur in parallel rather than in overlapping manner.

In contrast to *Cdh11*<sup>-/-</sup> mice, *Opn*<sup>-/-</sup> knockout mice have reduced pulmonary inflammation in the *Ada*<sup>-/-</sup> model (194) and the bleomycin models of pulmonary fibrosis (97, 98). Furthermore, studies demonstrate that OPN induces fibroblast migration and invasion through interactions with the putative OPN receptors (82, 97). In contrast, we have suggested that any CDH11-mediated cell migration would be the direct result of EMT. In addition, these processes are likely secondary to CDH11-dependent upregulations in TGF-β, interactions with other cadherins, or influence within tyrosine kinase receptor signaling pathways. Finally, there is discrepancy with regard to the influence of OPN on the levels of TGF-β *in vivo* (97, 194). In contrast, we report that CDH11 has a considerable affect on the expression of TGF-β in the bleomycin model.

However, one area where cadherin and OPN pathways may intersect is at the post-translational level. Findings in this dissertation of OPN mediated increases in MMP protein levels are consistent with OPN-mediated increases in MMP activity in the cancer literature and studies of *Opn*<sup>-/-</sup> mice in the bleomycin model. It has been reported recently that MMPs facilitate the disruption of E cadherin at adherens junctions promoting the process EMT (152). While we have shown CDH11 directly promotes EMT in lung epithelial cells *in vitro*, it is conceivable that this process may be aided by OPN-mediated increases in MMP activity *in vivo*. If further study of CDH11-directed fibrosis displays dependency or facilitation by MMP activity, the role of OPN in CDH11-dependent EMT *in vivo* may warrant investigation.

## **Conclusion**

This thesis demonstrates novel roles for OPN and CDH11 in the development of chronic lung diseases. This thesis exhibits the role of OPN-driven neutrophilia, increases in proteases, and angiogenesis in association with OPN-dependent alveolar air-space enlargement consistent with COPD *in vivo*. Further, in the context of CDH11-dependent pulmonary fibrosis, we demonstrate that CDH11 regulates epithelial to mesenchymal transition and production of TGF- $\beta$  from macrophages. These processes all have demonstrated roles in normal wound healing. These findings support the overriding hypothesis that mechanisms of chronic lung disease are a result of over-activity of normal wound healing processes. It follows that an overall understanding of factors shifting physiology from 'normal' to pathologic wound healing will be necessary as we continue to gain knowledge of the mechanisms of all diseases that are chronic in nature.

## **References**

1. Mannino, D.M. 2002. COPD: epidemiology, prevalence, morbidity and mortality, and disease heterogeneity. *Chest* 121:121S-126S.
2. Kung, H.C., Hoyert, D.L., Xu, J., and Murphy, S.L. 2008. Deaths: final data for 2005. *Natl Vital Stat Rep* 56:1-120.
3. Pauwels, R.A., and Rabe, K.F. 2004. Burden and clinical features of chronic obstructive pulmonary disease (COPD). *Lancet* 364:613-620.
4. Kemp, S.V., Polkey, M.I., and Shah, P.L. 2009. The epidemiology, etiology, clinical features, and natural history of emphysema. *Thorac Surg Clin* 19:149-158.
5. Tetley, T.D. 2005. Inflammatory cells and chronic obstructive pulmonary disease. *Curr Drug Targets Inflamm Allergy* 4:607-618.
6. Rabe, K.F., Hurd, S., Anzueto, A., Barnes, P.J., Buist, S.A., Calverley, P., Fukuchi, Y., Jenkins, C., Rodriguez-Roisin, R., van Weel, C., et al. 2007. Global strategy for the diagnosis, management, and prevention of chronic obstructive pulmonary disease: GOLD executive summary. *Am J Respir Crit Care Med* 176:532-555.
7. Wells, A.U., Steen, V., and Valentini, G. 2009. Pulmonary complications: one of the most challenging complications of systemic sclerosis. *Rheumatology (Oxford)* 48 Suppl 3:iii40-44.
8. Wynn, T.A. 2007. Common and unique mechanisms regulate fibrosis in various fibroproliferative diseases. *J Clin Invest* 117:524-529.
9. Morgenthau, A.S., and Padilla, M.L. 2009. Spectrum of fibrosing diffuse parenchymal lung disease. *Mt Sinai J Med* 76:2-23.
10. Collard, H.R., and King, T.E., Jr. 2001. Treatment of idiopathic pulmonary fibrosis: the rise and fall of corticosteroids. *Am J Med* 110:326-328.
11. Dempsey, O.J., Kerr, K.M., Gomersall, L., Remmen, H., and Currie, G.P. 2006. Idiopathic pulmonary fibrosis: an update. *Qjm* 99:643-654.
12. Elias, J.A., Lee, C.G., Zheng, T., Ma, B., Homer, R.J., and Zhu, Z. 2003. New insights into the pathogenesis of asthma. *J Clin Invest* 111:291-297.
13. Jeffery, P.K. 1999. Differences and similarities between chronic obstructive pulmonary disease and asthma. *Clin Exp Allergy* 29 Suppl 2:14-26.
14. Ward, P.A., and Hunninghake, G.W. 1998. Lung inflammation and fibrosis. *Am J Respir Crit Care Med* 157:S123-129.
15. Coultas, D.B., Zumwalt, R.E., Black, W.C., and Sobonya, R.E. 1994. The epidemiology of interstitial lung diseases. *Am J Respir Crit Care Med* 150:967-972.



16. Raghu, G., Weycker, D., Edelsberg, J., Bradford, W.Z., and Oster, G. 2006. Incidence and prevalence of idiopathic pulmonary fibrosis. *Am J Respir Crit Care Med* 174:810-816.
17. Hinz, B., Phan, S.H., Thannickal, V.J., Galli, A., Bochaton-Piallat, M.L., and Gabbiani, G. 2007. The myofibroblast: one function, multiple origins. *Am J Pathol* 170:1807-1816.
18. Wynn, T.A. 2008. Cellular and molecular mechanisms of fibrosis. *J Pathol* 214:199-210.
19. Sun, C.X., Young, H.W., Molina, J.G., Volmer, J.B., Schnermann, J., and Blackburn, M.R. 2005. A protective role for the A1 adenosine receptor in adenosine-dependent pulmonary injury. *J Clin Invest* 115:35-43.
20. Blackburn, M.R., Datta, S.K., and Kellems, R.E. 1998. Adenosine deaminase-deficient mice generated using a two-stage genetic engineering strategy exhibit a combined immunodeficiency. *J Biol Chem* 273:5093-5100.
21. Liaw, L., Birk, D.E., Ballas, C.B., Whitsitt, J.S., Davidson, J.M., and Hogan, B.L. 1998. Altered wound healing in mice lacking a functional osteopontin gene (spp1). *J Clin Invest* 101:1468-1478.
22. Young, H.W., Molina, J.G., Dimina, D., Zhong, H., Jacobson, M., Chan, L.N., Chan, T.S., Lee, J.J., and Blackburn, M.R. 2004. A3 adenosine receptor signaling contributes to airway inflammation and mucus production in adenosine deaminase-deficient mice. *J Immunol* 173:1380-1389.
23. Lee, D.M., Kiener, H.P., Agarwal, S.K., Noss, E.H., Watts, G.F., Chisaka, O., Takeichi, M., and Brenner, M.B. 2007. Cadherin-11 in synovial lining formation and pathology in arthritis. *Science* 315:1006-1010.
24. Horikawa, K., Radice, G., Takeichi, M., and Chisaka, O. 1999. Adhesive subdivisions intrinsic to the epithelial somites. *Dev Biol* 215:182-189.
25. Ashcroft, T., Simpson, J.M., and Timbrell, V. 1988. Simple method of estimating severity of pulmonary fibrosis on a numerical scale. *J Clin Pathol* 41:467-470.
26. Chunn, J.L., Molina, J.G., Mi, T., Xia, Y., Kellems, R.E., and Blackburn, M.R. 2005. Adenosine-dependent pulmonary fibrosis in adenosine deaminase-deficient mice. *J Immunol* 175:1937-1946.
27. Livak, K.J., and Schmittgen, T.D. 2001. Analysis of relative gene expression data using real-time quantitative PCR and the 2<sup>-</sup>(-Delta Delta C(T)) Method. *Methods* 25:402-408.
28. Mohsenin, A., Mi, T., Xia, Y., Kellems, R.E., Chen, J.F., and Blackburn, M.R. 2007. Genetic removal of the A2A adenosine receptor enhances pulmonary inflammation,

- mucin production, and angiogenesis in adenosine deaminase-deficient mice. *Am J Physiol Lung Cell Mol Physiol* 293:L753-761.
29. Thurston, G., Murphy, T.J., Baluk, P., Lindsey, J.R., and McDonald, D.M. 1998. Angiogenesis in mice with chronic airway inflammation: strain-dependent differences. *Am J Pathol* 153:1099-1112.
  30. Blackburn, M.R., Volmer, J.B., Thrasher, J.L., Zhong, H., Crosby, J.R., Lee, J.J., and Kellems, R.E. 2000. Metabolic consequences of adenosine deaminase deficiency in mice are associated with defects in alveogenesis, pulmonary inflammation, and airway obstruction. *J Exp Med* 192:159-170.
  31. Driver, A.G., Kukoly, C.A., Ali, S., and Mustafa, S.J. 1993. Adenosine in bronchoalveolar lavage fluid in asthma. *Am Rev Respir Dis* 148:91-97.
  32. Huszar, E., Vass, G., Vizi, E., Csoma, Z., Barat, E., Molnar Vilagos, G., Herjavec, I., and Horvath, I. 2002. Adenosine in exhaled breath condensate in healthy volunteers and in patients with asthma. *Eur Respir J* 20:1393-1398.
  33. Caruso, M., Varani, K., Tringali, G., and Polosa, R. 2009. Adenosine and adenosine receptors: their contribution to airway inflammation and therapeutic potential in asthma. *Curr Med Chem* 16:3875-3885.
  34. Auchampach, J.A. 2007. Adenosine receptors and angiogenesis. *Circ Res* 101:1075-1077.
  35. Feoktistov, I., Biaggioni, I., and Cronstein, B.N. 2009. Adenosine receptors in wound healing, fibrosis and angiogenesis. *Handb Exp Pharmacol*:383-397.
  36. Arch, J.R., and Newsholme, E.A. 1978. The control of the metabolism and the hormonal role of adenosine. *Essays Biochem* 14:82-123.
  37. Baldwin, S.A., Beal, P.R., Yao, S.Y., King, A.E., Cass, C.E., and Young, J.D. 2004. The equilibrative nucleoside transporter family, SLC29. *Pflugers Arch* 447:735-743.
  38. Eltzschig, H.K., Ibla, J.C., Furuta, G.T., Leonard, M.O., Jacobson, K.A., Enjyoji, K., Robson, S.C., and Colgan, S.P. 2003. Coordinated adenine nucleotide phosphohydrolysis and nucleoside signaling in posthypoxic endothelium: role of ectonucleotidases and adenosine A2B receptors. *J Exp Med* 198:783-796.
  39. Volmer, J.B., Thompson, L.F., and Blackburn, M.R. 2006. Ecto-5'-nucleotidase (CD73)-mediated adenosine production is tissue protective in a model of bleomycin-induced lung injury. *J Immunol* 176:4449-4458.

40. Reisin, I.L., Prat, A.G., Abraham, E.H., Amara, J.F., Gregory, R.J., Ausiello, D.A., and Cantiello, H.F. 1994. The cystic fibrosis transmembrane conductance regulator is a dual ATP and chloride channel. *J Biol Chem* 269:20584-20591.
41. Roman, R.M., Lomri, N., Braunstein, G., Feranchak, A.P., Simeoni, L.A., Davison, A.K., Mechetner, E., Schwiebert, E.M., and Fitz, J.G. 2001. Evidence for multidrug resistance-1 P-glycoprotein-dependent regulation of cellular ATP permeability. *J Membr Biol* 183:165-173.
42. Cotrina, M.L., Lin, J.H., and Nedergaard, M. 1998. Cytoskeletal assembly and ATP release regulate astrocytic calcium signaling. *J Neurosci* 18:8794-8804.
43. Bell, P.D., Lapointe, J.Y., Sabirov, R., Hayashi, S., Peti-Peterdi, J., Manabe, K., Kovacs, G., and Okada, Y. 2003. Macula densa cell signaling involves ATP release through a maxi anion channel. *Proc Natl Acad Sci U S A* 100:4322-4327.
44. Braunstein, G.M., Roman, R.M., Clancy, J.P., Kudlow, B.A., Taylor, A.L., Shylonsky, V.G., Jovov, B., Peter, K., Jilling, T., Ismailov, II, et al. 2001. Cystic fibrosis transmembrane conductance regulator facilitates ATP release by stimulating a separate ATP release channel for autocrine control of cell volume regulation. *J Biol Chem* 276:6621-6630.
45. Okada, S.F., O'Neal, W.K., Huang, P., Nicholas, R.A., Ostrowski, L.E., Craigen, W.J., Lazarowski, E.R., and Boucher, R.C. 2004. Voltage-dependent anion channel-1 (VDAC-1) contributes to ATP release and cell volume regulation in murine cells. *J Gen Physiol* 124:513-526.
46. Kaczmarek, E., Koziak, K., Seigny, J., Siegel, J.B., Anrather, J., Beaudoin, A.R., Bach, F.H., and Robson, S.C. 1996. Identification and characterization of CD39/vascular ATP diphosphohydrolase. *J Biol Chem* 271:33116-33122.
47. Resta, R., Yamashita, Y., and Thompson, L.F. 1998. Ecto-enzyme and signaling functions of lymphocyte CD73. *Immunol Rev* 161:95-109.
48. Fredholm, B.B., AP, I.J., Jacobson, K.A., Klotz, K.N., and Linden, J. 2001. International Union of Pharmacology. XXV. Nomenclature and classification of adenosine receptors. *Pharmacol Rev* 53:527-552.
49. Londos, C., Cooper, D.M., and Wolff, J. 1980. Subclasses of external adenosine receptors. *Proc Natl Acad Sci U S A* 77:2551-2554.
50. Palmer, T.M., Harris, C.A., Coote, J., and Stiles, G.L. 1997. Induction of multiple effects on adenylyl cyclase regulation by chronic activation of the human A3 adenosine receptor. *Mol Pharmacol* 52:632-640.

51. Yang, J.N., Wang, Y., Garcia-Roves, P.M., Bjornholm, M., and Fredholm, B.B. Adenosine A(3) receptors regulate heart rate, motor activity and body temperature. *Acta Physiol (Oxf)*.
52. Yang, J.N., Chen, J.F., and Fredholm, B.B. 2009. Physiological roles of A1 and A2A adenosine receptors in regulating heart rate, body temperature, and locomotion as revealed using knockout mice and caffeine. *Am J Physiol Heart Circ Physiol* 296:H1141-1149.
53. Johansson, B., Halldner, L., Dunwiddie, T.V., Masino, S.A., Poelchen, W., Gimenez-Llort, L., Escorihuela, R.M., Fernandez-Teruel, A., Wiesenfeld-Hallin, Z., Xu, X.J., et al. 2001. Hyperalgesia, anxiety, and decreased hypoxic neuroprotection in mice lacking the adenosine A1 receptor. *Proc Natl Acad Sci U S A* 98:9407-9412.
54. Ledent, C., Vaugeois, J.M., Schiffmann, S.N., Pedrazzini, T., El Yacoubi, M., Vanderhaeghen, J.J., Costentin, J., Heath, J.K., Vassart, G., and Parmentier, M. 1997. Aggressiveness, hypoalgesia and high blood pressure in mice lacking the adenosine A2a receptor. *Nature* 388:674-678.
55. Monteiro, E.C., and Ribeiro, J.A. 2000. Adenosine-dopamine interactions and ventilation mediated through carotid body chemoreceptors. *Adv Exp Med Biol* 475:671-684.
56. Hansen, P.B., and Schnermann, J. 2003. Vasoconstrictor and vasodilator effects of adenosine in the kidney. *Am J Physiol Renal Physiol* 285:F590-599.
57. Berne, R.M. 1963. Cardiac nucleotides in hypoxia: possible role in regulation of coronary blood flow. *Am J Physiol* 204:317-322.
58. Martin, C., Leone, M., Viviani, X., Ayem, M.L., and Guieu, R. 2000. High adenosine plasma concentration as a prognostic index for outcome in patients with septic shock. *Crit Care Med* 28:3198-3202.
59. Cargnoni, A., Ceconi, C., Boraso, A., Bernocchi, P., Monopoli, A., Curello, S., and Ferrari, R. 1999. Role of A2A receptor in the modulation of myocardial reperfusion damage. *J Cardiovasc Pharmacol* 33:883-893.
60. Okusa, M.D., Linden, J., Macdonald, T., and Huang, L. 1999. Selective A2A adenosine receptor activation reduces ischemia-reperfusion injury in rat kidney. *Am J Physiol* 277:F404-412.
61. Reece, T.B., Okonkwo, D.O., Ellman, P.I., Warren, P.S., Smith, R.L., Hawkins, A.S., Linden, J., Kron, I.L., Tribble, C.G., and Kern, J.A. 2004. The evolution of ischemic

- spinal cord injury in function, cytoarchitecture, and inflammation and the effects of adenosine A2A receptor activation. *J Thorac Cardiovasc Surg* 128:925-932.
62. Reece, T.B., Ellman, P.I., Maxey, T.S., Crosby, I.K., Warren, P.S., Chong, T.W., LeGallo, R.D., Linden, J., Kern, J.A., Tribble, C.G., et al. 2005. Adenosine A2A receptor activation reduces inflammation and preserves pulmonary function in an in vivo model of lung transplantation. *J Thorac Cardiovasc Surg* 129:1137-1143.
  63. Ross, S.D., Tribble, C.G., Linden, J., Gangemi, J.J., Lanpher, B.C., Wang, A.Y., and Kron, I.L. 1999. Selective adenosine-A2A activation reduces lung reperfusion injury following transplantation. *J Heart Lung Transplant* 18:994-1002.
  64. Ellman, P.I., Reece, T.B., Law, M.G., Gazoni, L.M., Singh, R., Laubach, V.E., Linden, J., Tribble, C.G., and Kron, I.L. 2008. Adenosine A2A activation attenuates nontransplantation lung reperfusion injury. *J Surg Res* 149:3-8.
  65. Lisle, T.C., Gazoni, L.M., Fernandez, L.G., Sharma, A.K., Bellizzi, A.M., Schifflett, G.D., Laubach, V.E., and Kron, I.L. 2008. Inflammatory lung injury after cardiopulmonary bypass is attenuated by adenosine A(2A) receptor activation. *J Thorac Cardiovasc Surg* 136:1280-1287; discussion 1287-1288.
  66. Sottofattori, E., Anzaldi, M., and Ottonello, L. 2001. HPLC determination of adenosine in human synovial fluid. *J Pharm Biomed Anal* 24:1143-1146.
  67. Reeves, J.J., Jones, C.A., Sheehan, M.J., Vardey, C.J., and Whelan, C.J. 1997. Adenosine A3 receptors promote degranulation of rat mast cells both in vitro and in vivo. *Inflamm Res* 46:180-184.
  68. Salvatore, C.A., Tilley, S.L., Latour, A.M., Fletcher, D.S., Koller, B.H., and Jacobson, M.A. 2000. Disruption of the A(3) adenosine receptor gene in mice and its effect on stimulated inflammatory cells. *J Biol Chem* 275:4429-4434.
  69. Zhong, H., Shlykov, S.G., Molina, J.G., Sanborn, B.M., Jacobson, M.A., Tilley, S.L., and Blackburn, M.R. 2003. Activation of murine lung mast cells by the adenosine A3 receptor. *J Immunol* 171:338-345.
  70. Ryzhov, S., Zaynagetdinov, R., Goldstein, A.E., Novitskiy, S.V., Blackburn, M.R., Biaggioni, I., and Feoktistov, I. 2008. Effect of A2B adenosine receptor gene ablation on adenosine-dependent regulation of proinflammatory cytokines. *J Pharmacol Exp Ther* 324:694-700.
  71. Sun, C.X., Zhong, H., Mohsenin, A., Morschl, E., Chunn, J.L., Molina, J.G., Belardinelli, L., Zeng, D., and Blackburn, M.R. 2006. Role of A2B adenosine receptor signaling in adenosine-dependent pulmonary inflammation and injury. *J Clin Invest* 116:2173-2182.

72. Zhong, H., Belardinelli, L., Maa, T., and Zeng, D. 2005. Synergy between A2B adenosine receptors and hypoxia in activating human lung fibroblasts. *Am J Respir Cell Mol Biol* 32:2-8.
73. Banerjee, S.K., Young, H.W., Volmer, J.B., and Blackburn, M.R. 2002. Gene expression profiling in inflammatory airway disease associated with elevated adenosine. *Am J Physiol Lung Cell Mol Physiol* 282:L169-182.
74. Franzen, A., and Heinegard, D. 1985. Isolation and characterization of two sialoproteins present only in bone calcified matrix. *Biochem J* 232:715-724.
75. Weber, G.F., and Cantor, H. 1996. The immunology of Eta-1/osteopontin. *Cytokine Growth Factor Rev* 7:241-248.
76. Denhardt, D.T., Noda, M., O'Regan, A.W., Pavlin, D., and Berman, J.S. 2001. Osteopontin as a means to cope with environmental insults: regulation of inflammation, tissue remodeling, and cell survival. *J Clin Invest* 107:1055-1061.
77. Mazzali, M., Kipari, T., Ophascharoensuk, V., Wesson, J.A., Johnson, R., and Hughes, J. 2002. Osteopontin--a molecule for all seasons. *Qjm* 95:3-13.
78. Barry, S.T., Ludbrook, S.B., Murrison, E., and Horgan, C.M. 2000. Analysis of the alpha4beta1 integrin-osteopontin interaction. *Exp Cell Res* 258:342-351.
79. Yokosaki, Y., Matsuura, N., Sasaki, T., Murakami, I., Schneider, H., Higashiyama, S., Saitoh, Y., Yamakido, M., Taooka, Y., and Sheppard, D. 1999. The integrin alpha(9)beta(1) binds to a novel recognition sequence (SVVYGLR) in the thrombin-cleaved amino-terminal fragment of osteopontin. *J Biol Chem* 274:36328-36334.
80. Liaw, L., Skinner, M.P., Raines, E.W., Ross, R., Cheresch, D.A., Schwartz, S.M., and Giachelli, C.M. 1995. The adhesive and migratory effects of osteopontin are mediated via distinct cell surface integrins. Role of alpha v beta 3 in smooth muscle cell migration to osteopontin in vitro. *J Clin Invest* 95:713-724.
81. Senger, D.R., Ledbetter, S.R., Claffey, K.P., Papadopoulos-Sergiou, A., Peruzzi, C.A., and Detmar, M. 1996. Stimulation of endothelial cell migration by vascular permeability factor/vascular endothelial growth factor through cooperative mechanisms involving the alphavbeta3 integrin, osteopontin, and thrombin. *Am J Pathol* 149:293-305.
82. Pardo, A., Gibson, K., Cisneros, J., Richards, T.J., Yang, Y., Becerril, C., Yousem, S., Herrera, I., Ruiz, V., Selman, M., et al. 2005. Up-regulation and profibrotic role of osteopontin in human idiopathic pulmonary fibrosis. *PLoS Med* 2:e251.
83. Weber, G.F., Ashkar, S., Glimcher, M.J., and Cantor, H. 1996. Receptor-ligand interaction between CD44 and osteopontin (Eta-1). *Science* 271:509-512.

84. Ashkar, S., Weber, G.F., Panoutsakopoulou, V., Sanchirico, M.E., Jansson, M., Zawaideh, S., Rittling, S.R., Denhardt, D.T., Glimcher, M.J., and Cantor, H. 2000. Eta-1 (osteopontin): an early component of type-1 (cell-mediated) immunity. *Science* 287:860-864.
85. Katagiri, Y.U., Sleeman, J., Fujii, H., Herrlich, P., Hotta, H., Tanaka, K., Chikuma, S., Yagita, H., Okumura, K., Murakami, M., et al. 1999. CD44 variants but not CD44s cooperate with beta1-containing integrins to permit cells to bind to osteopontin independently of arginine-glycine-aspartic acid, thereby stimulating cell motility and chemotaxis. *Cancer Res* 59:219-226.
86. Zohar, R., Suzuki, N., Suzuki, K., Arora, P., Glogauer, M., McCulloch, C.A., and Sodek, J. 2000. Intracellular osteopontin is an integral component of the CD44-ERM complex involved in cell migration. *J Cell Physiol* 184:118-130.
87. Marcondes, M.C., Poling, M., Watry, D.D., Hall, D., and Fox, H.S. 2008. In vivo osteopontin-induced macrophage accumulation is dependent on CD44 expression. *Cell Immunol*.
88. Rangaswami, H., and Kundu, G.C. 2007. Osteopontin stimulates melanoma growth and lung metastasis through NIK/MEKK1-dependent MMP-9 activation pathways. *Oncol Rep* 18:909-915.
89. Desai, B., Rogers, M.J., and Chellaiah, M.A. 2007. Mechanisms of osteopontin and CD44 as metastatic principles in prostate cancer cells. *Mol Cancer* 6:18.
90. Chakraborty, G., Jain, S., Patil, T.V., and Kundu, G.C. 2008. Down-regulation of osteopontin attenuates breast tumour progression in vivo. *J Cell Mol Med* 12:2305-2318.
91. Rabinowich, H., Lin, W.C., Amoscato, A., Herberman, R.B., and Whiteside, T.L. 1995. Expression of vitronectin receptor on human NK cells and its role in protein phosphorylation, cytokine production, and cell proliferation. *J Immunol* 154:1124-1135.
92. Nau, G.J., Guilfoile, P., Chupp, G.L., Berman, J.S., Kim, S.J., Kornfeld, H., and Young, R.A. 1997. A chemoattractant cytokine associated with granulomas in tuberculosis and silicosis. *Proc Natl Acad Sci U S A* 94:6414-6419.
93. O'Regan, A.W., Chupp, G.L., Lowry, J.A., Goetschkes, M., Mulligan, N., and Berman, J.S. 1999. Osteopontin is associated with T cells in sarcoid granulomas and has T cell adhesive and cytokine-like properties in vitro. *J Immunol* 162:1024-1031.

94. O'Regan, A.W., Hayden, J.M., Body, S., Liaw, L., Mulligan, N., Goetschkes, M., and Berman, J.S. 2001. Abnormal pulmonary granuloma formation in osteopontin-deficient mice. *Am J Respir Crit Care Med* 164:2243-2247.
95. Jansson, M., Panoutsakopoulou, V., Baker, J., Klein, L., and Cantor, H. 2002. Cutting edge: Attenuated experimental autoimmune encephalomyelitis in eta-1/osteopontin-deficient mice. *J Immunol* 168:2096-2099.
96. Xanthou, G., Alissafi, T., Semitekolou, M., Simoes, D.C., Economidou, E., Gaga, M., Lambrecht, B.N., Lloyd, C.M., and Panoutsakopoulou, V. 2007. Osteopontin has a crucial role in allergic airway disease through regulation of dendritic cell subsets. *Nat Med* 13:570-578.
97. Takahashi, F., Takahashi, K., Okazaki, T., Maeda, K., Ienaga, H., Maeda, M., Kon, S., Uede, T., and Fukuchi, Y. 2001. Role of osteopontin in the pathogenesis of bleomycin-induced pulmonary fibrosis. *Am J Respir Cell Mol Biol* 24:264-271.
98. Berman, J.S., Serlin, D., Li, X., Whitley, G., Hayes, J., Rishikof, D.C., Ricupero, D.A., Liaw, L., Goetschkes, M., and O'Regan, A.W. 2004. Altered bleomycin-induced lung fibrosis in osteopontin-deficient mice. *Am J Physiol Lung Cell Mol Physiol* 286:L1311-1318.
99. Keane, M.P., Donnelly, S.C., Belperio, J.A., Goodman, R.B., Dy, M., Burdick, M.D., Fishbein, M.C., and Strieter, R.M. 2002. Imbalance in the expression of CXC chemokines correlates with bronchoalveolar lavage fluid angiogenic activity and procollagen levels in acute respiratory distress syndrome. *J Immunol* 169:6515-6521.
100. Svetlečić, J., Molteni, A., Chen, Y., Al-Hamed, M., Quinn, T., and Herndon, B. 2005. Transplant-related bronchiolitis obliterans (BOS) demonstrates unique cytokine profiles compared to toxicant-induced BOS. *Exp Mol Pathol* 79:198-205.
101. Woodruff, P.G., Koth, L.L., Yang, Y.H., Rodriguez, M.W., Favoreto, S., Dolganov, G.M., Paquet, A.C., and Erle, D.J. 2005. A distinctive alveolar macrophage activation state induced by cigarette smoking. *Am J Respir Crit Care Med* 172:1383-1392.
102. Churg, A., Wang, R., Wang, X., Onnervik, P.O., Thim, K., and Wright, J.L. 2007. Effect of an MMP-9/MMP-12 inhibitor on smoke-induced emphysema and airway remodelling in guinea pigs. *Thorax* 62:706-713.
103. Hautamaki, R.D., Kobayashi, D.K., Senior, R.M., and Shapiro, S.D. 1997. Requirement for macrophage elastase for cigarette smoke-induced emphysema in mice. *Science* 277:2002-2004.



104. Demedts, I.K., Morel-Montero, A., Lebecque, S., Pacheco, Y., Cataldo, D., Joos, G.F., Pauwels, R.A., and Brusselle, G.G. 2006. Elevated MMP-12 protein levels in induced sputum from patients with COPD. *Thorax* 61:196-201.
105. Betsuyaku, T., Nishimura, M., Takeyabu, K., Tanino, M., Venge, P., Xu, S., and Kawakami, Y. 1999. Neutrophil granule proteins in bronchoalveolar lavage fluid from subjects with subclinical emphysema. *Am J Respir Crit Care Med* 159:1985-1991.
106. Kohan, M., Breuer, R., and Berkman, N. 2009. Osteopontin induces airway remodeling and lung fibroblast activation in a murine model of asthma. *Am J Respir Cell Mol Biol* 41:290-296.
107. Hunninghake, G.W., and Crystal, R.G. 1983. Cigarette smoking and lung destruction. Accumulation of neutrophils in the lungs of cigarette smokers. *Am Rev Respir Dis* 128:833-838.
108. Lacoste, J.Y., Bousquet, J., Chanez, P., Van Vyve, T., Simony-Lafontaine, J., Lequeu, N., Vic, P., Enander, I., Godard, P., and Michel, F.B. 1993. Eosinophilic and neutrophilic inflammation in asthma, chronic bronchitis, and chronic obstructive pulmonary disease. *J Allergy Clin Immunol* 92:537-548.
109. Koh, A., da Silva, A.P., Bansal, A.K., Bansal, M., Sun, C., Lee, H., Glogauer, M., Sodek, J., and Zohar, R. 2007. Role of osteopontin in neutrophil function. *Immunology* 122:466-475.
110. Trueblood, N.A., Xie, Z., Communal, C., Sam, F., Ngoy, S., Liaw, L., Jenkins, A.W., Wang, J., Sawyer, D.B., Bing, O.H., et al. 2001. Exaggerated left ventricular dilation and reduced collagen deposition after myocardial infarction in mice lacking osteopontin. *Circ Res* 88:1080-1087.
111. Ophascharoensuk, V., Giachelli, C.M., Gordon, K., Hughes, J., Pichler, R., Brown, P., Liaw, L., Schmidt, R., Shankland, S.J., Alpers, C.E., et al. 1999. Obstructive uropathy in the mouse: role of osteopontin in interstitial fibrosis and apoptosis. *Kidney Int* 56:571-580.
112. Roman, J., Rivera, H.N., Roser-Page, S., Sitaraman, S.V., and Ritzenthaler, J.D. 2006. Adenosine induces fibronectin expression in lung epithelial cells: implications for airway remodeling. *Am J Physiol Lung Cell Mol Physiol* 290:L317-325.
113. Song, W.D., Zhang, A.C., Pang, Y.Y., Liu, L.H., Zhao, J.Y., Deng, S.H., and Zhang, S.Y. 1995. Fibronectin and hyaluronan in bronchoalveolar lavage fluid from young patients with chronic obstructive pulmonary diseases. *Respiration* 62:125-129.

114. Blackburn, M.R. 2003. Too much of a good thing: adenosine overload in adenosine-deaminase-deficient mice. *Trends Pharmacol Sci* 24:66-70.
115. Senger, D.R., and Perruzzi, C.A. 1996. Cell migration promoted by a potent GRGDS-containing thrombin-cleavage fragment of osteopontin. *Biochim Biophys Acta* 1314:13-24.
116. Boucherat, O., Franco-Montoya, M.L., Thibault, C., Incitti, R., Chailley-Heu, B., Delacourt, C., and Bourbon, J.R. 2007. Gene expression profiling in lung fibroblasts reveals new players in alveolarization. *Physiol Genomics* 32:128-141.
117. Mehats, C., Franco-Montoya, M.L., Boucherat, O., Lopez, E., Schmitz, T., Zana, E., Evain-Brion, D., Bourbon, J., Delacourt, C., and Jarreau, P.H. 2008. Effects of phosphodiesterase 4 inhibition on alveolarization and hyperoxia toxicity in newborn rats. *PLoS One* 3:e3445.
118. Takahashi, F., Takahashi, K., Shimizu, K., Cui, R., Tada, N., Takahashi, H., Soma, S., Yoshioka, M., and Fukuchi, Y. 2004. Osteopontin is strongly expressed by alveolar macrophages in the lungs of acute respiratory distress syndrome. *Lung* 182:173-185.
119. Stockley, R.A. 2002. Neutrophils and the pathogenesis of COPD. *Chest* 121:151S-155S.
120. Coleman, K.R., Braden, G.A., Willingham, M.C., and Sane, D.C. 1999. Vitaxin, a humanized monoclonal antibody to the vitronectin receptor (alpha<sub>v</sub>beta<sub>3</sub>), reduces neointimal hyperplasia and total vessel area after balloon injury in hypercholesterolemic rabbits. *Circ Res* 84:1268-1276.
121. Gutheil, J.C., Campbell, T.N., Pierce, P.R., Watkins, J.D., Huse, W.D., Bodkin, D.J., and Cheresh, D.A. 2000. Targeted antiangiogenic therapy for cancer using Vitaxin: a humanized monoclonal antibody to the integrin alpha<sub>v</sub>beta<sub>3</sub>. *Clin Cancer Res* 6:3056-3061.
122. Noble, P.W. 2003. Idiopathic pulmonary fibrosis. New insights into classification and pathogenesis usher in a new era therapeutic approaches. *Am J Respir Cell Mol Biol* 29:S27-31.
123. Lenga, Y., Koh, A., Perera, A.S., McCulloch, C.A., Sodek, J., and Zohar, R. 2008. Osteopontin expression is required for myofibroblast differentiation. *Circ Res* 102:319-327.
124. Horowitz, J.C., Rogers, D.S., Simon, R.H., Sisson, T.H., and Thannickal, V.J. 2008. Plasminogen activation induced pericellular fibronectin proteolysis promotes fibroblast apoptosis. *Am J Respir Cell Mol Biol* 38:78-87.

125. Nomiya, T., Perez-Tilve, D., Ogawa, D., Gizard, F., Zhao, Y., Heywood, E.B., Jones, K.L., Kawamori, R., Cassis, L.A., Tschop, M.H., et al. 2007. Osteopontin mediates obesity-induced adipose tissue macrophage infiltration and insulin resistance in mice. *J Clin Invest* 117:2877-2888.
126. van Houwelingen, A.H., Weathington, N.M., Verweij, V., Blalock, J.E., Nijkamp, F.P., and Folkerts, G. 2008. Induction of lung emphysema is prevented by L-arginine-threonine-arginine. *Faseb J* 22:3403-3408.
127. Ramirez, A.M., Takagawa, S., Sekosan, M., Jaffe, H.A., Varga, J., and Roman, J. 2004. Smad3 deficiency ameliorates experimental obliterative bronchiolitis in a heterotopic tracheal transplantation model. *Am J Pathol* 165:1223-1232.
128. Fitzgerald, M.F., and Fox, J.C. 2007. Emerging trends in the therapy of COPD: novel anti-inflammatory agents in clinical development. *Drug Discov Today* 12:479-486.
129. Kalla, R.V., and Zablocki, J. 2009. Progress in the discovery of selective, high affinity A(2B) adenosine receptor antagonists as clinical candidates. *Purinergic Signal* 5:21-29.
130. Daniil, Z.D., Gilchrist, F.C., Nicholson, A.G., Hansell, D.M., Harris, J., Colby, T.V., and du Bois, R.M. 1999. A histologic pattern of nonspecific interstitial pneumonia is associated with a better prognosis than usual interstitial pneumonia in patients with cryptogenic fibrosing alveolitis. *Am J Respir Crit Care Med* 160:899-905.
131. Thannickal, V.J., Toews, G.B., White, E.S., Lynch, J.P., 3rd, and Martinez, F.J. 2004. Mechanisms of pulmonary fibrosis. *Annu Rev Med* 55:395-417.
132. Phillips, R.J., Burdick, M.D., Hong, K., Lutz, M.A., Murray, L.A., Xue, Y.Y., Belperio, J.A., Keane, M.P., and Strieter, R.M. 2004. Circulating fibrocytes traffic to the lungs in response to CXCL12 and mediate fibrosis. *J Clin Invest* 114:438-446.
133. Moore, B.B., Murray, L., Das, A., Wilke, C.A., Herrygers, A.B., and Toews, G.B. 2006. The role of CCL12 in the recruitment of fibrocytes and lung fibrosis. *Am J Respir Cell Mol Biol* 35:175-181.
134. Ruscetti, F., Varesio, L., Ochoa, A., and Ortaldo, J. 1993. Pleiotropic effects of transforming growth factor-beta on cells of the immune system. *Ann N Y Acad Sci* 685:488-500.
135. Wahl, S.M. 1994. Transforming growth factor beta: the good, the bad, and the ugly. *J Exp Med* 180:1587-1590.
136. Aluwihare, P., and Munger, J.S. 2008. What the lung has taught us about latent TGF-beta activation. *Am J Respir Cell Mol Biol* 39:499-502.

137. Blobel, G.A., Schiemann, W.P., and Lodish, H.F. 2000. Role of transforming growth factor beta in human disease. *N Engl J Med* 342:1350-1358.
138. Border, W.A., and Noble, N.A. 1994. Transforming growth factor beta in tissue fibrosis. *N Engl J Med* 331:1286-1292.
139. Khalil, N., O'Connor, R.N., Unruh, H.W., Warren, P.W., Flanders, K.C., Kemp, A., Berezney, O.H., and Greenberg, A.H. 1991. Increased production and immunohistochemical localization of transforming growth factor-beta in idiopathic pulmonary fibrosis. *Am J Respir Cell Mol Biol* 5:155-162.
140. Roy, S.G., Nozaki, Y., and Phan, S.H. 2001. Regulation of alpha-smooth muscle actin gene expression in myofibroblast differentiation from rat lung fibroblasts. *Int J Biochem Cell Biol* 33:723-734.
141. Cutroneo, K.R. 2007. TGF-beta-induced fibrosis and SMAD signaling: oligo decoys as natural therapeutics for inhibition of tissue fibrosis and scarring. *Wound Repair Regen* 15 Suppl 1:S54-60.
142. Arnoux, V., Nassour, M., L'Helgoualc'h, A., Hipkind, R.A., and Savagner, P. 2008. Erk5 controls Slug expression and keratinocyte activation during wound healing. *Mol Biol Cell* 19:4738-4749.
143. Ahmed, N., Maines-Bandiera, S., Quinn, M.A., Unger, W.G., Dedhar, S., and Auersperg, N. 2006. Molecular pathways regulating EGF-induced epithelial-mesenchymal transition in human ovarian surface epithelium. *Am J Physiol Cell Physiol* 290:C1532-1542.
144. Zeisberg, M., Yang, C., Martino, M., Duncan, M.B., Rieder, F., Tanjore, H., and Kalluri, R. 2007. Fibroblasts derive from hepatocytes in liver fibrosis via epithelial to mesenchymal transition. *J Biol Chem* 282:23337-23347.
145. Kim, K.K., Kugler, M.C., Wolters, P.J., Robillard, L., Galvez, M.G., Brumwell, A.N., Sheppard, D., and Chapman, H.A. 2006. Alveolar epithelial cell mesenchymal transition develops in vivo during pulmonary fibrosis and is regulated by the extracellular matrix. *Proc Natl Acad Sci U S A* 103:13180-13185.
146. Willis, B.C., duBois, R.M., and Borok, Z. 2006. Epithelial origin of myofibroblasts during fibrosis in the lung. *Proc Am Thorac Soc* 3:377-382.
147. Wheelock, M.J., and Johnson, K.R. 2003. Cadherins as modulators of cellular phenotype. *Annu Rev Cell Dev Biol* 19:207-235.

148. Islam, S., Carey, T.E., Wolf, G.T., Wheelock, M.J., and Johnson, K.R. 1996. Expression of N-cadherin by human squamous carcinoma cells induces a scattered fibroblastic phenotype with disrupted cell-cell adhesion. *J Cell Biol* 135:1643-1654.
149. Frixen, U.H., Behrens, J., Sachs, M., Eberle, G., Voss, B., Warda, A., Lochner, D., and Birchmeier, W. 1991. E-cadherin-mediated cell-cell adhesion prevents invasiveness of human carcinoma cells. *J Cell Biol* 113:173-185.
150. Takao, S., Che, X., Fukudome, T., Natsugoe, S., Ozawa, M., and Aikou, T. 2000. Down-regulation of E-cadherin by antisense oligonucleotide enhances basement membrane invasion of pancreatic carcinoma cells. *Hum Cell* 13:15-21.
151. Nieman, M.T., Prudoff, R.S., Johnson, K.R., and Wheelock, M.J. 1999. N-cadherin promotes motility in human breast cancer cells regardless of their E-cadherin expression. *J Cell Biol* 147:631-644.
152. Zheng, G., Lyons, J.G., Tan, T.K., Wang, Y., Hsu, T.T., Min, D., Succar, L., Rangan, G.K., Hu, M., Henderson, B.R., et al. 2009. Disruption of E-cadherin by matrix metalloproteinase directly mediates epithelial-mesenchymal transition downstream of transforming growth factor-beta1 in renal tubular epithelial cells. *Am J Pathol* 175:580-591.
153. Veerasamy, M., Nguyen, T.Q., Motazed, R., Pearson, A.L., Goldschmeding, R., and Dockrell, M.E. 2009. Differential regulation of E-cadherin and alpha-smooth muscle actin by BMP 7 in human renal proximal tubule epithelial cells and its implication in renal fibrosis. *Am J Physiol Renal Physiol* 297:F1238-1248.
154. Pozharskaya, V., Torres-Gonzalez, E., Rojas, M., Gal, A., Amin, M., Dollard, S., Roman, J., Stecenko, A.A., and Mora, A.L. 2009. Twist: a regulator of epithelial-mesenchymal transition in lung fibrosis. *PLoS One* 4:e7559.
155. Selman, M., Pardo, A., Barrera, L., Estrada, A., Watson, S.R., Wilson, K., Aziz, N., Kaminski, N., and Zlotnik, A. 2006. Gene expression profiles distinguish idiopathic pulmonary fibrosis from hypersensitivity pneumonitis. *Am J Respir Crit Care Med* 173:188-198.
156. Borchers, A., David, R., and Wedlich, D. 2001. Xenopus cadherin-11 restrains cranial neural crest migration and influences neural crest specification. *Development* 128:3049-3060.
157. Pishvaian, M.J., Feltes, C.M., Thompson, P., Bussemakers, M.J., Schalken, J.A., and Byers, S.W. 1999. Cadherin-11 is expressed in invasive breast cancer cell lines. *Cancer Res* 59:947-952.

158. Valencia, X., Higgins, J.M., Kiener, H.P., Lee, D.M., Podrebarac, T.A., Dascher, C.C., Watts, G.F., Mizoguchi, E., Simmons, B., Patel, D.D., et al. 2004. Cadherin-11 provides specific cellular adhesion between fibroblast-like synoviocytes. *J Exp Med* 200:1673-1679.
159. Kiener, H.P., Niederreiter, B., Lee, D.M., Jimenez-Boj, E., Smolen, J.S., and Brenner, M.B. 2009. Cadherin 11 promotes invasive behavior of fibroblast-like synoviocytes. *Arthritis Rheum* 60:1305-1310.
160. Hinz, B., Pittet, P., Smith-Clerc, J., Chaponnier, C., and Meister, J.J. 2004. Myofibroblast development is characterized by specific cell-cell adherens junctions. *Mol Biol Cell* 15:4310-4320.
161. Gardner, H., Shearstone, J.R., Bandaru, R., Crowell, T., Lynes, M., Trojanowska, M., Pannu, J., Smith, E., Jablonska, S., Blaszczyk, M., et al. 2006. Gene profiling of scleroderma skin reveals robust signatures of disease that are imperfectly reflected in the transcript profiles of explanted fibroblasts. *Arthritis Rheum* 54:1961-1973.
162. Whitfield, M.L., Finlay, D.R., Murray, J.I., Troyanskaya, O.G., Chi, J.T., Pergamenschikov, A., McCalmont, T.H., Brown, P.O., Botstein, D., and Connolly, M.K. 2003. Systemic and cell type-specific gene expression patterns in scleroderma skin. *Proc Natl Acad Sci U S A* 100:12319-12324.
163. Moeller, A., Ask, K., Warburton, D., Gauldie, J., and Kolb, M. 2008. The bleomycin animal model: a useful tool to investigate treatment options for idiopathic pulmonary fibrosis? *Int J Biochem Cell Biol* 40:362-382.
164. Homer, R.J., Zheng, T., Chupp, G., He, S., Zhu, Z., Chen, Q., Ma, B., Hite, R.D., Gobran, L.I., Rooney, S.A., et al. 2002. Pulmonary type II cell hypertrophy and pulmonary lipoproteinosis are features of chronic IL-13 exposure. *Am J Physiol Lung Cell Mol Physiol* 283:L52-59.
165. Konigshoff, M., Kramer, M., Balsara, N., Wilhelm, J., Amarie, O.V., Jahn, A., Rose, F., Fink, L., Seeger, W., Schaefer, L., et al. 2009. WNT1-inducible signaling protein-1 mediates pulmonary fibrosis in mice and is upregulated in humans with idiopathic pulmonary fibrosis. *J Clin Invest* 119:772-787.
166. Khalil, N., Berezney, O., Sporn, M., and Greenberg, A.H. 1989. Macrophage production of transforming growth factor beta and fibroblast collagen synthesis in chronic pulmonary inflammation. *J Exp Med* 170:727-737.
167. Phan, S.H., and Kunkel, S.L. 1992. Lung cytokine production in bleomycin-induced pulmonary fibrosis. *Exp Lung Res* 18:29-43.

168. Bringardner, B.D., Baran, C.P., Eubank, T.D., and Marsh, C.B. 2008. The role of inflammation in the pathogenesis of idiopathic pulmonary fibrosis. *Antioxid Redox Signal* 10:287-301.
169. Forino, M., Torregrossa, R., Ceol, M., Murer, L., Della Vella, M., Del Prete, D., D'Angelo, A., and Anglani, F. 2006. TGFbeta1 induces epithelial-mesenchymal transition, but not myofibroblast transdifferentiation of human kidney tubular epithelial cells in primary culture. *Int J Exp Pathol* 87:197-208.
170. Sarrio, D., Rodriguez-Pinilla, S.M., Hardisson, D., Cano, A., Moreno-Bueno, G., and Palacios, J. 2008. Epithelial-mesenchymal transition in breast cancer relates to the basal-like phenotype. *Cancer Res* 68:989-997.
171. Vered, M., Dayan, D., Yahalom, R., Dobriyan, A., Barshack, I., Bello, I.O., Kantola, S., and Salo, T. Cancer-associated fibroblasts and epithelial-mesenchymal transition in metastatic oral tongue squamous cell carcinoma. *Int J Cancer*.
172. Reneker, L.W., Bloch, A., Xie, L., Overbeek, P.A., and Ash, J.D. Induction of corneal myofibroblasts by lens-derived transforming growth factor beta1 (TGFbeta1): a transgenic mouse model. *Brain Res Bull* 81:287-296.
173. Willis, B.C., Liebler, J.M., Luby-Phelps, K., Nicholson, A.G., Crandall, E.D., du Bois, R.M., and Borok, Z. 2005. Induction of epithelial-mesenchymal transition in alveolar epithelial cells by transforming growth factor-beta1: potential role in idiopathic pulmonary fibrosis. *Am J Pathol* 166:1321-1332.
174. Munger, J.S., Huang, X., Kawakatsu, H., Griffiths, M.J., Dalton, S.L., Wu, J., Pittet, J.F., Kaminski, N., Garat, C., Matthay, M.A., et al. 1999. The integrin alpha v beta 6 binds and activates latent TGF beta 1: a mechanism for regulating pulmonary inflammation and fibrosis. *Cell* 96:319-328.
175. Crawford, S.E., Stellmach, V., Murphy-Ullrich, J.E., Ribeiro, S.M., Lawler, J., Hynes, R.O., Boivin, G.P., and Bouck, N. 1998. Thrombospondin-1 is a major activator of TGF-beta1 in vivo. *Cell* 93:1159-1170.
176. Yu, Q., and Stamenkovic, I. 2000. Cell surface-localized matrix metalloproteinase-9 proteolytically activates TGF-beta and promotes tumor invasion and angiogenesis. *Genes Dev* 14:163-176.
177. Noren, N.K., Niessen, C.M., Gumbiner, B.M., and Burridge, K. 2001. Cadherin engagement regulates Rho family GTPases. *J Biol Chem* 276:33305-33308.

178. Cai, G.Q., Zheng, A., Tang, Q., White, E.S., Chou, C.F., Gladson, C.L., Oltman, M.A., and Ding, Q. Downregulation of FAK-related non-kinase mediates the migratory phenotype of human fibrotic lung fibroblasts. *Exp Cell Res*.
179. Kono, Y., Nishiuma, T., Nishimura, Y., Kotani, Y., Okada, T., Nakamura, S., and Yokoyama, M. 2007. Sphingosine kinase 1 regulates differentiation of human and mouse lung fibroblasts mediated by TGF-beta1. *Am J Respir Cell Mol Biol* 37:395-404.
180. Xiao, Y.Q., Freire-de-Lima, C.G., Schiemann, W.P., Bratton, D.L., Vandivier, R.W., and Henson, P.M. 2008. Transcriptional and translational regulation of TGF-beta production in response to apoptotic cells. *J Immunol* 181:3575-3585.
181. Nagatoya, K., Moriyama, T., Kawada, N., Takeji, M., Oseto, S., Murozono, T., Ando, A., Imai, E., and Hori, M. 2002. Y-27632 prevents tubulointerstitial fibrosis in mouse kidneys with unilateral ureteral obstruction. *Kidney Int* 61:1684-1695.
182. Salazar, K.D., Lankford, S.M., and Brody, A.R. 2009. Mesenchymal stem cells produce Wnt isoforms and TGF-beta1 that mediate proliferation and procollagen expression by lung fibroblasts. *Am J Physiol Lung Cell Mol Physiol* 297:L1002-1011.
183. Chilosi, M., Poletti, V., Zamo, A., Lestani, M., Montagna, L., Piccoli, P., Pedron, S., Bertaso, M., Scarpa, A., Murer, B., et al. 2003. Aberrant Wnt/beta-catenin pathway activation in idiopathic pulmonary fibrosis. *Am J Pathol* 162:1495-1502.
184. Konigshoff, M., Balsara, N., Pfaff, E.M., Kramer, M., Chrobak, I., Seeger, W., and Eickelberg, O. 2008. Functional Wnt signaling is increased in idiopathic pulmonary fibrosis. *PLoS One* 3:e2142.
185. Kam, Y., and Quaranta, V. 2009. Cadherin-bound beta-catenin feeds into the Wnt pathway upon adherens junctions dissociation: evidence for an intersection between beta-catenin pools. *PLoS One* 4:e4580.
186. Korfhagen, T.R., Swantz, R.J., Wert, S.E., McCarty, J.M., Kerlakian, C.B., Glasser, S.W., and Whitsett, J.A. 1994. Respiratory epithelial cell expression of human transforming growth factor-alpha induces lung fibrosis in transgenic mice. *J Clin Invest* 93:1691-1699.
187. Hamada, N., Kuwano, K., Yamada, M., Hagimoto, N., Hiasa, K., Egashira, K., Nakashima, N., Maeyama, T., Yoshimi, M., and Nakanishi, Y. 2005. Anti-vascular endothelial growth factor gene therapy attenuates lung injury and fibrosis in mice. *J Immunol* 175:1224-1231.
188. Fehrenbach, H., Haase, M., Kasper, M., Koslowski, R., Schuh, D., and Muller, M. 1999. Alterations in the immunohistochemical distribution patterns of vascular endothelial



- growth factor receptors Flk1 and Flt1 in bleomycin-induced rat lung fibrosis. *Virchows Arch* 435:20-31.
189. Chaudhary, N.I., Roth, G.J., Hilberg, F., Muller-Quernheim, J., Prasse, A., Zissel, G., Schnapp, A., and Park, J.E. 2007. Inhibition of PDGF, VEGF and FGF signalling attenuates fibrosis. *Eur Respir J* 29:976-985.
  190. Pece, S., and Gutkind, J.S. 2000. Signaling from E-cadherins to the MAPK pathway by the recruitment and activation of epidermal growth factor receptors upon cell-cell contact formation. *J Biol Chem* 275:41227-41233.
  191. Boscher, C., and Mege, R.M. 2008. Cadherin-11 interacts with the FGF receptor and induces neurite outgrowth through associated downstream signalling. *Cell Signal* 20:1061-1072.
  192. Williams, E.J., Williams, G., Howell, F.V., Skaper, S.D., Walsh, F.S., and Doherty, P. 2001. Identification of an N-cadherin motif that can interact with the fibroblast growth factor receptor and is required for axonal growth. *J Biol Chem* 276:43879-43886.
  193. Calera, M.R., Venkatakrishnan, A., and Kazlauskas, A. 2004. VE-cadherin increases the half-life of VEGF receptor 2. *Exp Cell Res* 300:248-256.
  194. Schneider, D.J., Lindsay, J.C., Zhou, Y., Molina, J.G., and Blackburn, M.R. 2009. Adenosine and osteopontin contribute to the development of chronic obstructive pulmonary disease. *Faseb J*.

# Vita

Name of author: Daniel Joseph Schneider

Date and place of birth: April 15<sup>th</sup>, 1981, Iowa City, IA

High School: Class of 1999 – Lincoln East High School, Lincoln, NE

Undergraduate: B.S. in Biochemistry with Honors,  
University of Texas at Austin, 2003

Post-graduate: University of Texas at Houston medical school  
Graduate School of Biomedical Sciences (MD/PhD Program)

## Publications:

Cadherin 11 contributes to epithelial to mesenchymal transition and the pathogenesis of pulmonary fibrosis

**Schneider DJ**, Wu M, Huang M, Le T, Brenner MB, Blackburn MR, Agarwal SK

In final preparations for submission

Adenosine and osteopontin contribute to the development of chronic obstructive pulmonary disease

**Schneider DJ**, Lindsay JC, Zhou Y, Molina JG, Blackburn MR

FASEB J. 2010 Jan;24(1):70-80. Epub 2009 Aug 31.

Adenosine signaling and the regulation of chronic lung diseases

Zhou Y, **Schneider DJ**, Blackburn MR

Pharmacol Ther. 2009 Jul;123(1):105-16.

Osteopontin in systemic sclerosis and its role in dermal fibrosis

Wu M, **Schneider DJ**, Huang M, Mayes MD, Assassi S, Arnett FC, Tan FK, Blackburn MR, Agarwal SK

In final preparations for submission

Interleukin 6 contributes to inflammation and fibrosis in a model of adenosine-mediated pulmonary injury

Pedroza M, **Schneider DJ**, Corrigan R, Molina JM, Gelinas R, Blackburn MR

In final preparations for submission

A<sub>2B</sub> adenosine receptor activation is essential for potentiation of epithelial ciliary motility and clearance

Allen-Gipson DS, Blackburn MR, **Schneider DJ**, Bluit DL, Jarrell JC, Sisson JH, Wyatt TA

In final preparations for submission.

Abstracts

Effect of osteopontin on baseline airway responsiveness and ozone-induced pulmonary injury and inflammation

Johnston RA, Hernandez CB, Hallberg LM, **Schneider DJ**, Blackburn MR

Poster at American Thoracic Society: May 2010 meeting – New Orleans, LA

Contribution of osteopontin to adenosine-dependent lung disease

**Schneider DJ**, Molina JG, Chunn JL, Zhou Y, Blackburn MR

Poster presented at American Thoracic Society: May, 2009 meeting – San Diego, CA

Adenosine and osteopontin contribute to chronic obstructive pulmonary disease

**Schneider DJ**, Molina JG, Chunn JL, Zhou Y, Blackburn MR

Poster presented at American Physician Scientist Association: April, 2009 – Chicago, IL

Purinergic stimulation of ciliary beat frequency in adenosine receptor knockout mouse tracheal rings is dependent on A<sub>2B</sub> adenosine receptor activation

Allen-Gipson DS, Jarrell JC, **Schneider DJ**, Wyatt TA, Sisson JH, Blackburn MR

Submitted and accepted by 2008 Purines meeting – Copenhagen, Denmark

Voltage gated Na<sup>+</sup> and Ca<sup>2+</sup> currents in rodent vestibular ganglion cells

**Schneider DJ**, Hurley KM, Eatock RA

Abstract/Poster presented @ ARO conference: February, 2006 – Baltimore, MD

Awards

CCTS T32 training grant fellowship	4/2008 to 4/2010
GSEC Research Poster Competition – 2 <sup>nd</sup> Place	2/11/2009
GSBS/UTHSC Student Travel Award	2/26/2009
Biochemistry Retreat Poster Competition – 1 <sup>st</sup> place	3/10/2009
ASCI/AAP Joint Meeting Travel Awardee	4/26/2009
Biochemistry Retreat Talks Competition – 1 <sup>st</sup> place	3/10/2010